EXACT QUANTUM DYNAMICS OF SPIN SYSTEMS USING THE POSITIVE-P REPRESENTATION

EXACT QUANTUM DYNAMICS OF SPIN SYSTEMS USING THE POSITIVE-P REPRESENTATION

By

RAY NG YEH YI, BSc.

A Thesis

Submitted to the School of Graduate Studies

in Partial Fulfilment of the Requirements

for the Degree

Master of Science

McMaster University

August 2010

MASTER OF SCIENCE (2010)
(Physics and Astronomy)

McMaster University
Hamilton, Ontario

TITLE: Exact Quantum Dyanmics of Spin Systems Using the Positive-P Representation

AUTHOR: Ray Ng Yeh Yi, B.Sc. (Simon Fraser University)

SUPERVISOR: Professor Erik Sörensen

NUMBER OF PAGES: xii, 82

Dedicated to Zoey Forsyth

"Do or do not. There is no try" – Master Jedi Yoda

Abstract

In this thesis, we discuss a scheme for simulating the *real time* quantum quench dynamics of interacting quantum spin systems within the positive-P formalism. As model systems we study the transverse field Ising model as well as the Heisenberg model undergoing a quench away from the classical ferromagnetic ordered state. The connection to the positive-P formalism, as it is used in quantum optics, is established by mapping the spin operators on to Scwhwinger bosons. In doing so, the dynamics of the interacting quantum spin system is mapped onto a set of stochastic differential equations (SDEs) the number of which scales *linearly* with the number of spins, N, compared to an exact solution through diagonalization that in the case of the Heisenberg model would require matrices exponentially large in N. This mapping is *exact* and can be extended to higher dimensional interacting systems as well as to systems with an explicit coupling to the environment.

Acknowledgements

Above all, I would like to thank my parents, Harold and Christine for always being supportive for all my endeavors. You have inculcated excellent values and principles that will aid me in achieving my goals. My siblings, Dawn and Jed, have been a source of inspiration in their own ways and we share a special bond from being brought up in the 'Ng' household. When I first moved to Canada, it was the other 'Ng' family (Harry, Lucy, Darrell and Rachel) who have always looked out for me and for that I am grateful.

I would like to thank my supervisor, Erik Sörensen for being encouraging and reassuring me during the worst times of resultless research. It was this encouragement that has enabled me to keep the faith and not give up, resulting in this humble thesis. Having someone believe in you is a very powerful thing.

Thank you to my thesis defence committee members, Duncan O'Dell and Maikel Rheinstadter for indulging me and allowing me to share my research with them.

I cannot stress how important and crucial my email correspondences with Piotr Deuar and Murray Olsen have been. You two have provided extremely enlightening discussions, like pieces to the jigsaw puzzle to my understanding of the positive-P representation. I would surely not have come this far without your useful consultations. Thank you so much. I would also like to thank Dmitry Pelinovski from McMaster's Department of Mathematics, who has been patient with me. Dmitry was the professor of a Math course that I audited and has since been eager to have dicussions with me.

Thank you to my senior graduate students, especially Allan Bayntun and Sedigh Ghamari for always being willing to discuss physics outside their own areas of specialties and to Phillip Ashby and Prasanna Venkatesh for always providing useful insight. My group members, Misha Thesberg and Andreas Deschner, have been delightful and I am grateful for their accompaniment as office mates. To my cohort, I would like to thank Andrew Louca for being the perfect study 'wingman' and Sarah Purdy for always being there for me inside and outside of physics.

Last but not least, I would like to thank my friends of Kawasaki Judo club whom I have grown to love and treasure very much. My Sensei (Mitchell Kawasaki) has been

very encouraging towards my Judo aspirations despite my interest in the sport at such a mature age. I do not believe I would have made it this far without the fun times at the dojo, especially the intense games of hand-ball. They have always helped me recharge my zest for research. My 'surrogate family': The Forsyths (Scott, Mary-Lisa, Delaney, Zoe and Georgia) and my 'Asian' family': (Woo Tak, Woo Deok and Woo Cheol), who are a part of Kawasaki, have showered unconditional love and care when it was needed the most. I cannot begin to express how lucky I feel every day to have you all in my life. Thank you all.

Contents

List of Figures

List of Tables

Chapter 1

Introduction

1.1 Motivation

A central model in condensed matter physics is rooted in the celebrated Heisenberg Hamiltonian [1]:

$$\hat{H} = -\vec{\mathbf{J}} \sum_{\langle i,j \rangle} \hat{\mathbf{S}}_i . \hat{\mathbf{S}}_j, \tag{1.1.1}$$

which describes the phenomena of quantum magnetism arising from exchange interactions between spins in insulating solids. Despite its deceivingly simple form, the Heisenberg model is a very successful one[1]. In accordance with the predictions of eq. 1.1.1, antiferromagnetic ($J < 0$) and ferromagnetic ($J > 0$) ordering have been experimentally observed in all dimensions and different geometries, such as in Kagome [2, 3] or square lattices [4, 5] to name a few.

Due to the macroscopic number of spins, N, in real materials however, solving eq. 1.1.1 (even in $1D$) exactly, from a theoretical point of view, is a difficult problem because of the exponential scaling of the Hilbert space. Considering that the number of spins in a typical solid is to the order of Avogadro's number: $N \sim 10^{23}$, a material consisting of spin-$\frac{1}{2}$ particles would have 2^N eigenstates, requiring resources that cannot be met even with today's most powerful computers. As a result of this predicament, numerous methods have been developed over the years in a bid to circumvent it. For such lattice-based models, the most straightforward and brute force approach is by way of exact diagonalization [6–8]. While this method has been developed significantly, exact diagonalization is still only able to simulate systems of relatively small sizes (~ 20), due to the aforementioned Hilbert space problem. Standard quantum Monte Carlo techniques yield results only in the imaginary time domain and requires an explicit analytic continuation to access real times, a notoriously difficult procedure. In recent years, methods rooted in the density matrix renormalization group (DMRG) such as TEBD [9] and t-DMRG [10] have been

[1] see table 1.1 for variants of the Heisenberg model[2] arising from eq. 1.1.1

developed to study real-time dynamics, but are applicable only to one-dimension. Most recently, the infinite size TEBD (iTEBD) has been tuned to yield results for the time dependence of the transverse-field Ising model (TFIM) out to surprisingly large times of order $tJ/\hbar \sim 6 - 10$ [11]. How well such methods will perform in higher dimensions or in the presence of a coupling to the environment is presently unclear.

Name	Exchange interaction	Hamiltonian: $\hat{H}$:
Ising	$J_x = J_y = 0$	$\sum_{\langle i,j \rangle} J_z \hat{S}_i^z \hat{S}_j^z$
XXX (isotropic)	$J_x = J_y = J_z = J$	$\sum_{\langle i,j \rangle} J \left[\hat{S}_i^x \hat{S}_j^x + \hat{S}_i^y \hat{S}_j^y + \hat{S}_i^z \hat{S}_j^z \right]$ $= \sum_{\langle i,j \rangle} J \left[\hat{S}_i^z \hat{S}_j^z + \frac{1}{2} \left(\hat{S}_i^+ \hat{S}_j^- + \hat{S}_i^- \hat{S}_j^+ \right) \right]$
XY	$J_z = 0$	$\sum_{\langle i,j \rangle} \left[J_x \hat{S}^x f_i \hat{S}_j^x + J_y \hat{S}_i^y \hat{S}_j^y \right]$
XXZ	$J_x = J_y = \Delta, J_z = J$	$\sum_{\langle i,j \rangle} \left[J \hat{S}_i^z \hat{S}_j^z + \frac{\Delta}{2} \left(\hat{S}_i^+ \hat{S}_j^- + \hat{S}_i^- \hat{S}_j^+ \right) \right]$
XYZ (anisotropic)	$J_x \neq J_y \neq J_z$	$\sum_{\langle i,j \rangle} \left[J_x \hat{S}_i^x \hat{S}_j^x + J_y \hat{S}_i^y \hat{S}_j^y + J_z \hat{S}_i^z \hat{S}_j^z \right]$

Table 1.1: Different Heisenberg spin models.

In this thesis, we present a novel idea of overcoming the Hilbert space problem by employing quantum phase space methods [12]; traditionally tailored towards quantum optics systems. The upshot of this method is that it in principle allows us to solve both the real time and imaginary time dynamics for macroscopic system sizes in all dimensions and geometries, potentially surpassing other traditional techniques mentioned above. The essence of quantum phase space methods is to rework the complicated dynamics of a quantum mechanical Hamiltonian in such a way that a classical interpretation of the physics arises. As an example, consider the pioneering quantum phase space method discovered by Wigner [13, 14] in 1960, known as the Wigner representation. Wigner derived a distribution function, f_W called the Wigner function:

$$f_W(p,q) = \frac{1}{2\pi\hbar} \int_{-\infty}^{\infty} e^{\frac{i}{\hbar}ps} \langle q - \frac{s}{2} | \psi \rangle \langle \psi | q + \frac{s}{2} \rangle ds \tag{1.1.2}$$

which had certain characteristics of a classical probability in the sense that

$$\int_{-\infty}^{\infty} f_W(p,q) dp = |\psi(q)|^2 \tag{1.1.3}$$

$$\int_{-\infty}^{\infty} f_W(p,q) dq = |\tilde{\psi}(p)|^2. \tag{1.1.4}$$

$$\int_{-\infty}^{\infty} f_W(p,q) dp dq = 1. \tag{1.1.5}$$

are obeyed [15], where $|\tilde{\psi}(p)|^2$ yields the probability distribution in momentum space and $|\tilde{\psi}(q)|^2$ yields the probability distribution in position space. In the Wigner representation,

$f_W(p,q)$ behaves almost like a joint probability distribution in the momentum, p and position, q analogous to a classical canonical ensemble probability distribution. We say *almost* because the Wigner function can take on negative values as well and therefore cannot be interpreted strictly as a phase space probability distribution. Nonetheless, it is a noble attempt at bridging the gap between classical and quantum physics.

The quantum phase space method that we will be using however, is known as the positive-P representation (PPR) [16], discovered by Drummond and Gardiner in 1980. The PPR, like Glauber-Sudarshan's P representation is based upon the bosonic coherent states which were fashioned by Roy J. Glauber[17] as the most 'classical', quantum mechanical state. In the PPR, we obtain a classical statistical interpretation of quantum mechanics in the sense that expectation values of normal-ordered operators[3] are replaced by the equivalent statistical expression

$$\langle \hat{O}(\hat{a}^\dagger, \hat{a}) \rangle = tr\left[\hat{\rho}\hat{O}(\hat{a}, \hat{a}^\dagger)\right] \tag{1.1.6}$$

$$= \int O(\alpha, \alpha^+) P(\alpha, \alpha^+) d^2\alpha d^2\alpha^+, \tag{1.1.7}$$

where $P(\alpha, \alpha^+)$ is the positive-P distribution function that plays the role of a joint probability distribution function for the complex variables α and α^+. This is made possible by the existence of correspondence relations which allows one to map the bosonic operators: $\hat{a}, \hat{a}^\dagger$ on to a pair of independent complex variables, α, α^+ (for the single mode case). Normal ordered operators such as $\hat{O}(\hat{a}^{dg}, \hat{a})$ are then mapped on to complex functions: $\hat{O}(\alpha^+, \alpha)$ instead. Instead of solving the dynamics of the probability distribution function, $P(\alpha, \alpha^+)$ (as in the Wigner distribution), it is possible to simulate the system dynamics via Ito Stochastic Differential equations (SDEs) instead.

This is done in the following way. Using the correspondence relations in an equation of motion for the density operator generally allows one to obtain a Fokker-Planck equation (FPE). According to the theory of Stochastic calculus [18] then, the FPE can in turn be equivalently described by a set of N, coupled Ito stochastic differential equations (SDEs). This reduces the dimensionality of the problem to one that scales linearly with N, thereby overcoming the Hilbert space problem and making many-body physics tractable. The beauty of utilizing SDEs is that, in the limit of an infinite number of trajectories (n_{traj}), stochastic averaging of complex phase space functions corresponds to the statistical expression in eq. 1.1.7 and converges to the exact quantum mechanical expectation value, i..e

$$tr\left[\hat{\rho}\hat{O}(\hat{a}, \hat{a}^\dagger)\right] = \lim_{n_{traj}\to\infty} \langle\langle O(\alpha, \alpha^+)\rangle\rangle, \tag{1.1.8}$$

where $\langle\langle . \rangle\rangle$ denotes a stochastic average and assuming we are dealing with normal-ordered operator observables. Calculating complicated quantum mechanical expectation values now reduces to the task of trivial averaging.

The PPR has been traditionally applied to quantum optics applications [19, 20], especially the realm of Bose-Einstein condensates (BECs) [21–23] of late. However, it has not

[3] This means operators of the form $(\hat{a}^\dagger)^m(\hat{a})^n$, i.e. all $\hat{a}^\dagger$s appear on the left and all $\hat{a}$s appear on the right.

yet to our knowledge been applied to simulating the dynamics of condensed matter spin systems such as the Heisenberg model. We have therefore picked two $1D$ simple models as an initial test bed for this novel idea, i.e. (i) the transverse-field Ising model (TFIM):

$$\hat{H}_o = -\sum_{\langle i,j \rangle} J\hat{S}_i^z \hat{S}_j^z - h\sum_i \hat{S}_i^x \tag{1.1.9}$$

and (ii) the transverse field-XXZ anisotropic model (see table 1.1 for other possible models as well):

$$\hat{H}_o = -\sum_{\langle i,j \rangle} \left[J\hat{S}_i^z \hat{S}_j^z + \frac{\Delta}{2}\left(\hat{S}_i^+ \hat{S}_j^- + \hat{S}_i^- \hat{S}_j^+ \right) \right] - h\sum_i \hat{S}_i^x. \tag{1.1.10}$$

Instead of viewing (i) and (ii) as materials being described by a single Hamiltonian, $\hat{H}_o$ and observing the evolution of the system under the latter, we will take the alternate view that eq. 1.1.9 and eq. 1.1.10 represent quantum quench systems [24]. That is to say, we wish to study the dynamics of a system after subjecting it to a sudden change of a parameter of the system, where by "a sudden change" we mean that this change occurs on a time scale much shorter than the relevant time scale of the system. Physically this means that at $t < 0$, the system is described by some initial Hamiltonian, $\hat{H}_i$ and at $t \geq 0$ allowed to evolve under a different Hamiltonian, $\hat{H}_f$. In such quench systems, it is of interest to see if equilibration (thermalization) into a new eigenstate of $\hat{H}_f$ occurs or if new nonequilibrium dynamics arises. Although it is common practice to begin the system in an eigenstate of the the initial Hamiltonian, it is certainly not essential [25].

If we assume the initial Hamiltonian as an Ising chain, then the parameters we would like to tune are the transverse magnetic field, h and the measure of anisotropy, Δ. Such control over the system is not just theoretical, and in fact can be achieved experimentally with ultracold two level atoms in optical lattices [26]. These experiments are currently under development [27, 28]. Using the PPR, we will show that it is possible to simulate the quantum quench dynamics of (i) and (ii) by employing stochastic differential equations. We will concern ourselves with both FM $J(>0)$ and AFM $(J<0)$ material prepared in the either the FM ground state: $|\uparrow\uparrow \ldots \uparrow\rangle$ or the classical AFM Neel state: $|\uparrow\downarrow\uparrow\downarrow \ldots \uparrow\downarrow\rangle$ respectively, and observe its dynamics after a magnetic field((i) and (ii)) and anisotropic quench ((ii) only).

This thesis report is outlined as follows. For readers without any background in stochastic differential equations (SDEs), it is recommended that a detour to appendix A is made. We have written appendix A in such a fashion that it will provide the reader with the mathematical background necessary to understand the details of this thesis. In chapter 2, we present a thorough review of the PPR. We will answer the question: "What is the PPR?" and go through the derivations and certain technical details of the formalism. In particular, we will show how a master equation can be converted to a FPE and in turn mapped on a set of Ito SDEs which is our final goal. To reinforce these ideas, we will derive the SDEs explicitly for the examples presented in [29] and [19]. In chapter 3, we introduce the idea of Schwinger bosons which allows us to write spin operators in terms of bosonic operators,

in preparation for the PPR. We then demonstrate its validity by reproducing the results of [30]. Finally, in chapter 4, we present our results for the quantum quench dynamics of the TFIM and the isotropic Heisenberg model for the FM case, from stochastic simulations and compare them with exact diagonalization results. For the case of AFM interactions, we simulate the anisotropic Heisenberg model and compare the results once again with exact calculations. The details of the derivations in chapter 4 have been relegated to Appendix B and the numerical algorithm used is discussed in Appendix C. Lastly, the conclusion follows in chapter 5 where we summarize our results and discuss the future direction of our research.

Chapter 2

What is the positive-P representation?

The main problem-solving tool or method that is used in our research is known as the positive-P representation (PPR) and we dedicate this chapter to the technical details of its derivation and application. The PPR is an exact quantum phase space method that was originally developed to solve simple quantum optics problems [19, 20, 31] but has lately shifted focus to the realm of many-body physics, in particular, simulating the dynamics of Bose-Einstein condensates (BECs) [21, 23, 32]. For instance, Ghanbari et al [21] have recently applied the positive-P representation to the imaginary time evolution of the Bose-Hubbard model and successfully calculated finite temperature correlations for up to 11 lattice sites. In a different work [22] , Deuar and Drummond used the PPR to simulate the real time dynamics of two colliding Bose gases, comprising of up to 150,000 atoms, by measuring its first-order and second order correlation functions. The PPR has therefore displayed evidence of being a very effective technique in simulating many-body systems and deserves some scrutiny.

To provide the reader with some overall idea about the PPR, I will first provide a summary of how the PPR is used, before indulging in the technical details. This will serve as a guide for the material presented in this chapter so that is able to see the motivation of its layout. For readers who are unfamiliar with stochastic differential equations (SDEs) then it is recommended that a detour to Appendix A is made, where an abridged introduction to SDEs is provided. This will help familiarize the reader with certain jargon and terminology used in this branch of mathematics.

Broadly speaking, the PPR is the expansion of the quantum density operator, $\hat{\rho}$, in terms of bosonic coherent states. The benefit of doing so is that in this form, the equation of motion for $\hat{\rho}$ may take the form of a Fokker-Planck Equation (FPE) (see section A.1), which can then be mapped onto a set of Ito SDES (see section A), that are more readily simulated. This is the final goal of using the PPR i.e. being able to derive Ito SDEs that

just as equivalently describe the quantum system, while requiring lesser degrees of freedom. This is clearly advantageous in simulating quantum many-body systems, which are susceptible to the exponential Hilbert space problem. The reader should keep this central theme in mind while reading this chapter.

In section 2.1, we will first review some properties of bosonic coherent states on which the PPR is based on [17]. We have decided not to relegate this to an appendix section for easy access during reading. Readers who are already familiar with bosonic coherent states can skip ahead section 2.2. In section 2.2, we will review Glauber-Sudarshan's P-representation which is the the predecessor of the PPR. There, we explain the pitfalls of the P-representation and why the latter method does not always yield SDEs. This provides the motivation for the PPR where SDEs can always be derived. From section 2.3- 2.4, the technical details of the PPR will be examined thoroughly. Finally, we conclude the chapter by explicitly deriving SDEs for two simple quantum systems, namely the damped harmonic oscillator [29] and the single-mode interferometer [19], in order to make the PPR more lucid. Simulation results for the latter example will be showed as well.

2.1 Review of Coherent states

Before we dive into the details of the PPR, let us review some properties of bosonic coherent states [33] which will be instrumental in our understanding of the method. In this section, we will only cover certain properties of coherent states that are necessary to understand the details of the PPR. We would like to point out however, that there are many more properties [29] that have been omitted (for brevity) but this by no means implies that they are in general unimportant.

1. A coherent state is a quantum mechanical state that is labeled by a complex number, $\alpha \in \mathbb{C}$ so that every point in the complex plane represents a unique coherent state [1]. The mathematical definition of a normalized coherent state has the following equivalent forms:

$$|\alpha\rangle = e^{-\frac{1}{2}\alpha^*\alpha} e^{\alpha\hat{a}^\dagger}|0\rangle, \tag{2.1.1}$$

which tells us that it can be generated by the action of the annihilation operator $\hat{a}^\dagger$ on the vacuum state $|0\rangle$ or alternatively:

$$|\alpha\rangle = e^{-\frac{1}{2}\alpha^*\alpha} \sum_{n=0}^{\infty} \frac{\alpha^n}{\sqrt{n!}}|n\rangle, \quad n = 0, 1, 2, \ldots, \tag{2.1.2}$$

which expresses it as a superposition of Fock or number states:

2. It is interesting to note that coherent states are often described as the "most classical" quantum mechanical states as they are minimum uncertainty states. What we mean by this is that they minimize the Heisenberg uncertainty product, i.e.

[1] This is analogous to a continuous position state where every point on the real line represents a position basis state.

$$\langle \Delta\hat{x} \rangle \langle \Delta\hat{p} \rangle = \frac{\hbar}{2}, \tag{2.1.3}$$

where expectation values are taken with respect to $|\alpha\rangle$ and the position operator, $\hat{x}$ and momentum operator $\hat{p}$ take the usual definitions:

$$\hat{x} = \sqrt{\frac{\hbar}{2m\omega}} \left(\hat{a} + \hat{a}^\dagger \right) \tag{2.1.4}$$

and

$$\hat{p} = i\sqrt{\frac{2m\omega}{\hbar}} \left(\hat{a} - \hat{a}^\dagger \right). \tag{2.1.5}$$

3. A Coherent state is the eigenfunction of the destruction operator

$$\hat{a}|\alpha\rangle = \alpha|\alpha\rangle, \quad \langle\alpha|\hat{a}^\dagger = \langle\alpha|\alpha^*, \tag{2.1.6}$$

with a complex eigenvalue $\alpha \in \mathbb{C}$.

4. The set of Coherent states are non-orthogonal, which implies that there is a redundancy and we do not need every single Coherent state in the complex plane to form a complete basis. Using eq. 2.1.2, the overlap of two states $|\alpha\rangle$ and $|\beta\rangle$ can be calculated to be

$$\langle\alpha|\beta\rangle = e^{-\frac{1}{2}|\alpha^2|} e^{-\frac{1}{2}|\beta^2|} e^{\alpha^*\beta} \tag{2.1.7}$$

or

$$|\langle\alpha|\beta\rangle|^2 = e^{|\alpha|^2} e^{|\beta|^2} e^{\alpha^*\beta} e^{\alpha\beta^*} = e^{-|\alpha-\beta|^2}, \tag{2.1.8}$$

unlike complete orthogonal basis states. For example, if we work with the position basis $\langle x|x'\rangle = \delta(x - x')$ and every single state on the real line is necessary to span the Hilbert space.

5. The Coherent states are overcomplete and so an integration of all Coherent states over the entire complex plane does not yield the identity, instead:

$$\int d^2\alpha |\alpha\rangle\langle\alpha| = \pi, \tag{2.1.9}$$

which can be seen as a consequence of the property of non-orthogonality in eq. 2.1.7.

6. Using a Coherent state basis, it is possible to express any operator in terms of just diagonal terms i.e. any operator is determined by its expectation value in all Coherent states. We can show this by using eq. 2.1.2 to calculate

$$\langle\alpha|\hat{T}|\alpha\rangle = \sum_{m,n} \langle n|\hat{T}|m\rangle e^{|\alpha|^2} (\alpha^*)^n (\alpha)^m \frac{1}{n!m!}, \tag{2.1.10}$$

which upon simple differentiation with respect to α and α^* gives

$$\langle n|\hat{T}|m\rangle = \sqrt{m!n!}\frac{\partial^n}{\partial\alpha^{*n}}\frac{\partial^m}{\partial\alpha^m}(e^{\alpha\alpha^*}\langle\alpha|\hat{T}|\alpha\rangle). \tag{2.1.11}$$

Thus the matrix elements of any operator, $\hat{T}$ can be expressed in terms of the diagonal elements of $\hat{T}$ in the Coherent state basis.

2.2 Glauber-Sudarshan's P-representation

The P-representation can be thought of as the predecessor of the PPR and was originally developed in 1963 by 2005 Nobel Prize winner, Roy J. Glauber[2] [33, 34]. It is therefore worthwhile to spend some time on it as the ideas presented are very analogous to the PPR.

In describing quantum systems, what we are interested in particular, is the density operator, $\hat{\rho}$ as it contains all the necessary information about the system. According to property 6 in section 2.1, the diagonal matrix elements of any operator in a Coherent state basis, are all we need to span the operator. Using this property then, we can simply expand $\hat{\rho}$ in terms of a sum of diagonal matrix elements using some distribution function $P(\alpha,\alpha^*)$:

$$\hat{\rho} = \int d^2\alpha|\alpha\rangle\langle\alpha|P(\alpha,\alpha^*). \tag{2.2.1}$$

This representation of $\hat{\rho}$ is known as the Glauber-Sudarshan P-representation. The benefit in using the P-representation is in calculating expectation values of normal-ordered operators as they take the trivial form:

$$\begin{aligned}\langle\hat{a}^{\dagger p}\hat{a}^q\rangle &\equiv tr(\rho\hat{a}^{\dagger p}\hat{a}^q)\\ &= tr\left(\int d^2\alpha|\alpha\rangle\langle\alpha|P(\alpha,\alpha^*)\hat{a}^{\dagger p}\hat{a}^q\right)\\ &= \int d^2\alpha P(\alpha,\alpha^*)\langle\alpha|\hat{a}^{\dagger p}\hat{a}^q|\alpha\rangle\\ &= \int d^2\alpha P(\alpha,\alpha^*)\alpha^{*p}\alpha^q,\end{aligned} \tag{2.2.2}$$

which makes it tempting to interpret $P(\alpha,\alpha^*)$ as a probability distribution function, i.e. $P(\alpha) = \langle\alpha|\hat{\rho}|\alpha\rangle$ being the probability of the system occupying the state $|\alpha\rangle$. Furthermore, $P(\alpha,\alpha^*)$ is normalized as well:

[2]The nobel prize was attributed to his contribution to the quantum theory of optical coherence

$$\begin{aligned}\int d^2\alpha P(\alpha,\alpha^*) &= \int d^2\alpha \langle\alpha|\alpha\rangle P(\alpha) \\ &= tr\left(\int d^2\alpha |\alpha\rangle\langle\alpha| P(\alpha)\right) \\ &= tr(\hat{\rho}) \\ &= 1, \end{aligned} \tag{2.2.3}$$

where we used the normalization of the trace of $\hat{\rho}$. However, this interpretation must be made with reservation. Because of the overcompleteness of the Coherent states, $P(\alpha,\alpha^*)$ is not unique. It is therefore not strictly positive and may even take on negative values, in which case, it would be incorrect to interpret it as a probability distribution function. In fact, if we were to calculate $\langle\alpha|\hat{\rho}|\alpha\rangle$ explicitly, we see that:

$$\langle\alpha|\hat{\rho}|\alpha\rangle = \int d^2\lambda e^{-|\lambda-\alpha|^2} P(\lambda) \tag{2.2.4}$$

which implies that $P(\alpha,\alpha^*)$ is not the probability of being in a Coherent state $|\alpha\rangle$ contrary to our intuition (since $e^{-|\lambda-\alpha|^2}$ is not equal to a delta function: $\delta(\lambda-\alpha)$). The P-representation therefore may prevent us from having a classical statistical interpretation of quantum mechanics as seen in eq. 2.2.2, which is the central theme of quantum phase space methods.

2.3 The positive-P representation

In 1980 however, Drummond and Gardiner [16] formulated the positive-P representation of the density operator which circumvents the problems associated with the P-representation. Broadly speaking, they expanded the density operator in terms of off-diagonal elements using the Coherent state basis, effectively doubling the phase space involved, i.e.:

$$\hat{\rho} = \int d^2\alpha d^2\alpha^+ \frac{|\alpha\rangle\langle(\alpha^+)^*|}{\langle(\alpha^+)^*|\alpha\rangle} P(\alpha,\alpha^+) = \int d^2\alpha d^2\alpha^+ \hat{\Lambda}(\alpha,\alpha^+) P(\alpha,\alpha^+), \tag{2.3.1}$$

where $\hat{\Lambda}(\alpha,\alpha^+) = \frac{|\alpha\rangle\langle(\alpha^+)^*|}{\langle(\alpha^+)^*|\alpha\rangle}$ is called the projection operator. While previously in the P-representation we integrated over one complex variable α, in the positive-P representation we integrate over two independent complex variables, α and α^+. The upshot of this is that as long as a distribution for the P-representations exists, a corresponding distribution given by

$$P(\alpha,\alpha^+) = \frac{1}{4\pi^2} e^{-|\alpha-\alpha^{+*}|^2/4} \langle \frac{(\alpha+(\alpha^+)^*)}{2} |\hat{\rho}| \frac{(\alpha+(\alpha^+)^*)}{2} \rangle, \tag{2.3.2}$$

does as well [16], where $P(\alpha,\alpha^+)$ is real and positive by definition (since $\hat{\rho}$ is a positive-definite operator) and can therefore be interpreted as a probability distribution[3]. This doubling of phase space requires that normalization is now given by

[3] A proof of this can be found in [16] but we will simply state it here

$$\begin{aligned} \int P(\alpha,\alpha^+)d^2\alpha d^2\alpha^+ &= tr(\hat{\rho}) \\ &= 1 \end{aligned} \tag{2.3.3}$$

instead. Also, the expression for the expectation value of normal-ordered operators is slightly modified with the replacement $\alpha^* \to \alpha^+$ in eq. 2.2.2, i.e.:

$$\begin{aligned} \langle \hat{a}^{\dagger p}\hat{a}^q \rangle &\equiv tr(\hat{\rho}\hat{a}^{\dagger p}\hat{a}^q) \\ &= \int d^2\alpha d^2\alpha^+ P(\alpha,\alpha^+)(\alpha^+)^p\alpha^q, \end{aligned} \tag{2.3.4}$$

and we see that just by doubling the phase space, we obtain a quantum phase space method that allows us to calculate the expectation values of normal-ordered operators, in an analogous fashion to calculating averages of α and α^+ statistically, using a probability distribution function $P(\alpha,\alpha^+)$.

2.3.1 Master equation to Fokker-Planck equation

The usefulness of the PPR is in calculating the dynamics of a quantum mechanical system, which is equivalent to solving for the dynamics of the density operator, $\hat{\rho}$. In general, it is possible to solve for two kinds of dynamics, either in real-time or imaginary-time (as long as an equation of motion for the latter exists). But for this thesis, we will focus our discussion on real time dynamics only. The equation of motion for $\hat{\rho}$ of a closed system in real time is given by Heisenberg's equation of motion:

$$\frac{d}{dt}\hat{\rho} = -\frac{i}{\hbar}\left[\hat{H},\hat{\rho}\right], \tag{2.3.5}$$

and we will show how it is possible to obtain an FPE by using the PPR. This is done by substituting eq. 2.3.1 into eq. 2.3.5 to obtain:

$$\begin{aligned} \int \frac{\partial}{\partial t}P(\alpha,\alpha^+)\hat{\Lambda}(\alpha,\alpha^+)d^2\alpha d^2\alpha^+ &= -\frac{i}{\hbar}\int P(\alpha,\alpha^+)\Big[\hat{H}(\hat{a},\hat{a}^\dagger)\hat{\Lambda}(\alpha,\alpha^+) \\ &\quad -\hat{\Lambda}(\alpha,\alpha^+)\hat{H}(\hat{a},\hat{a^\dagger})\Big]d^2\alpha d^2\alpha^+, \end{aligned} \tag{2.3.6}$$

which is an operator equation that is usually difficult to solve exactly. We have also made the additional assumption that our Hamiltonian: $\hat{H}(\hat{a},\hat{a}^\dagger)$ consists of bosonic annihilation and creation operators, which is common in quantum optics systems. For the case that this assumption holds, there exist correspondence relations which will allow us to write the master equation in terms of a partial differential equation for α and α^+ in place of an operator equation for a and $\hat{a}^\dagger$.

In general, the master equation will contain combinations of $\hat{a}$ and $\hat{a}^\dagger$ on the left hand side (LHS) and right hand side (RHS) of the projection operator: $\hat{\Lambda}(\alpha,\beta)$ and we can in fact

replace them with algebraic operations. The two straightforward correspondence relations are given by the of action $\hat{a}$ and $\hat{a}^\dagger$ on the LHS and RHS of $\hat{\Lambda}(\alpha, \alpha^+)$ respectively:

$$\begin{aligned} \hat{a}\hat{\Lambda} &= \frac{(\hat{a}|\alpha\rangle)\langle\alpha^{+*}|}{\langle\alpha^{+*}|\alpha\rangle} \\ &= \alpha\hat{\Lambda} \end{aligned} \tag{2.3.7}$$

and

$$\begin{aligned} \hat{\Lambda}\hat{a}^\dagger &= \frac{|\alpha\rangle\langle(\alpha^{+*}|\hat{a}^\dagger)}{\langle\alpha^{+*}|\alpha\rangle} \\ &= \alpha^+\hat{\Lambda}, \end{aligned} \tag{2.3.8}$$

which can be seen from a direct application of eq. 2.1.6. We can therefore replace $\hat{a}$ and $\hat{a}^\dagger$ by complex phase space variables α and α^+ if they act on the LHS and RHS of $\hat{\Lambda}(\alpha, \alpha^+)$ respectively. If this were not the case however, i.e. $\hat{\Lambda}(\alpha, \alpha^+)\hat{a}$ and $\hat{a}^\dagger\hat{\Lambda}(\alpha, \alpha^+)$ then things are a little less straightforward. To derive the correspondence relations for the latter case, we will take our expression for $\hat{\Lambda}$ and use eq. 2.1.1 and the overlap relation in eq. 2.1.7 to write it explicitly as:

$$\begin{aligned} \hat{\Lambda}(\alpha, \alpha^+) &= \frac{|\alpha\rangle|\langle\alpha^{+*}|}{\langle\alpha^{+*}|\alpha\rangle} \\ &= e^{(\alpha\hat{a}^\dagger - \alpha\alpha^+)}|0\rangle\langle 0|e^{\alpha^+\hat{a}}. \end{aligned} \tag{2.3.9}$$

We then differentiate eq. 2.3.9 with respect to α

$$\begin{aligned} \frac{\partial}{\partial\alpha}\hat{\Lambda} &= \frac{\partial}{\partial\alpha}(e^{(\alpha\hat{a}^\dagger - \alpha\alpha^+)})|0\rangle\langle 0|e^{\alpha^+\hat{a}} \\ &= (\hat{a}^\dagger - \alpha^+)\hat{\Lambda}(\alpha, \alpha^+), \end{aligned} \tag{2.3.10}$$

and carry out a simple rearrangement to get

$$\hat{a}^\dagger\hat{\Lambda} = (\alpha^+ + \frac{\partial}{\partial\alpha})\hat{\Lambda}. \tag{2.3.11}$$

On the other hand, by taking the derivative with respect to α^+ and rearranging we get:

$$\hat{\Lambda}\hat{a} = (\alpha + \frac{\partial}{\partial\alpha^+})\hat{\Lambda}. \tag{2.3.12}$$

To summarize then, the correspondence relations for the positive-P representation are:

$$\begin{aligned} \hat{\Lambda}\hat{a}^\dagger &= \alpha^+\hat{\Lambda}. \\ \hat{a}\hat{\Lambda} &= \alpha\hat{\Lambda}. \\ \hat{a}^\dagger\hat{\Lambda} &= (\alpha^+ + \frac{\partial}{\partial\alpha})\hat{\Lambda} \\ \hat{\Lambda}\hat{a} &= (\alpha + \frac{\partial}{\partial\alpha^+})\hat{\Lambda}. \end{aligned} \tag{2.3.13}$$

which can be thought of as its signature.

2.3.2 Fokker-Planck equation to stochastic differential equations

If were to substitute the correspondence relations. 2.3.13 into the Master equation in eq. 2.3.5, it is generally possible to convert the latter to the form:

$$\begin{aligned}\frac{\partial\hat{\rho}}{\partial t} &= \int\int \hat{\Lambda}(\alpha,\alpha^+)\frac{\partial P(\alpha,\alpha^+)}{\partial t}d^2\alpha d^2\alpha^+ \\ &= \int\int P(\alpha,\alpha^+)\left\{(A^\mu(\boldsymbol{\alpha})\frac{\partial}{\partial\alpha^\mu}+\frac{1}{2}D^{\mu\nu}(\boldsymbol{\alpha})\frac{\partial}{\partial\alpha^\mu}\frac{\partial}{\partial\alpha^\nu})\hat{\Lambda}(\boldsymbol{\alpha})\right\}d^2\alpha d^2\alpha^+, \quad (2.3.14)\end{aligned}$$

where in the simple case of a single mode system described by $\hat{a}$, we denote $\alpha^0 = \alpha, \alpha^1 = \alpha^+$. In other words, $\vec{\alpha}^i$ is used to specify both α and α^+. Already, this is reminiscent of a Fokker-Planck equation (FPE) (see section A.2) and we can intuitively identify the first term $A(\alpha,\alpha^+)$ as the drift vector and the second term: $D(\alpha,\alpha^+)$ as the diffusion matrix[4]. The next key step is an integration by parts of eq. 2.3.14 with the assumption that boundary terms vanish. Let us just focus on the drift term for which an integration by parts yields:

$$\begin{aligned}\int\int P(\alpha,\alpha^+)A^\mu(\alpha,\alpha^+)\frac{\partial}{\partial\alpha^\mu}\hat{\Lambda}(\alpha,\alpha^+)d^2\alpha d^2\alpha^+ &= \int d^2\alpha^+\Big[P(\alpha,\alpha^+)A^0(\alpha,\alpha^+) \quad (2.3.15)\\ \hat{\Lambda}(\alpha,\alpha^+)\Big]\,|_{\alpha=boundaries} &+ \int d^2\alpha\left[P(\alpha,\alpha^+)A^1(\alpha,\alpha^+)\hat{\Lambda}(\alpha,\alpha^+)\right]|_{\alpha^+=boundaries}\\ &- \int\int \hat{\Lambda}(\alpha,\alpha^+)\frac{\partial}{\partial\alpha^\mu}\left[A^\mu P(\alpha,\alpha^+)\right]d^2\alpha d^2\alpha^+.\end{aligned}$$

If we have an unbounded phase space, then the first two terms are evaluated at the regions $\alpha,\alpha^+\to\infty$. We assume that these terms vanish at the boundaries[5], which is true when we have a distribution function that decays much more rapidly than the growth of the term $A^\mu(\alpha,\alpha^+)\hat{\Lambda}(\alpha,\alpha^+)$ as $\alpha,\alpha^+\to\infty$. The effect of integrating by parts then is the introduction of a negative sign to the drift term and a transfer of derivatives away from the projection operator $\hat{\Lambda}(\alpha,\alpha^+)$, i.e.:

$$\int\int P(\alpha,\alpha^+)A^\mu(\alpha,\alpha^+)\frac{\partial}{\partial\alpha^\mu}\hat{\Lambda}(\alpha,\alpha^+)d^2\alpha d^2\alpha^+ = -\int\int \hat{\Lambda}(\alpha,\alpha^+)\frac{\partial}{\partial\alpha^\mu}\left[A^\mu P(\alpha,\alpha^+)\right]d^2\alpha d^2\alpha^+. \quad (2.3.16)$$

If we repeat this process for the diffusion term, then we see that there is no change in sign since we integrate by parts twice. However, the derivatives will also be removed from $\hat{\Lambda}(\alpha,\alpha^+)$ and transferred to the remaining terms: $D^{\mu\nu}P(\boldsymbol{\alpha})$. The final result is eq. 2.3.14 being converted to:

[4] We will see later that this does indeed correspond to the drift and diffusion terms of an FPE

[5] We will refer to these as boundary terms

$$\int\int \hat{\Lambda}(\alpha,\alpha^+)\frac{\partial P(\alpha,\alpha^+)}{\partial t}d^2\alpha d^2\alpha^+ = \int\int \hat{\Lambda}(\alpha,\alpha^+)\left\{-\frac{\partial}{\partial\alpha^\mu}A^\mu(\alpha,\alpha^+)+ \frac{1}{2}\frac{\partial}{\partial\alpha^\mu}\frac{\partial}{\partial\alpha^\nu}D^{\mu\nu}(\boldsymbol{\alpha})\right\}P(\boldsymbol{\alpha})d^2\alpha d^2\alpha^+$$

from which we can tell that at least one solution that exists is given by:

$$\frac{\partial P(\alpha,\alpha^+)}{\partial t} = \left[-\frac{\partial}{\partial\alpha^\mu}A^\mu(\alpha,\alpha^+)+\frac{1}{2}\frac{\partial}{\partial\alpha^\mu}\frac{\partial}{\partial\alpha^\nu}D^{\mu\nu}(\alpha,\alpha^+)\right]P(\alpha,\alpha^+). \tag{2.3.17}$$

Eq. 2.3.17 has the exact form of the Fokker-Planck equation (FPE) (see eq. A.1.1), which by definition is the equation of motion for a probability distribution function. Since we have established that $P(\alpha,\alpha^+)$ in section 2.3 does have the properties of probability distribution then this interpretation is valid as long as $\mathbf{D}$ is symmetric and positive semi-definite. The symmetricality of $\mathbf{D}$ depends on the form of the master equation whereas its positive semi-definiteness is automatically guaranteed by use of the PPR as will be shown in section 2.3.3.

Solving the FPE analytically at this point is in general a difficult task and in fact only feasible for a few special cases [35]. It is however possible to instead map the dynamics of an FPE onto a set of Ito Stochastic differential equations (SDEs) [18] that are in general easier to simulate. The equivalent SDEs that describe the evolution of our phase space variables are given by (see Appendix A):

$$d\alpha^\mu = A^\mu(\alpha,\alpha^+)dt + B^{\mu\nu}(\alpha,\alpha^+)dW^\nu(t) \tag{2.3.18}$$

where $\mathbf{B}$ is called the noise matrix and is related to the diffusion matrix via the following factorization:

$$\mathbf{D}(\alpha,\alpha^+) = \mathbf{B}(\alpha,\alpha^+)\mathbf{B}^T(\alpha,\alpha^+). \tag{2.3.19}$$

The condition imposed by eq. 2.3.19 grants us the freedom in constructing a noise matrix with a variable second dimension, N_w. Thus if $\mathbf{D}$ is an $N\times N$ matrix then $\mathbf{B}$ has dimensions: $N\times N_w$. Since in eq. 2.3.18, $\mu = 1\ldots 2N$ and $\nu = 1\ldots N_w$, this in turn may result in more or less independent Wiener increments than the dimensionality of the system, N. The terms $dW^\nu(t)$ where $\nu = 1\ldots N_w$ are independent Wiener increments or white noise terms with the statistical properties that

$$\begin{aligned}\langle dW^\mu(t)\rangle &= 0\\ \langle dW^\mu(t)dW^\nu(t')\rangle &= \delta_{\mu\nu}\delta(t-t')dt.\end{aligned} \tag{2.3.20}$$

and can be easily sampled using a gaussian distribution with mean 0 and variance 1, i.e. $\sim N(0,1)$ via the relation

$$dW^\mu(t) \sim \sqrt{dt}N(0,1). \tag{2.3.21}$$

Noise matrix factorization

In general for non-diagonal diffusion matrices, finding the noise matrix $\mathbf{B}$ that satisfies eq. 2.3.19 is not an easy task if we do not have a purely diagonal diffusion matrix, especially so for the multidimensional case. There are two ways to go about this. The first way utilizes the symmetry of $\mathbf{D}$, i.e. since

$$\mathbf{D} = \mathbf{D}^T = \mathbf{B}\mathbf{B}^T \tag{2.3.22}$$

then we can write

$$\mathbf{D} = \mathbf{B}^2 \tag{2.3.23}$$

and a straightforward decomposition is given by the square root of the diffusion matrix:

$$\mathbf{B} = \sqrt{\mathbf{D}}, \tag{2.3.24}$$

which can be carried out using common symbolic manipulation software such as *Maple* or *Mathematica*. While this is a straightforward means of calculating the noise matrix, it generally yields matrices with complicated expressions that makes calculating Stratonovich correction terms[6] a potentially difficult task.

The other method of factorization makes use of the ambiguity of second dimension of $\mathbf{B}$. Note that since $\mathbf{D}$ is an $N \times N$ matrix then any noise matrix of dimension $N \times N_w$, will preserve the dimensionality of $\mathbf{D}$. With that being said, it is possible to break up $\mathbf{D}$ into N_c constituents such that:

$$\mathbf{D} = \sum_{i=1}^{N_c} \mathbf{D}^{(\mathbf{i})}. \tag{2.3.25}$$

Of course, one should be strategic in choosing these constituents so that factorizing each $\mathbf{D}^{(i)}$ is a considerably easier task. Mathematically this means finding an $N \times N_w^i$ matrix, $\mathbf{B}^{(\mathbf{i})}$ so that $\mathbf{D}^{(\mathbf{i})} = \mathbf{B}^{(\mathbf{i})}\mathbf{B}^{(\mathbf{i})\mathbf{T}}$. Using this strategy then, the total noise matrix is obviously given by

$$\mathbf{B} = \left[\mathbf{B}^1\mathbf{B}^2 \ldots\ldots \mathbf{B}^{N_c}\right] \tag{2.3.26}$$

since

[6] We will see why this is important later on.

$$\begin{aligned}
\mathbf{B}\mathbf{B}^{\mathrm{T}} &= \left[\mathbf{B}^{(1)}\mathbf{B}^{(2)}\cdots+\mathbf{B}^{(\mathrm{N_c})}\right]\begin{bmatrix}\mathbf{B}^{(1)\mathrm{T}}\\ \mathbf{B}^{(2)\mathrm{T}}\\ \vdots\\ \vdots\\ \mathbf{B}^{(\mathrm{N_c})\mathrm{T}}\end{bmatrix}\\
&= \mathbf{B}^{(1)}\mathbf{B}^{(1)\mathrm{T}}+\mathbf{B}^{(2)}\mathbf{B}^{(2)\mathrm{T}}+\cdots+\mathbf{B}^{(\mathrm{N_c})}\mathbf{B}^{(\mathrm{N_c})\mathrm{T}}\\
&= \mathbf{D}^{(1)}+\mathbf{D}^{(2)}+\cdots+\mathbf{D}^{(\mathrm{N_c})}\\
&= \mathbf{D} \qquad (2.3.27)
\end{aligned}$$

as required. The benefit of using the square root factorization is that we only require N noise terms (recall eq. 2.3.18), at the cost of a (usually) much more complicated expression for the noise matrix. On the other hand, using the latter trick we end up introducing $\sum_i N_w^{(i)}$ noise terms which may be more than N. This increases the stochasticity of the simulations and may result in larger sampling errors.

2.3.3 Positive-definite Diffusion matrix

As mentioned in section 2.3.2, it is essential for the diffusion matrix to be positive semi-definite [16] in order to interpret eq. 2.3.17 as an FPE. Only then is it possible to obtain equivalent Ito SDEs, and we will now show that the doubling of the phase space guarantees this automatically.

Assuming the factorization of $\mathbf{D}(\boldsymbol{\alpha})$[7] exists:

$$D(\boldsymbol{\alpha}) = B(\boldsymbol{\alpha})B^T(\boldsymbol{\alpha}), \qquad (2.3.28)$$

we can separate the drift vector and noise matrix into its real and imaginary parts explicitly

$$\begin{aligned}
A(\boldsymbol{\alpha}) &= A_x(\boldsymbol{\alpha}) + iA_y(\boldsymbol{\alpha}) \qquad (2.3.29)\\
B(\boldsymbol{\alpha}) &= B_x(\boldsymbol{\alpha}) + iB_y(\boldsymbol{\alpha}) \qquad (2.3.30)
\end{aligned}$$

where A_x, A_y, B_x, B_y are real. We then make use of the analyticity of $\hat{\Lambda}(\alpha, \alpha^+)$ (see eq. 2.3.9)

[7] We will abbreviate (α, α^+) with $\boldsymbol{\alpha}$ where we see fit

to make the replacement (where appropriate) $\frac{\partial}{\partial\alpha^\mu} \leftrightarrow \partial^x_\mu \leftrightarrow -i\partial^y_\mu$ in eq. 2.3.17 to get:

$$\begin{aligned}
\int\int d^2\alpha d^2\alpha^+ \hat{\Lambda}(\boldsymbol{\alpha})\frac{\partial P(\boldsymbol{\alpha})}{\partial t} &= \int\int P(\boldsymbol{\alpha})\Big\{(A^\mu_x(\boldsymbol{\alpha}) + iA^\mu_y(\boldsymbol{\alpha}))\partial\alpha^\mu + \frac{1}{2}(B_xB_x^T \\
&\quad + iB_yB_x^T + iB_xB_y^T - B_yB_y^T)^{\mu\nu}(\partial\alpha^\mu\partial\alpha^\nu)\Big\}\hat{\Lambda}(\boldsymbol{\alpha})d^2\alpha d^2\alpha^+ \\
&= \int\int P(\boldsymbol{\alpha})\Big\{(A^\mu_x(\boldsymbol{\alpha})\partial\alpha^\mu + iA^\mu_y(\boldsymbol{\alpha})\partial\alpha^\mu) + \frac{1}{2}((B_xB_y^T)^{\mu\nu}(\partial\alpha^\mu\partial\alpha^\nu) \\
&\quad + i(B_yB_x^T)^{\mu\nu}(\partial\alpha^\mu\partial\alpha^\nu) + i(B_xB_y^T)^{\mu\nu}(\partial\alpha^\mu\partial\alpha^\nu) \\
&\quad - (B_yB_y^T)^{\mu\nu}(\partial\alpha^\mu\partial\alpha^\nu)\Big\}\hat{\Lambda}(\boldsymbol{\alpha})d^2\alpha d^2\alpha^+ \\
&= \int\int P(\boldsymbol{\alpha})\Big\{(A^\mu_x(\boldsymbol{\alpha})\partial^x_\mu + iA^\mu_y(\boldsymbol{\alpha})(-i\partial^y_\mu)) + \frac{1}{2}((B_xB_x^T)^{\mu\nu}(\partial^x_\mu)(\partial^x_\mu) \\
&\quad + i(B_yB_x^T)^{\mu\nu}(-i\partial^\mu_y)(\partial^\nu_x) + i(B_xB_y^T)^{\mu\nu}(\partial^\mu_x)(-i\partial^\nu_y) \\
&\quad - (B_yB_y^T)^{\mu\nu}(-i\partial^y_\mu)(-i\partial^y_\mu))\Big\}\hat{\Lambda}(\boldsymbol{\alpha})d^2\alpha d^2\alpha^+ \\
&= \int\int P(\boldsymbol{\alpha})\Big\{A^\mu_x(\boldsymbol{\alpha})\partial^x_\mu + A^\mu_y(\boldsymbol{\alpha})\partial^y_\mu + \frac{1}{2}\Big[B^{\mu\sigma}_xB^{\nu\sigma}_x\partial^x_\mu\partial^x_\nu \qquad (2.3.31) \\
&\quad + B^{\mu\sigma}_yB^{\nu\sigma}_y\partial^y_\mu\partial^y_\nu + B^{\mu\sigma}_xB^{\nu\sigma}_y\partial^x_\mu\partial^y_\nu + B^{\mu\sigma}_yB^{\nu\sigma}_x\partial^y_\mu\partial^x_\nu\Big]\Big\}\hat{\Lambda}(\boldsymbol{\alpha})d^2\alpha d^2\alpha^+. \\
&= \int\int P(\boldsymbol{\alpha})\Big\{A^\mu_x(\boldsymbol{\alpha})\partial^x_\mu + A^\mu_y(\boldsymbol{\alpha})\partial^y_\mu + \frac{1}{2}\Big[B^{\mu\sigma}_xB^{\nu\sigma}_x\partial^x_\mu\partial^x_\nu \\
&\quad + B^{\mu\sigma}_yB^{\nu\sigma}_y\partial^y_\mu\partial^y_\nu + 2B^{\mu\sigma}_xB^{\nu\sigma}_y\partial^x_\mu\partial^y_\nu\Big]\Big\}\hat{\Lambda}(\boldsymbol{\alpha})d^2\alpha d^2\alpha^+. \qquad (2.3.32)
\end{aligned}$$

Integrating by parts and removing surface terms yields the following Fokker-Planck equation:

$$\begin{aligned}
\frac{\partial P(\boldsymbol{\alpha})}{\partial t} &= \Big[-\partial^x_\mu A^x_\mu(\boldsymbol{\alpha}) - \partial^y_\mu A^\mu_y(\boldsymbol{\alpha}) + \frac{1}{2}\Big\{\partial^x_\mu\partial^x_\nu B^{\mu\sigma}_xB^{\nu\sigma}_x + 2\partial^x_\mu\partial^y_\nu B^{\mu\sigma}_xB^{\nu\sigma}_y \\
&\quad + \partial^y_\mu\partial^y_\nu B^{\mu\sigma}_yB^{\nu\sigma}_y\Big\}\Big]P(\boldsymbol{\alpha}). \qquad (2.3.33)
\end{aligned}$$

Now in this form, the Fokker-Planck equation possesses a positive semi-definite diffusion matrix in a four dimensional space whose vectors are

$$(\alpha^{(1)}_x, \alpha^{(2)}_x, \alpha^{(1)}_y, \alpha^{(2)}_y) \equiv (\alpha_x, \alpha^+_x, \alpha_y, \alpha^+_y) \qquad (2.3.34)$$

with drift vector

$$\vec{A}(\boldsymbol{\alpha}) \equiv (A^{(1)}_x(\boldsymbol{\alpha}), A^{(2)}_x(\boldsymbol{\alpha}), A^{(1)}_y(\boldsymbol{\alpha}), A^{(2)}_y(\boldsymbol{\alpha})) \qquad (2.3.35)$$

and diffusion matrix

$$\mathbf{D}(\boldsymbol{\alpha}) = \begin{bmatrix} \mathbf{B_x}.\mathbf{B_x^T} & \mathbf{B_x}.\mathbf{B_y^T} \\ \mathbf{B_y}.\mathbf{B_x^T} & \mathbf{B_y}.\mathbf{B_y^T} \end{bmatrix}(\boldsymbol{\alpha}) \equiv \mathbf{B}(\boldsymbol{\alpha})\mathbf{B}^T(\boldsymbol{\alpha}).$$

In this form, $\mathbf{D}(\boldsymbol{\alpha})$ is explicitly positive semidefinite[8] which is exactly what we wanted to show, as long as we identify:

$$\mathbf{B}(\boldsymbol{\alpha}) \equiv \begin{bmatrix} \mathbf{B_x} & 0 \\ \mathbf{B_y} & 0 \end{bmatrix} (\boldsymbol{\alpha}).$$

The corresponding Ito stochastic differential equations can then be written as :

$$\frac{\partial}{\partial t}\begin{pmatrix} \alpha_x \\ \alpha_y \end{pmatrix} = \begin{pmatrix} A_x(\boldsymbol{\alpha}) \\ A_y(\boldsymbol{\alpha}) \end{pmatrix} + \begin{pmatrix} B_x(\boldsymbol{\alpha}).\xi(t) \\ B_y(\boldsymbol{\alpha}).\xi(t) \end{pmatrix}$$

or in its more compact form

$$\frac{\partial \boldsymbol{\alpha}}{\partial t} = \vec{A}(\boldsymbol{\alpha}) + \mathbf{B}(\boldsymbol{\alpha}).\xi(t), \tag{2.3.36}$$

where $\alpha_x^{(1)} = \alpha_x^{(1)} + i\alpha_y^{(1)} = \alpha_x + i\alpha_y$ and $\alpha_x^{(2)} = \alpha_x^{(2)} + i\alpha_y^{(2)} = \alpha_x^+ + i\alpha_y^+$.

2.4 Calculation of observables

The advantage of using SDEs is in the relative ease in calculating normal ordered expectation values. As mentioned in section 2.3.2, the calculation of quantum mechanical normal ordered observables is given by the statistical expression in eq. 2.3.4:

$$\langle \hat{a}^{\dagger p} \hat{a}^q \rangle = \int P(\alpha, \alpha^+)(\alpha^+)^p \alpha^q d^2\alpha d^2\alpha^+. \tag{2.4.1}$$

From the correspondence relations in eq. 2.3.13, we see that there is a direct relation between the bosonic operators: $\hat{a}^\dagger$ and $\hat{a}$ with α^+ and α, respectively. It is no surprise then that in the limit of an infinite number of trajectories (n_{traj}), we can get an exact correspondence between the quantum mechanical average and the stochastic average of their respective phase space variable functions, i.e.:

$$\langle \hat{a}^{\dagger p} \hat{a}^q \rangle = \lim_{ntraj \to \infty} \langle\langle (\alpha^+)^p \alpha^q \rangle\rangle, \tag{2.4.2}$$

where

$$\langle\langle (\alpha^+)^p \alpha^q \rangle\rangle = \sum_{i=1}^{ntraj} \left[(\alpha^+)_i^p \alpha_i^q \right] \tag{2.4.3}$$

and i labels the individual realization of each trajectory of the phase space function $(\alpha^+)^p \alpha^q$. The dynamics of any normal ordered operator can therefore be monitored by numerically integrating SDEs of the form 2.3.18 and calculating simple stochastic averages. Although the exact correspondence is achieved in the limit that the total number of trajectories tends to infinity, in practice it is usually sufficient to use $\sim 10^4 - 10^7$ trajectories, depending on the nature of the problem.

[8] An $n \times n$ real matrix, M is said to be positive semidefinite if $x^T M x \geq 0$ for all $x \in \mathbb{R}$. One can show that $\mathbf{D}(\boldsymbol{\alpha})$ is positive-semidefinite by showing that $\mathbf{x}^T D \mathbf{x} \geq 0$ for any $\vec{x}$

2.5 Example 1: The damped harmonic oscillator

So far, we have carried out a rather general discussion of the PPR with a focus on the technical details and establishing the proofs of the validity of the formalism. Deriving SDEs is a fairly standard process and can in fact be broken down into the few steps below:

1. Start with a master equation describing the system of interest.
2. Express $\hat{\rho}$ in terms of off-diagonal Coherent state projection operators, $\hat{\Lambda}$.
3. Substitute the correspondence relations in eq. 2.3.13 into the new master equation
4. Integrate by parts once and ignore boundary terms to obtain an FPE
5. Factorize the diffusion matrix.
6. Map FPE on Ito SDEs

Bearing these points in mind, we will now carry out an explicit derivation of the SDEs describing a damped harmonic oscillator [29] with frequency, ω_o. Because this is an open quantum system, the master equation is no longer just given by heisenberg's equation of motion for $\hat{\rho}$. There will be additional terms in the master equation that take into consideration the damping effects caused by the oscillator's interaction with a bosonic heat bath. The master equation is given by [29]

$$\begin{aligned}\frac{d\hat{\rho}}{dt} &= -i\omega_o[\hat{a}^\dagger\hat{a},\hat{\rho}] + \frac{\gamma}{2}(2\hat{a}\hat{\rho}\hat{a}^\dagger - \hat{a}^\dagger\hat{a}\hat{\rho} - \hat{\rho}\hat{a}^\dagger\hat{a}) \\ &\quad +\gamma\bar{n}(\hat{a}\rho\hat{a}^\dagger + \hat{a}^\dagger\hat{\rho}\hat{a} - \hat{a}^\dagger\hat{a}\rho - \hat{\rho}\hat{a}\hat{a}^\dagger), \end{aligned} \tag{2.5.1}$$

where γ is the damping rate and $\bar{n}$ is the average number of particles in the heat bath. Upon substituting the positive-P representation for the density operator, eq. 2.5.1 becomes

$$\begin{aligned}\int\int \hat{\Lambda}(\boldsymbol{\alpha})\frac{\partial P(\boldsymbol{\alpha})}{\partial t}d^2\alpha d^2\alpha^+ &= \int\int \Big\{-i\omega_o(\hat{a}^\dagger\hat{a}\hat{\Lambda} - \hat{a}\hat{a}^\dagger\hat{\Lambda}) + \frac{\gamma}{2}(2\hat{a}\hat{\Lambda}\hat{a}^\dagger - \hat{a}^\dagger\hat{a}\hat{\Lambda} - \hat{\Lambda}\hat{a}^\dagger\hat{a}) \\ &\quad +\gamma\bar{n}(\hat{a}\hat{\Lambda}\hat{a}^\dagger + \hat{a}^\dagger\hat{\Lambda}\hat{a} - \hat{a}^\dagger\hat{a}\hat{\Lambda} - \hat{\Lambda}\hat{a}\hat{a}^\dagger)\Big\} P(\boldsymbol{\alpha})d^2\alpha d^2\alpha^+. \end{aligned} \tag{2.5.2}$$

Now if we recall the correspondence relations for $\hat{\Lambda}$ in eq. 2.3.13, we can show the obvious relations

$$\hat{a}^\dagger\hat{a}\hat{\Lambda} = \alpha\left(\hat{a}^\dagger\hat{\Lambda}\right) = \alpha(\frac{\partial}{\partial\alpha} + \alpha^+)\hat{\Lambda} \tag{2.5.3}$$

$$\hat{\Lambda}\hat{a}^\dagger\hat{a} = \alpha^+\left(\hat{\Lambda}\hat{a}\right) = \alpha^+(\frac{\partial}{\partial\alpha^+} + \alpha)\hat{\Lambda} \tag{2.5.4}$$

$$\hat{a}\hat{\Lambda}\hat{a}^\dagger = \left(\alpha^+ + \frac{\partial}{\partial\alpha}\right)\left(\hat{\Lambda}\hat{a}\right) = (\alpha^+ + \frac{\partial}{\partial\alpha})(\frac{\partial}{\partial\alpha^+} + \alpha)\hat{\Lambda} \tag{2.5.5}$$

and

$$\hat{\Lambda}\hat{a}\hat{a}^\dagger = \left(\frac{\partial}{\partial\alpha^+} + \alpha\right)\left(\hat{\Lambda}\hat{a}^\dagger\right) = \left(\frac{\partial}{\partial\alpha^+} + \alpha\right)\alpha^+\hat{\Lambda}, \tag{2.5.6}$$

which are all the operator combinations that occur in eq. 2.5.1. If we then substitute eq. 2.5.3 to eq. 2.5.6 into eq. 2.3.14, we get the following differential equation:

$$\begin{aligned}
\frac{d\hat{\rho}}{dt} &= \int\int P(\alpha,\alpha^+)\left\{-i\omega_o\left(\alpha(\alpha^+ + \frac{\partial}{\partial\alpha}) - \alpha^+(\alpha + \frac{\partial}{\partial\alpha^+})\right) - \alpha^+(\alpha + \frac{\partial}{\partial\alpha^+})\right) \\
&\quad +\gamma\bar{n}\left(\alpha\alpha^+ + (\alpha^+ + \frac{\partial}{\partial\alpha})(\alpha + \frac{\partial}{\partial\alpha^+}) - \alpha(\alpha^+ + \frac{\partial}{\partial\alpha})\right. \qquad (2.5.7) \\
&\quad \left.-(\alpha + \frac{\partial}{\partial\alpha^+})\alpha^+\right)\Big\}\hat{\Lambda}d^2\alpha d^2\alpha^+ \\
&= \int\int P(\alpha,\alpha^+)\left\{-i\omega_o\left(\alpha\alpha^+ + \alpha\frac{\partial}{\partial\alpha} - \alpha^+\alpha - \alpha^+\frac{\partial}{\partial\alpha^+}\right)\right. \\
&\quad +\frac{\gamma}{2}\left(2\alpha\alpha^+ - \alpha\alpha^+ - \alpha\frac{\partial}{\partial\alpha} - \alpha\alpha^+ - \alpha^+\frac{\partial}{\partial\alpha^+}\right) \qquad (2.5.8) \\
&\quad \gamma\bar{n}\left(\alpha\alpha^+ + \alpha\alpha^+ + \frac{\partial}{\partial\alpha}\alpha + \alpha^+\frac{\partial}{\partial\alpha^+} + \frac{\partial^2}{\partial\alpha\partial\alpha^+} - \alpha\alpha^+ - \alpha\frac{\partial}{\partial\alpha} - \alpha\alpha^+\right. \\
&\quad \left.\left.-\frac{\partial}{\partial\alpha^+}\alpha^+\right)\right\}\hat{\Lambda}d^2\alpha d^2\alpha^+ \\
&= \int\int P(\alpha,\alpha^+)\left\{-i\omega_o\left(\alpha\frac{\partial}{\partial\alpha} - \alpha^+\frac{\partial}{\partial\alpha^+}\right)\right. \qquad (2.5.9) \\
&\quad +\frac{\gamma}{2}\left(-\alpha\frac{\partial}{\partial\alpha} - \alpha^+\frac{\partial}{\partial\alpha^+}\right) + \gamma\bar{n}\left(\alpha\frac{\partial}{\partial\alpha} + 1 + \alpha^+\frac{\partial}{\partial\alpha^+} + \frac{\partial^2}{\partial\alpha\partial\alpha^+} - \alpha\frac{\partial}{\partial\alpha} -\right. \\
&\quad \left.\left.\alpha^+\frac{\partial}{\partial\alpha^+} - 1\right)\right\}\hat{\Lambda}d^2\alpha d^2\alpha^+ \\
&= \int\int P(\alpha,\alpha^+)\left\{(-i\omega_o - \frac{\gamma}{2})\alpha\frac{\partial}{\partial\alpha} + (i\omega_o - \frac{\gamma}{2})\alpha^+\frac{\partial}{\partial\alpha^+}\right] \\
&\quad \left.+\gamma\bar{n}\frac{\partial^2}{\partial\alpha\partial\alpha^+}\right\}d^2\alpha d^2\alpha^+, \qquad (2.5.10)
\end{aligned}$$

which has the form of eq. 2.3.14 before carrying out partial integration. Note that in eq. 2.5.9, we have carried out the differentiation of the terms $\alpha\hat{\Lambda}$ and $\alpha^+\hat{\Lambda}$ in order to transfer all derivatives onto $\hat{\Lambda}$. This is a necessary step so that partial integration of eq. 2.5.10 will transfer all derivatives away from $\hat{\Lambda}$, i.e.

$$\begin{aligned}\int\int \hat{\Lambda}\frac{\partial P(\boldsymbol{\alpha})}{\partial t}d^2\alpha d^2\alpha^+ &= \int\int P(\boldsymbol{\alpha})\left[-(\frac{\gamma}{2}+i\omega_o)\frac{\partial}{\partial\alpha}\alpha-(\frac{\gamma}{2}-i\omega_o)\frac{\partial}{\partial\alpha^+}\alpha^+\right.\\ &\quad\left.+\gamma\bar{n}\frac{\partial^2}{\partial\alpha\partial\alpha^+}\right]\hat{\Lambda}(\boldsymbol{\alpha})d^2\alpha d^2\alpha^+.\\ &= \int\int d\alpha d\alpha^+\hat{\Lambda}(\boldsymbol{\alpha})\left[\frac{\partial}{\partial\alpha}(\frac{\gamma}{2}+i\omega_o)\alpha+\frac{\partial}{\partial\alpha^+}(\frac{\gamma}{2}-i\omega_o)\alpha^+\right.\\ &\quad\left.+\frac{\partial^2}{\partial\alpha\partial\alpha^+}\gamma\bar{n}\right]P(\boldsymbol{\alpha}),\end{aligned} \tag{2.5.11}$$

where *boundary terms* have been removed as in eq. 2.3.17. This gives the final FPE:

$$\frac{\partial P(\boldsymbol{\alpha})}{\partial t}=\left\{(\frac{\gamma}{2}+i\omega_o)\frac{\partial}{\partial\alpha}\alpha+(\frac{\gamma}{2}-i\omega_o)\frac{\partial}{\partial\alpha^+}\alpha^++\frac{1}{2}(\gamma\bar{n}\frac{\partial^2}{\partial\alpha\partial\alpha^+}+\gamma\bar{n}\frac{\partial^2}{\partial\alpha^+\partial\alpha})\right\}P(\boldsymbol{\alpha}). \tag{2.5.12}$$

with an off-diagonal diffusion matrix

$$\mathbf{D}=\begin{bmatrix}0 & \gamma\bar{n}\\ \gamma\bar{n} & 0\end{bmatrix} \tag{2.5.13}$$

that has a trivial noise matrix factorization

$$\mathbf{B}=\sqrt{\frac{\gamma\bar{n}}{2}}\begin{bmatrix}-1 & -i\\ -1 & +i\end{bmatrix}. \tag{2.5.14}$$

This then allows us to write the corresponding SDEs for α and α^+ (see eq. 2.3.18) as a system of linear equations:

$$d\begin{bmatrix}\alpha\\ \alpha^+\end{bmatrix}=\begin{bmatrix}-(\frac{\gamma}{2}+i\omega_o)\alpha\\ -(\frac{\gamma}{2}-i\omega_o)\alpha^+\end{bmatrix}dt+\sqrt{\frac{\gamma\bar{n}}{2}}\begin{bmatrix}-1 & -i\\ -1 & +i\end{bmatrix}\begin{bmatrix}dW_1(t)\\ dW_2(t)\end{bmatrix} \tag{2.5.15}$$

or explicitly as

$$d\alpha = -\left(\frac{\gamma}{2}+i\omega_o\right)\alpha dt-\sqrt{\frac{\gamma\bar{n}}{2}}\left(dW_1(t)+dW_2(t)\right) \tag{2.5.16}$$

$$d\alpha^+ = -\left(\frac{\gamma}{2}-i\omega_o\right)\alpha^+dt-\sqrt{\frac{\gamma\bar{n}}{2}}\left(dW_1(t)-dW_2(t)\right), \tag{2.5.17}$$

where the white noise terms are delta-correlated in the usual sense since $\langle dW_i(t)dW_j(t')\rangle = dt\delta(t-t')\delta_{ij}$ and $\langle dW_i(t)\rangle = 0$.

2.6 Example 2: single-mode interferometer

For the second example, we will derive the SDES for a single mode interferometer [19] and present some results from actual numerical simulations. On a side note, this was our

first exposure to the PPR as we attempted to reproduce the results of [19]. We will not derive the SDEs in a rigorous way as it is simply a repetitive process that has already been carried out in section 2.5. Instead, the key equations will be stated without proof so as not to lengthen this thesis unnecessarily.

The interferometer can be modeled as a harmonic oscillator of frequency ω, damped by linear and non-linear couplings to zero-temperature reservoirs. In the interaction picture, this is described by the master equation

$$\frac{\partial\hat{\rho}}{\partial t} = \frac{\kappa}{2}\left(2\hat{a}^2\hat{\rho}\hat{a}^{\dagger 2} - \hat{a}^{\dagger 2}a^2\hat{\rho} - \rho\hat{a}^{\dagger 2}\hat{a}^2\right) + \frac{1}{2}\kappa\gamma\left(2\hat{a}\hat{\rho}\hat{a}^\dagger - \hat{a}^\dagger\hat{a}\hat{\rho} - \hat{\rho}\hat{a}^\dagger\hat{a}\right), \tag{2.6.1}$$

where κ is the nonlinear decay rate and $\gamma\kappa$ is the linear damping rate. γ therefore describes the ratio between the linear and non-linear damping rates and can be thought of as a measure of nonlinearity. Once again, we will follow the usual prescription and use the positive-P representation of the density operator in eq. 2.3.1 to obtain the following FPE[9]:

$$\begin{aligned}\frac{\partial P(\alpha,\alpha^+)}{\partial t} &= \left[\frac{\partial}{\partial\alpha}\left(\frac{1}{2}\gamma\kappa\alpha + \kappa\alpha^+\alpha^2\right) + \frac{\partial}{\partial\alpha^+}\left(\frac{1}{2}\gamma\kappa\alpha^+ + \kappa\alpha\alpha^{+2}\right)\right.\\ &\quad \left. -\frac{1}{2}\left[\frac{\partial^2}{\partial\alpha^2}\kappa\alpha^2 + \frac{\partial}{\partial\alpha^{+2}}\kappa\alpha^{+2}\right]\right]P(\alpha,\alpha^+).\end{aligned} \tag{2.6.2}$$

The diffusion matrix takes the convenient diagonal form:

$$\mathbf{D} = \begin{bmatrix} -\kappa\alpha^2 & 0 \\ 0 & \kappa\alpha^{+2} \end{bmatrix}, \tag{2.6.3}$$

with the obvious square root factorization

$$\mathbf{B} = \begin{bmatrix} i\sqrt{\kappa}\alpha & 0 \\ 0 & i\sqrt{\kappa}\alpha^+ \end{bmatrix}. \tag{2.6.4}$$

The SDEs that correspond to the Fokker-Planck in eq. 2.6.2 are then given by:

$$d\alpha = -\kappa(\frac{1}{2}\gamma\alpha + \alpha^+\alpha^2)dt + i(\kappa)^{\frac{1}{2}}\alpha dW_1(t), \tag{2.6.5}$$

$$d\alpha^+ = -\kappa(\frac{1}{2}\gamma\alpha^+ + \alpha\alpha^{+2})dt + i(\kappa)^{\frac{1}{2}}\alpha^+ dW_2(t), \tag{2.6.6}$$

where $dW_i(t)$ are Wiener increments. Now for this system, the observable that we are interested in is the average occupation number of the photon modes: $\hat{n} = \hat{a}^\dagger\hat{a}$ which can be represented by the function (of phase space variables) $n(\alpha,\alpha^+) = \alpha\alpha^+$. In accordance with

[9] We will omit the details of the derivation since it is the same as that in section. 2.5)

the rules of Ito calculus, we can derive an SDE for the variable n, i.e.

$$\begin{aligned} dn &= d\alpha\alpha^{+} + d\beta\alpha + d\alpha d\beta \\ &= -\kappa(\frac{1}{2}\gamma\alpha + \beta\alpha^2)\beta dt + i(\kappa)^{\frac{1}{2}}\alpha\beta dW_1(t) \\ &\quad -\kappa(\frac{1}{2}\gamma\beta + \alpha\beta^2)\alpha dt + i(\kappa)^{\frac{1}{2}}\beta\alpha dW_2(t) \\ &= -2\kappa\left(\frac{1}{2}\gamma n + n^2\right)dt + i\sqrt{\kappa}n\left(dW_1(t) + dW_2(t)\right). \end{aligned} \tag{2.6.7}$$

In this example, we are lucky in that the SDE for n decouples nicely so that instead of

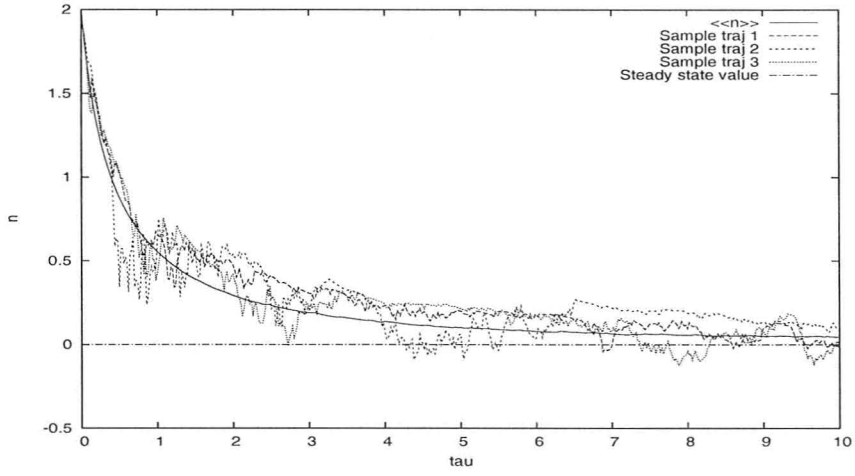

Figure 2.1: Ensemble average of particle number $Re(n)$ vs $\tau = 2\kappa t$ (solid line) using SDE. 2.6.7 and 15000 trials. Simulation parameters: $\gamma = 1.0, dt = 0.02, N_x(0) = 2, N_y(0) = 0$. Three independent stochastic trajectories (non-solid lines) are shown with the steady state value given by the horizontal line at 0.

simulating SDEs for both α and β, we only have to simulate one. This is a luxury that does not usually happen but is not essential, just a matter of convenience. In fact, we could have just as well derived an Ito SDE for n for the damped harmonic oscillator example in section 2.5. However, this would have not resulted in a standalone SDE in n and therefore doing so serves no purpose.

In eq. 2.6.7, terms that arise from multiplying the differentials: $d\alpha d\beta$ scales greater than dt and does not produce significant terms. It would appear that the rules of ordinary calculus are obeyed but we would like to emphasize that this is just a coincidence. In general, the extra $d\alpha d\alpha^{+}$ product may result in additional terms in our Ito SDE and cannot be naively discarded. For instance, if we get terms that $\sim dW_i(t) \propto \sqrt{dt}$ or $\sim dW_i^2(t) \propto dt$ then the latter will modify the original drift terms. For now, we will look at the results obtained from our simulation[10] for the photon number $\langle \hat{n} \rangle$ in fig. 2.1 which plots the stochastic average

[10]Explicit details on the actual numerical algorithm can be found in [19]. The algorithm is unfortunately out-

of $\langle \hat{n} \rangle = \langle\langle \alpha\beta \rangle\rangle$ using 15000 independent trajectories.

In [19], the steady state values when $\gamma < 2$ is given by

$$\langle n(t) \rangle_{SS} = \frac{1-\gamma}{2} \tag{2.6.8}$$

and

$$\langle n(t) \rangle_{SS} = 0. \tag{2.6.9}$$

when $\gamma \geq 2$. We will use these steady state values as a guide that our simulations are producing correct results. In fig. 2.1, we show three different trajectories as well as the ensemble averaged result for the case $\gamma = 1.0$. Taken individually, independent trajectories exhibit wild fluctuations and look different from each other, even though they do produce the expected qualitative behavior. An average of 15000 trajectories however, produces a smooth curve and the correct asymptotic behavior as predicted by eq. 2.6.8. This illustrates the idea of stochastic averaging and how it can be used to calculate quantum mechanical expectation values.

2.7 Generalization of the positive-P representation

Although our discussion carried out so far has been for the single mode case, the PPR can also be generalized to a system with N-modes, taking the form:

$$\hat{\rho} = \int \hat{\Lambda}(\vec{\alpha}, \vec{\alpha}^{+}) P(\vec{\alpha}, \vec{\alpha}^{+}) d^2\vec{\alpha} d^2\vec{\alpha}^{+} \tag{2.7.1}$$

where the generalized off-diagonal Coherent state projection operator is[11]:

$$\hat{\Lambda}(\vec{\alpha}, \vec{\alpha^{+}}) = \prod_{i}^{N} \otimes \frac{|\alpha_i\rangle\langle(\alpha_i^{+})^{*}|}{|(\alpha_i^{+})^{*}\rangle\langle\alpha_i|} \tag{2.7.2}$$

and α_i and α_i^{+} for $i = 1 \ldots N$ are independent complex variables. The quantum mechanics averaged of normal ordered moments are then simply given by an analogous expression:

$$\langle \prod_{i}^{N} (\hat{a_i}^{\dagger})^{p_i} (\hat{a}_i)^{q_i} \rangle = \int P(\vec{\alpha}, \vec{\beta}) \prod_{i}^{N} (\alpha_i)^{p_i} (\alpha_i^{+})^{q_i} d^2\vec{\alpha} d^2\vec{\beta} \tag{2.7.3}$$

which is also equivalent to:

$$\lim_{ntraj \to \infty} \langle\langle \prod_{i}^{N} (\alpha_i)^{p_i} (\alpha_i^{+})^{q_i} . \rangle\rangle \tag{2.7.4}$$

dated and was not used to simulate subsequent examples in this thesis.

[11] where we have change notation from α to α^{+} instead.

So we see that the PPR can be easily generalized to multimode systems and that the number of variables required to simulate the system scales linearly with N. In this respect, exact many-body dynamics is reduced to a tractable one that is not computationally exhaustive.

2.8 Short lifetimes

In principle, the positive-P representation allows us to simulate the exact dynamics of a bosonic system and seems to be a very powerful method. However, there is a notorious problem associated with the method; its short lifetime: t_{life}. This means that beyond $t > t_{life}$, simulations fail to produce correct results. Because we are simulating SDEs, every trajectory is completely random and for sufficiently large times, depending on the nature of the SDEs, there may exist errant trajectories that eventually wander to infinity. The breakdown of the PPR is quite obvious and takes the form of sudden spikes in trajectories. If we do indeed use an infinite number of trajectories to calculate stochastic averages then this would not be a problem. However, since we are in a world with finite computers, this would be impossible and so we are limited to $t < t_{life}$ for useful results. For example, suppose we had a single trajectory that wandered off to an unmanageably large number of 10^{40}, then we would require at least 10^{40} trajectories to neutralize its effect. This type of error is known as sampling errors and is usually what limits the use of the PPR.

Unfortunately, there is no way apriori to know what t_{life} will be or how many trajectories are needed to obtain convergence[12]. The latter usually ranges from $10^4 - 10^7$ depending on the problem and the nature of the SDEs, and has to be determined empirically. The positive-P representation is therefore a method that is particularly useful in simulating systems where the interesting physics occur at short time scales before sampling errors dominate.

This issue of numerical spikes has been first investigated thoroughly in [36] where it was discovered that the cause of divergences was due to the nature of the SDEs itself and not because of an unstable numerical algorithm. This eventually resulted in the development of the gauge-P representation [37] which has been successfully applied in extending t_{life} of systems that would otherwise experience early divergences.

In Deaur's [38] PhD thesis, he has examined in detail the causes of singular trajectories and discovered that divergences occur when nonlinearities arise in either the drift or stochastic parts of an SDE. This is closely linked to the step in our derivation where we ignored boundary terms during partial integration of the FPE. If nonlinearities exist, then it may not be true at all times that boundary terms vanish, in which case we no longer have a direct correspondence with the dynamics of the master equation. However, since this thesis is based on the 'barebones' application of the PPR, we will not go into details of this issue. We will however just state a key result of Deaur's [38] thesis that drift and noise instabilities arise unless the two conditions:

[12] Convergence here implies a lack of change in numerical results even if we increase the number of trajectories.

$$\lim_{|\alpha_j|\to\infty} \frac{A_j}{|\alpha_j|} = 0 \tag{2.8.1}$$

and

$$\lim_{|\alpha_j|\to\infty} \frac{B_{jk}}{|\alpha_j|} = 0, \tag{2.8.2}$$

for all k are satisfied. This simple check will give us a good idea if simulation of our SDEs will be the victim of early peril or not.

Chapter 3

The Schwinger Bosons

As mentioned in chapter 1, we wish to apply the PPR to simulate the quantum quench dynamics of the Heisenberg model:

$$\hat{H} = -\vec{\mathbf{J}} \sum_{\langle i,j \rangle} \hat{\mathbf{S}}_i . \hat{\mathbf{S}}_j, \tag{3.0.1}$$

which describes either a FM ($\vec{J} > 0$) or AFM ($\vec{J} < 0$) material. At first glance however, this does not seem possible since the Heisenberg Hamiltonian in eq. 3.0.1 is expressed in terms of spin operators $\hat{\mathbf{S}}$ whereas the PPR formalism presented in chapter 2 relies solely on bosonic annihilation and creation operators, $\hat{a}$ and $\hat{a}^\dagger$.

$\hat{\mathbf{S}}$ and $\hat{a}$ are very different classes of operators as they obey different commutation relations. The bosonic operators obey the commutation relation

$$\left[\hat{a}, \hat{a}^\dagger\right] = 1, \tag{3.0.2}$$

while the spin operators obey an analogous relation:

$$[\hat{S}^-, \hat{S}^+] = -2\hat{S}^z, \tag{3.0.3}$$

where we define

$$\hat{S}^+ = \hat{S}^x + i\hat{S}^y \tag{3.0.4}$$

$$\hat{S}^- = \hat{S}^x - i\hat{S}^y \tag{3.0.5}$$

as the usual ladder spin operators. In addition to eq. 3.0.3, the other commutation relations that $\hat{\mathbf{S}}$ must preserve are given by:

$$\left[\hat{S}^i, \hat{S}^j\right] = i\epsilon_{ijk}\hat{S}^k, \tag{3.0.6}$$

$$\left[\hat{S}^-, \hat{S}^z\right] = 2\hat{S}^-, \tag{3.0.7}$$

where $\{i, j, k\} = x, y, z$ and

$$\left[\hat{S}^+, \hat{S}^z\right] = 2\hat{S}^+. \tag{3.0.8}$$

What we need then, is a clever way to map the spin operators onto some combination of bosonic creation and annihilation operators so that eq. 3.0.3- 3.0.7 still hold. One way of mapping quantum mechanical spins to bosonic operators is known as *Schwinger representation* [39, 40] with the correspondence given by:

$$\hat{S}^+ \to \hat{b}\hat{a}^\dagger, \hat{S}^- \to \hat{b}^\dagger\hat{a}, \hat{S}^z \to \frac{1}{2}\left(\hat{a}^\dagger\hat{a} - \hat{b}^\dagger\hat{b}\right) \tag{3.0.9}$$

and as required, preserves all the required spin commutation relations:

$$\left[\hat{S}^+, \hat{S}^-\right] \to \left[\hat{a}^\dagger\hat{b}, \hat{b}^\dagger\hat{a}\right] = \hat{a}^\dagger\hat{a} - \hat{a}^\dagger\hat{a} \to 2\hat{S}^z, \tag{3.0.10}$$

$$\left[\hat{S}^-, \hat{S}^z\right] \to \left[\hat{b}^\dagger\hat{a}, \tfrac{1}{2}(\hat{a}^\dagger\hat{a} - \hat{b}^\dagger\hat{b})\right] = 2\hat{b}^\dagger\hat{a} \to 2\hat{S}^-, \tag{3.0.11}$$

$$\left[\hat{S}^+, \hat{S}^z\right] \to \left[\hat{a}^\dagger\hat{b}, \tfrac{1}{2}(\hat{a}^\dagger\hat{a} - \hat{b}^\dagger\hat{b})\right] = 2\hat{a}^\dagger\hat{b} \to 2\hat{S}^+. \tag{3.0.12}$$

This shows that the physics is unchanged if we introduce two kinds of uncoupled bosons $\hat{a}$ and $\hat{b}$ to replace a Heisenberg spin, where by uncoupled we mean that they commute:

$$\left[\hat{a}, \hat{b}^\dagger\right] = \left[\hat{b}, \hat{a}^\dagger\right] = 0. \tag{3.0.13}$$

Since it is trivial to show eq. 3.0.10- 3.0.12, we will just derive the first relation as an exercise, i.e.

$$\begin{aligned}
\left[\hat{S}^+, \hat{S}^-\right] &= \left[\hat{a}^\dagger\hat{b}, \hat{b}^\dagger\hat{a}\right] \\
&= \hat{a}^\dagger\hat{b}\hat{b}^\dagger\hat{a} - \hat{b}^\dagger\hat{a}\hat{a}^\dagger\hat{b} \\
&= \hat{a}^\dagger\hat{a}\left(1 + \hat{b}^\dagger\hat{b}\right) - \left(1 + \hat{a}^\dagger\hat{a}\right)\hat{b}^\dagger\hat{b} \\
&= \left(\hat{a}^\dagger\hat{a} - \hat{b}^\dagger\hat{b}\right) \\
&= 2\hat{S}^z,
\end{aligned} \tag{3.0.14}$$

where we have used eq. 3.0.9 and the usual bosonic commutation relations: $\left[\hat{a}^\dagger, \hat{a}\right] = \left[\hat{b}^\dagger, \hat{b}\right] = 1$.

The next question is, how do we know what bosonic state corresponds to the correct spin state, i.e., we need to determine n_a and n_b such that $|n_a, n_b\rangle \equiv |s, m\rangle$. For a spin-$\frac{1}{2}$ case,

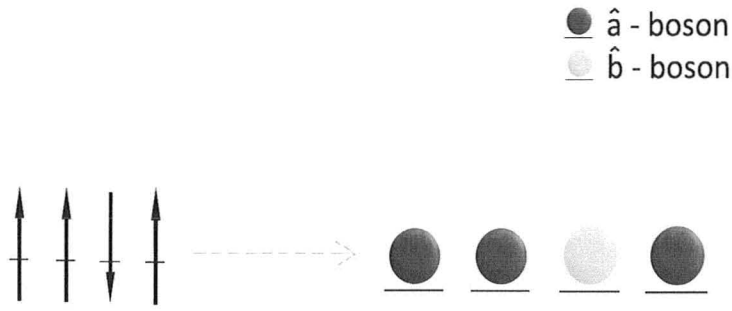

Figure 3.1: Schwinger representation of spin. This figure demonstrates a spin-$\frac{1}{2}$ chain with four sites, equivalently described in terms of Schwinger bosons. A down spin is replaced by an $\hat{a}$-type boson (light shaded), while an up spin is replaced by a $\hat{b}$-boson (dark shaded) .

we can deduce this just by examining the form of the Schwinger operators in eq. 3.0.9. Suppose we had a particle in the $|\downarrow\rangle$ state, then the action of the raising operator, $\hat{S}^+$, serves to increase its spin by 1 and change it to the $|\uparrow\rangle$ state. This operation is associated with the bosonic operator combination $\hat{S}^+ \rightarrow \hat{a}^\dagger \hat{b}$ which increases the number of $\hat{a}$-bosons by one and decreases the number of $\hat{b}$-bosons by one. On the other hand, the $\hat{S}^- \rightarrow \hat{b}^\dagger \hat{a}$ flips the $|\uparrow\rangle$ state onto $|\downarrow\rangle$ and is equivalent to increasing the number of $\hat{b}$-bosons by one and decreasing the number of $\hat{a}$-bosons by one. In either case, the total number of particles is conserved and there is only one type of either $\hat{a}$- or $\hat{b}$-boson at all times. We can then intuitively assign:

$$|n_a, n_b\rangle = |1,0\rangle \equiv |\uparrow\rangle \tag{3.0.15}$$

and

$$|n_a, n_b\rangle = |0,1\rangle \equiv |\downarrow\rangle. \tag{3.0.16}$$

To verify this, we will apply the projection operator: $\hat{S}^z \rightarrow \frac{1}{2}(\hat{n}_a - \hat{n}_b)$ on both $|\uparrow\rangle = |1,0\rangle$ and $|\downarrow\rangle = |0,1\rangle$ and see that:

$$\frac{1}{2}(\hat{n}_a - \hat{n}_b)\,|1,0\rangle = \frac{1}{2}|1,0\rangle \tag{3.0.17}$$

and

$$\frac{1}{2}(\hat{n}_a - \hat{n}_b)\,|0,1\rangle = -\frac{1}{2}|0,1\rangle, \tag{3.0.18}$$

which produces the correct eigenvalues as required. If we have a spin-$\frac{1}{2}$ particle, then its two states are now described by either a single $\hat{a}-$boson or a $\hat{b}$-boson per site as shown in fig. 3.1. A spin-up state: $|\uparrow\rangle$ is the same as having a single $\hat{a}$-boson and no $\hat{b}$-bosons, whereas a spin down-state: $|\downarrow\rangle$ is the same as having a single $\hat{b}$-boson but no $\hat{a}$-bosons. In

this way, it is possible to replace spin operators with bosonic operators using the Schwinger boson representation in eq. 3.0.9 thus allowing us to apply the PPR in the usual way.

Admittedly, the argument presented above is not very rigorous and a more precise treatment of Schwinger representation can be found in [40] or [39]. In general, it is possible to represent arbitrary spin systems with $s > \frac{1}{2}$ using Schwinger bosons. It can be shown that the general spin s state with projection m is given by

$$|s,m\rangle = \frac{\left(\hat{a}^\dagger\right)^{s+m}\left(\hat{b}^\dagger\right)^{s-m}}{\sqrt{(s+m)!(s-m)!}}|0\rangle, \tag{3.0.19}$$

where $|0\rangle$ is the vacuum state. Eq. 3.0.19 has the physical interpretation that the state $|s,m\rangle$ is equivalent to the number state with $(s+m)$ $\hat{a}$-bosons and $(s-m)$ $\hat{b}-$bosons. One can also view a spin with $s > \frac{1}{2}$ as being comprised of many spin-$\frac{1}{2}$ particles. Substituting $s = \frac{1}{2}$ and $m = \pm\frac{1}{2}$ into eq. 3.0.19 does indeed reproduce the states eq. 3.0.16 and eq. 3.0.15 as required.

Before we proceed, we would like to mention that the Schwinger boson representation is not the only bosonic mapping available. One mapping we came across which proved unfavorable was the Holstein-Primakoff transformation [41]. This is because the latter involves a square root term, which is essentially an infinite series that cannot be represented exactly without some form of truncation. Another mapping which we attempted to use to derive SDEs was the Dyson-Maleev transformation [42]. This representation required the presence of a fictitious infinite potential term in order to preserve the correct Hilbert space. Unfortunately, it was this potential term which rendered numerical simulations of SDES impractical with extremely short life times. Lastly, we would also like to point out that Drummond et al [43] developed an analogous formalism to the PPR, using Radcliffe coherent states [44] instead, but only simulated the classical TFIM, albeit for larger simulation times.

3.1 Example: Bosonic spontaneous emission

The idea of using Schwinger bosons first came to our attention in a resarch article by Olsen et al [30] in which the PPR and the truncated Wigner approximation [45] (TWA) was used to simulate the dynamics of spontaneous emission in two-level bosonic atoms. The system was initialized in an excited state and allowed to decay into a zero-temperature thermal bath, being described by the master equation

$$\frac{d\hat{\rho}}{dt} = \frac{\kappa'}{2}\left(2\hat{\sigma}^-\hat{\rho}\hat{\sigma}^+ - \hat{\sigma}^+\hat{\sigma}^-\hat{\rho} - \hat{\rho}\hat{\sigma}^+\sigma^-\right), \tag{3.1.1}$$

where $\hat{\sigma}^i$ are the usual Pauli spin matrices and are related to $\hat{S}^i$ by a factor of $\frac{1}{2}$, i.e. $\hat{S}^i = \frac{1}{2}\hat{\sigma}^i$[1]. By redefining κ', we can write our master equation in terms of the bosonic operators:

$$\frac{d\hat{\rho}}{dt} = \frac{\kappa}{2}\left(2\hat{a}^\dagger\hat{b}\hat{\rho}\hat{a}\hat{b}^\dagger - \hat{a}\hat{b}^\dagger\hat{a}^\dagger\hat{b}\hat{\rho} - \hat{\rho}\hat{a}\hat{b}^\dagger\hat{a}^\dagger\hat{b}\right). \tag{3.1.3}$$

Using the PPR formalism outlined in chapter 2, the following FPE was obtained:

$$\begin{aligned}\frac{\partial P}{\partial t} &= \left\{-\frac{\kappa}{2}\left[\frac{\partial}{\partial\alpha}\beta\beta^+\alpha + \frac{\partial}{\partial\alpha^+}\beta^+\beta\alpha^+ - \frac{\partial}{\partial\beta}(\alpha^+\alpha+1)\beta - \frac{\partial}{\partial\beta^+}\right]\right. \\ &\left.+\frac{\kappa}{2}\left[\frac{\partial^2}{\partial\alpha\partial\alpha^+}2\beta^+\beta - \frac{\partial^2}{\partial\alpha\partial\beta}\alpha\beta - \frac{\partial^2}{\partial\alpha^+\partial\beta^+}\alpha^+\beta^+\right],\right. \end{aligned}\tag{3.1.4}$$

for which the diffusion matrix reads:

$$\mathbf{D} = \begin{bmatrix} 0 & \beta\beta^+ & -\frac{1}{2}\alpha\beta & 0 \\ \beta\beta^+ & 0 & 0 & -\frac{1}{2}\alpha^+\beta^+ \\ -\frac{1}{2}\alpha\beta & 0 & 0 & 0 \\ 0 & -\frac{1}{2}\alpha^+\beta^+ & 0 & 0 \end{bmatrix}. \tag{3.1.5}$$

In the article, it was shown that $\mathbf{D}$ can be factorized to yield a noise matrix, $\mathbf{B}$ of the form:

$$B = \sqrt{\kappa}\begin{bmatrix} \frac{i}{2}\sqrt{\alpha\beta} & 0 & -\frac{1}{2}\sqrt{\alpha\beta} & 0 & \sqrt{\frac{\beta^+\beta}{2}} & i\sqrt{\frac{\beta\beta^+}{2}} \\ 0 & \frac{i}{2}\sqrt{\alpha^+\beta^+} & 0 & -\frac{1}{2}\sqrt{\alpha^+\beta^+} & \sqrt{\frac{\beta^+\beta}{2}} & -i\sqrt{\frac{\beta^+\beta}{2}} \\ \frac{i}{2}\sqrt{\alpha\beta} & 0 & \frac{1}{2}\sqrt{\alpha\beta} & 0 & 0 & 0 \\ 0 & \frac{i}{2}\sqrt{\alpha^+\beta^+} & 0 & \frac{1}{2}\sqrt{\alpha^+\beta^+} & 0 & 0 \end{bmatrix}, \tag{3.1.6}$$

which immediately yields the Ito SDEs

$$\begin{aligned} d\alpha &= \frac{\kappa}{2}\beta^+\beta\alpha dt - \frac{1}{2}\sqrt{\kappa\alpha\beta}(dW_3 + idW_1) + \sqrt{\frac{\kappa\beta\beta^+}{2}}(dW_5 + idW_6), \\ d\alpha^+ &= \frac{\kappa}{2}\beta^+\beta\alpha^+ dt - \frac{1}{2}\sqrt{\kappa\alpha^+\beta^+}(dW_4 - idW_2) + \sqrt{\frac{\kappa\beta+\beta}{2}}(dW_5 - idW_6), \\ d\beta &= -\frac{\kappa}{2}(\alpha^+\alpha+1)\beta + \frac{1}{2}\sqrt{\kappa\alpha\beta}(dW_3 + idW_1), \\ d\beta^+ &= -\frac{\kappa}{2}(\alpha\alpha^+ + 1)\beta^+ + \frac{1}{2}\sqrt{\kappa\alpha^+\beta^+}(dW_4 + idW_2). \end{aligned}\tag{3.1.7}$$

[1] We would like to point out that in [30], the following transformation was used:

$$\hat{S}^+ \to \hat{a}\hat{b}^\dagger, \hat{S}^- \to \hat{a}^\dagger\hat{b}, \hat{S}^z \to \frac{1}{2}\left(\hat{b}^\dagger\hat{b} - \hat{a}^\dagger\hat{a}\right), \tag{3.1.2}$$

and a quick comparison with eq. 3.0.9 tells us that this just reverses the role of $\hat{a}$-bosons and $\hat{b}$-bosons. This is nothing more than an issue of notation. Only for the remainder of this section will the mappings in eq. 3.1.2 be used, and in Chapter 4 we will revert to the notation in eq. 3.0.9. We used the notation in eq. 3.1.2 so that it aligns directly with the results and equations found in [30].

Note that even though the diffusion matrix is of dimension 4×4, our noise matrix is given by a 4×6 matrix, which means that we have introduced two additional Wiener increment terms at the expense of a simpler noise matrix. The naive choice would be to take the square root decomposition to generate a 4×4 noise matrix by taking advantage of the symmetry of $\mathbf{D}$. However, this would leave us with a complicated $\mathbf{B}$, which could make calculating Stratonovich correction terms more difficult than it already is. If we were to write eq. 3.1.7 as a system of linear SDEs, we get:

$$d\begin{bmatrix} \alpha \\ \alpha^+ \\ \beta \\ \beta^+ \end{bmatrix} = \begin{bmatrix} \frac{\kappa}{2}\beta^+\beta\alpha \\ \frac{\kappa}{2}\beta^+\beta\alpha^+ \\ -\frac{\kappa}{2}(\alpha\alpha^+ + 1)\beta \\ -\frac{\kappa}{2}(\alpha^+\alpha + 1)\beta^+ \end{bmatrix} dt \tag{3.1.8}$$

$$+\sqrt{\kappa}\begin{bmatrix} \frac{i}{2}\sqrt{\alpha\beta} & 0 & -\frac{1}{2}\sqrt{\alpha\beta} & 0 & \sqrt{\frac{\beta^+\beta}{2}} & i\sqrt{\beta\beta^+2} \\ 0 & \frac{i}{2}\sqrt{\alpha^+\beta^+} & 0 & -\frac{1}{2}\sqrt{\alpha^+\beta^+} & \sqrt{\frac{\beta^+\beta}{2}} & -i\sqrt{\frac{\beta^+\beta}{2}} \\ \frac{i}{2}\sqrt{\alpha\beta} & 0 & \frac{1}{2}\sqrt{\alpha\beta} & 0 & 0 & 0 \\ 0 & \frac{i}{2}\sqrt{\alpha^+\beta^+} & 0 & \frac{1}{2}\sqrt{\alpha^+\beta^+} & 0 & 0 \end{bmatrix} \begin{bmatrix} dW_1 \\ dW_2 \\ dW_3 \\ dW_4 \\ dW_5 \\ dW_6 \end{bmatrix}.$$

Using eq. A.2.28, the following Stratonovich correction terms were calculated:

$$S_\alpha = \frac{\alpha}{8} \tag{3.1.9}$$

$$S_{\alpha^+} = \frac{\alpha^+}{8} \tag{3.1.10}$$

$$S_\beta = \frac{\beta}{8} \tag{3.1.11}$$

$$S_{\beta^+} = \frac{\beta^+}{8}, \tag{3.1.12}$$

and the Stratonovich version of eq. 3.1.13 is given by

$$d\begin{bmatrix} \alpha \\ \alpha^+ \\ \beta \\ \beta^+ \end{bmatrix} = \begin{bmatrix} \frac{\kappa}{2}\beta^+\beta\alpha + \frac{\alpha}{8} \\ \frac{\kappa}{2}\beta^+\beta\alpha^+ + \frac{\alpha^+}{8} \\ -\frac{\kappa}{2}(\alpha\alpha^+ + 1)\beta + \frac{\beta}{8} \\ -\frac{\kappa}{2}(\alpha^+\alpha + 1)\beta^+ + \frac{\beta^+}{8} \end{bmatrix} dt \tag{3.1.13}$$

$$+\sqrt{\kappa}\begin{bmatrix} \frac{i}{2}\sqrt{\alpha\beta} & 0 & -\frac{1}{2}\sqrt{\alpha\beta} & 0 & \sqrt{\frac{\beta^+\beta}{2}} & i\sqrt{\beta\beta^+2} \\ 0 & \frac{i}{2}\sqrt{\alpha^+\beta^+} & 0 & -\frac{1}{2}\sqrt{\alpha^+\beta^+} & \sqrt{\frac{\beta^+\beta}{2}} & -i\sqrt{\frac{\beta^+\beta}{2}} \\ \frac{i}{2}\sqrt{\alpha\beta} & 0 & \frac{1}{2}\sqrt{\alpha\beta} & 0 & 0 & 0 \\ 0 & \frac{i}{2}\sqrt{\alpha^+\beta^+} & 0 & \frac{1}{2}\sqrt{\alpha^+\beta^+} & 0 & 0 \end{bmatrix} \circ \begin{bmatrix} dW_1 \\ dW_2 \\ dW_3 \\ dW_4 \\ dW_5 \\ dW_6 \end{bmatrix},$$

where we have used $\circ$ to denote a Stratonovich SDE.

In this system the obvious observables of interest are given by the population of the excited and ground states which are represented by the operators $\hat{N}_b = \hat{b}^\dagger \hat{b}$ and $\hat{N}_a = \hat{a}^\dagger \hat{a}$ respectively. The dynamics for these operators are mapped on to the following phase space variable functions: $\hat{N}_b \to N_b = \beta^+ \beta$ and $\hat{N}_a \to N_a = \alpha^+ \alpha$ and can be easily simulated. Lucky for us, this problem is simple enough that analytic solutions for the population stochastic averages can be worked out, to allow us to compare our simulation results against them. Let us now derive these expressions. Using Ito calculus and the SDES in eq. 3.1.13, we can obtain an SDE for N_b:

$$\begin{aligned} dN_b = d(\beta^+\beta) &= \beta d\beta^+ + \beta^+ d\beta + d\beta d\beta^+ \\ &= -\frac{\kappa}{2}(N_a+1)N_b dt + \frac{1}{2}\sqrt{\kappa\alpha^+\beta^+}(dW_4 + i dW_2)\beta \qquad (3.1.14) \\ &\quad -\frac{\kappa}{2}(N_a+1)N_b dt + \frac{1}{2}\sqrt{\kappa\alpha\beta}(dW_3 + i dW_1)\beta^+ \\ &= -\kappa(N_a+1)N_b dt + \frac{1}{2}\sqrt{\kappa\alpha^+\beta^+}(dW_4 + i dW_2)\beta \qquad (3.1.15) \\ &\quad +\frac{1}{2}\sqrt{\kappa\alpha\beta}(dW_3 + i dW_1)\beta^+, \end{aligned}$$

where we have ignored terms that are of $O(dt^{3/2})$ and also used the fact that $\langle dW_i dW_j \rangle = \delta_{ij} dt$ to ignore potential correction terms (arising from $d\beta^+ d\beta$). If we were to take the stochastic average of the resulting equation then what we are left with is just:

$$d\langle N_b \rangle = -\kappa(\langle N_a N_b \rangle + \langle N_b \rangle)dt, \qquad (3.1.16)$$

where we have used the property $\langle dW_i \rangle = 0$ for all i.

For the stochastic variables N_a, the SDE is given by:

$$
\begin{aligned}
dN_a = d(\alpha^+\alpha) &= \alpha d\alpha^+ + \alpha^+ d\alpha + d\alpha d\alpha^+ \\
&= \left(\frac{\kappa}{2}\beta^+\beta\alpha dt - \frac{1}{2}\sqrt{\kappa\alpha\beta}(dW_3 + idW_1) + \sqrt{\frac{\kappa\beta\beta^+}{2}}(dW_5 + idW_6)\right)\alpha^+ \\
&\quad + \left(\frac{\kappa}{2}\beta^+\beta\alpha^+ dt - \frac{1}{2}\sqrt{\kappa\alpha^+\beta^+}(dW_4 - idW_2) + \sqrt{\frac{\kappa\beta+\beta}{2}}(dW_5 - idW_6)\right)\alpha \\
&\quad + \left(\frac{\kappa}{2}\beta^+\beta\alpha dt - \frac{1}{2}\sqrt{\kappa\alpha\beta}(dW_3 + idW_1) + \sqrt{\frac{\kappa\beta\beta^+}{2}}(dW_5 + idW_6)\right) \\
&\quad \times \left(\frac{\kappa}{2}\beta^+\beta\alpha^+ dt - \frac{1}{2}\sqrt{\kappa\alpha^+\beta^+}(dW_4 - idW_2) + \sqrt{\frac{\kappa\beta+\beta}{2}}(dW_5 - idW_6)\right) \\
&= \left(\frac{\kappa}{2}N_aN_b dt + \ldots dW_3 + \ldots dW_1 + \ldots dW_5 + \ldots dW_6\right) \\
&\quad + \left(\frac{\kappa}{2}N_aN_b dt + \ldots dW_4 + \ldots dW_2 + \ldots dW_5 + \ldots dW_6\right) \\
&\quad + \kappa\frac{N_b}{2}(dW_5)^2 + \kappa\frac{N_b}{2}(dW_6)^2,
\end{aligned}
\tag{3.1.17}
$$

so that taking a stochastic average results in

$$
\begin{aligned}
d\langle N_a\rangle &= \kappa\langle\, N_aN_b\rangle dt + \kappa\langle\frac{N_b}{2}\rangle\langle(dW_5)^2\rangle + \kappa\frac{\langle N_b\rangle}{2}\langle(dW_6)^2\rangle \\
&= \kappa\left(\langle\, N_aN_b\rangle dt + \kappa\langle\frac{N_b}{2}\rangle dt + \kappa\frac{\langle N_b\rangle}{2}\langle\right)dt \\
&= \kappa\left(\langle N_aN_b\rangle + \langle N_b\rangle\right)dt,
\end{aligned}
\tag{3.1.18}
$$

where we have again used the property that $\langle dW_i dW_j\rangle = \delta_{ij}dt$. If we let N_T be the total number of particles then (even in the mean) we must have

$$
\frac{dN_T}{dt} = \frac{d\langle N_a\rangle}{dt} + \frac{d\langle N_b\rangle}{dt} = 0, \tag{3.1.19}
$$

and hence

$$
N_T = \langle N_a\rangle + \langle N_b\rangle \tag{3.1.20}
$$

at all times. We see that eq. 3.1.19 is indeed satisfied by adding eq. 3.1.18 to 3.1.16. The solution of $\langle N_b\rangle$ is obtained by solving the ordinary differential equation (ODE):

$$
\frac{d\langle N_b\rangle}{dt} = -\kappa\left(\langle N_aN_b\rangle + \langle N_b\rangle\right) = \kappa\left(N_T - \langle N_b\rangle + 1\right)\langle N_b\rangle, \tag{3.1.21}
$$

where we have used eq. 3.1.20 and which has the solution:

$$
\langle N_b(t)\rangle = \frac{\langle N_b(0)\rangle\left(N_T + 1\right)}{\langle N_b(0)\rangle\left[N_T + 1 - \langle N_b(0)\rangle\right]e^{(N_T+1)\kappa t}}. \tag{3.1.22}
$$

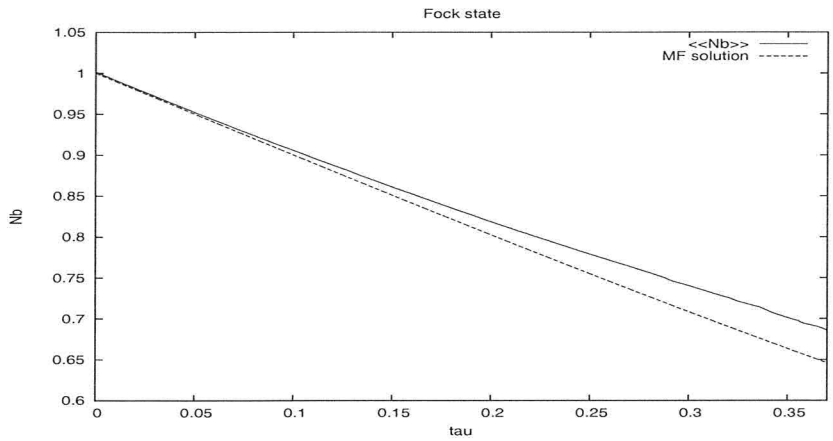

Figure 3.2: Plot of N_b vs $\tau = \kappa t$: the decay of an $N = 1$ fock state initially in the excited level. We compare the stochastic average $\langle\langle N_b \rangle\rangle$ with the mean field (MF) solution calculated in eq. 3.1.23. Simulation parameters: 4×10^5 trajectories. $d\tau = 0.0001$

If we assume that only one atom is initially excited, i.e. $N_b(0) = 1$, then this further simplifies to:

$$N_b(t) = sech(\kappa t)e^{-\kappa t}. \tag{3.1.23}$$

The simulations were carried out using a Stratonovich semi-implicit algorithm [46] with the results shown in Fig. 3.3 to 3.4 for a variety of initial conditions, namely: the Coherent state and Fock state. This raises another crucial point regarding the PPR: "How does one initialize the distribution: $P(\alpha, \alpha^+)$?". A pedagogical article which addresses this issue can be found in [47] but we will review the necessary results in section 3.2.

3.2 Representation of quantum states

The two quantum states that we wish to represent are the (i) Coherent state and the (ii) Fock state. As mentioned in section 2.3, any density matrix $\hat{\rho}$ has the following form of the distribution function:

$$P(\alpha, \alpha^+) = \frac{1}{4\pi^2} |\langle (\alpha + \alpha^+)^* | \hat{\rho} | (\alpha + \alpha^+)^* \rangle|^2 e^{-|\alpha - (\alpha^+)^*|^2/4} \tag{3.2.1}$$

and can be used to represent different quantum states.

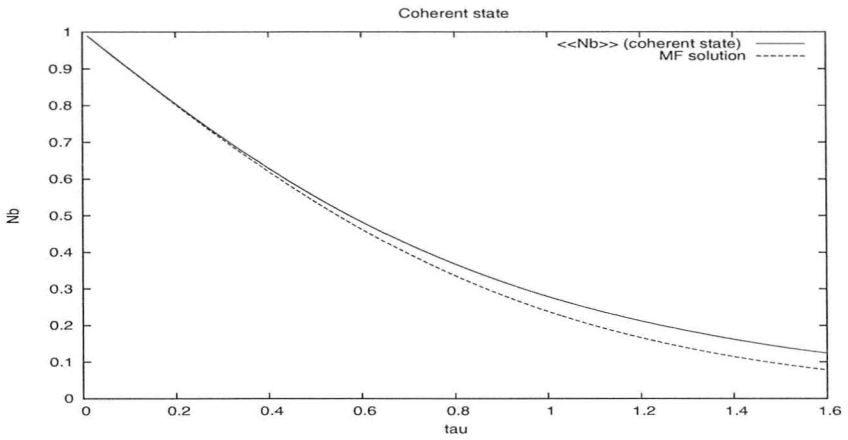

Figure 3.3: Plot of N_b vs $\tau = \kappa t$: the decay of an $N = 1$ coherent state initially in the excited level. We compare the stochastic average $\langle\langle N_b \rangle\rangle$ with the mean field (MF) solution calculated in eq. 3.1.23. Simulation parameters: 10^6 trajectories. $d\tau = 0.001$

3.2.1 Coherent states

The most convenient case about using the PPR is in constructing a density operator corresponding to a pure coherent state:

$$\hat{\rho} = |\beta\rangle\langle\beta|. \tag{3.2.2}$$

First let us recall the expression for the density operator in the PPR:

$$\hat{\rho} = \int d^2\alpha d^2\alpha^+ \frac{|\alpha\rangle\langle(\alpha^+)^*|}{\langle(\alpha^+)^*|\alpha\rangle} P(\alpha, \alpha^+). \tag{3.2.3}$$

In order to represent the coherent state of eq. 3.2.2, it is obvious that we need the following PP-distribution:

$$P(\alpha, \alpha^+) = \delta(\alpha - \beta)\delta(\alpha^+ - \beta^*), \tag{3.2.4}$$

which is easy enough to compute. Numerically this means that using the same complex conjugate pair, β and β^* for every stochastic trajectory will generate an initial coherent state $|\beta\rangle$. The values of β and β^* are usually chosen to agree with the initial particle number. For example, suppose we require that $\langle\hat{a}^\dagger\hat{a}\rangle = n(0)$ initially. For the single mode case, the number operator is simply given by $\hat{n} \to \alpha^+\alpha$ which is constrained to $n(0)$. An obvious choice for our initial phase space variables would then be $\alpha = \sqrt{n(0)}e^{i\theta}$ and $\alpha^+ = \sqrt{n(0)}e^{-i\theta}$ where $\theta \in [0, 2\pi)$.

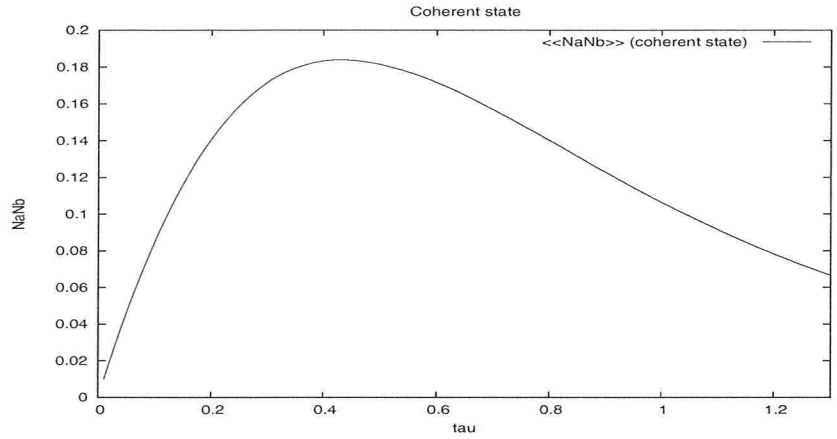

Figure 3.4: Plot of $N_a N_b$ vs $\tau = \kappa t$: the decay of the correlation function for a system with an initial coherent state in the excited level. There is no analytic solution available for comparison. Simulation parameters: 4×10^5 trajectories. $d\tau = 0.001$

3.2.2 Fock states

Another quantum state of interest is the Fock state, whose density operator is given by:

$$\hat{\rho} = |n\rangle\langle n| \tag{3.2.5}$$

where $|n\rangle$ is the Fock state representing n quanta i.e. $\hat{a}^\dagger \hat{a}|n\rangle = n|n\rangle$. The distribution for the Fock state is obtained by substituting eq. 3.2.5 into eq. 3.2.1 directly and using the change of variables

$$\mu = \frac{\alpha - (\alpha^+)^*}{2} \tag{3.2.6}$$

$$\gamma = \frac{\alpha + (\alpha^+)^*}{2}. \tag{3.2.7}$$

This gives:

$$P(\mu,\gamma) = \frac{1}{4\pi^2}|\langle\mu|n\rangle\langle n|\mu\rangle|e^{-|\gamma|^2}.J_{\mu\gamma}, \tag{3.2.8}$$

where $J_{\mu\gamma}$ is the Jacobian for the transformation:

$$J_{\mu\gamma} = \left|\frac{\mu,\mu^*,\gamma,\gamma^*}{\alpha,\alpha^*,\alpha^+,\alpha^{+*}}\right| = 4. \tag{3.2.9}$$

A little algebra shows that we can write eq. 3.2.8 in the separable form:

$$P(\mu,\gamma) = \frac{e^{-|\gamma|^2}}{\pi^2}\frac{|\mu^{2n}e^{-|\mu|^2}|}{\pi n!} = \frac{e^{-|\gamma|^2}}{\pi}\frac{\Gamma(|\mu|^2,n+1)}{\pi}, \tag{3.2.10}$$

where

$$\Gamma(x,n) = \frac{e^{-x}x^{n-1}}{(n-1)!} \tag{3.2.11}$$

is the Gamma distribution. The normal distribution with 0 mean has the generic form:

$$f(x) = \frac{1}{\sqrt{2\pi\sigma^2}}e^{-\frac{|\gamma|^2}{2\sigma^2}} \tag{3.2.12}$$

and a quick comparison of eq. 3.2.12 and eq. 3.2.10 tells us γ can be sampled by setting:

$$\gamma = (n_1 + in_2)/\sqrt{2}, \tag{3.2.13}$$

where $n_i \equiv N(0,1)$, i.e. is a standard normal random variable. $|\mu|^2$ on the other hand is readily sampled by using a Gamma distribution which has a simple yet efficient algorithm [48]. This allows us to sample $\mu = \sqrt{z}e^{i\theta}$ where $z \equiv |\mu|^2$ is sampled from the Gamma distribution and θ is uniform in $[0, 2\pi)$. Finally, we only need to invert eq. 3.2.6 and 3.2.7 to get the result:

$$\alpha = \mu + \gamma \tag{3.2.14}$$
$$\alpha^+ = \mu^* - \gamma^*. \tag{3.2.15}$$

3.3 Discussion

The results for the N_b vs $\tau = \kappa t$ are shown in Fig. 3.3 and Fig. 3.2 for an initial coherent and Fock state respectively. They do not agree exactly with the mean-field solution since the latter is just an approximation but do exhibit the same qualitative behavior, i.e. an exponential decay. In addition, the stochastic solution of the correlation function, $\langle \hat{N}_a\hat{N}_b\rangle = \alpha^+\alpha\beta^+\beta$ for an initial coherent state is shown in Fig. 3.4. In accordance with the PPR, $\langle N_b\rangle$ was calculated by simulating the SDEs for the stochastic variables in eq. 3.1.7 and stochastic averaging the corresponding function: $\beta^+\beta$. Similarly for N_aN_b, the corresponding function is given by $\alpha^+\alpha\beta^+\beta$.

All three plots show good agreement with the results published in [30] which is a positive sign that we are on the right track. We would also like to point out the rather short life times of the simulations, terminating at $\tau \sim 0.38$ for the initial Fock state and at $\tau \sim 1.6$ for the initial coherent state. Beyond these time scales, numerical instabilities occur and our simulations fail to produce accurate results.

Chapter 4

Quantum quench dynamics of the TFIM and anisotropic Heisenberg model

The Schwinger bosons provide a convenient way of mapping spin operators onto bosonic operators thereby allowing us to apply the PPR. The two variants of the Heisenberg Hamiltonian which we examined were the (i) transverse-field Ising Model (TFIM), (ii) the isotropic Heisenberg model with an anisotropy of $\Delta/J = 1.0$ and (iii) other anisotropic Heisenberg system. What we are interested in is being able to derive the SDEs that describe the dynamics of (i)-(iii). For brevity however, we will focus mainly on the derivations of (i) but present results for both (i) and (ii) in section 4.3.

4.1 Deriving SDEs for the TFIM

We will view the $1D$ TFIM model as a material with Ising interactions subject to quantum quench in the x-direction described by the Hamiltonian

$$\hat{H} = -\left[J\sum_{\langle i,j\rangle}\hat{S}_i^z.\hat{S}_j^z + h(t)\sum_i \hat{S}_i^x\right] = \sum_{\langle i,j\rangle}\left[-J\hat{S}_i^z.\hat{S}_j^z\right] - \frac{1}{2}h(t)\sum_i\left[\hat{S}_i^+ + \hat{S}_i^-\right], \tag{4.1.1}$$

with $J > 0$, i.e. FM interactions. This means that at $t = 0$ a transverse-field is instantaneously switched on, which we can write as an interaction of the form: $h(t)\sum_i \hat{S}_i^x$ where

$$h(t) = \begin{cases} h, & t \geq 0 \\ 0, & t < 0 \end{cases} \tag{4.1.2}$$

Using the Schwinger representation in eq. 3.0.9, the Hamiltonian for the $1D$ TFIM can be mapped on to the equivalent bosonic Hamiltonian:

$$\begin{aligned}\hat{H} &= -\frac{J}{4}\sum_{\langle i,j\rangle}\left(\hat{a}_i^\dagger\hat{a}_i\hat{a}_j^\dagger\hat{a}_j - \hat{a}_i^\dagger\hat{a}_i\hat{b}_j^\dagger\hat{b}_j - \hat{b}_i^\dagger\hat{b}_i\hat{a}_j^\dagger\hat{a}_j + \hat{b}_i^\dagger\hat{b}_i\hat{b}_j^\dagger\hat{b}_j\right) - \frac{1}{2}\left(h(t)\sum_i \hat{a}_i^\dagger\hat{b}_i + \hat{b}_i^\dagger\hat{a}_i\right)\\ &= -\frac{J}{4}\sum_{i=0}^{N-1}\left(\hat{a}_i^\dagger\hat{a}_i\hat{a}_{i+1}^\dagger\hat{a}_{i+1} - \hat{a}_i^\dagger\hat{a}_i\hat{b}_{i+1}^\dagger\hat{b}_{i+1} - \hat{b}_i^\dagger\hat{b}_i\hat{a}_{i+1}^\dagger\hat{a}_{i+1} + \hat{b}_i^\dagger\hat{b}_i\hat{b}_{i+1}^\dagger\hat{b}_{i+1}\right)\\ &\quad -\frac{1}{2}\left(h(t)\sum_i \hat{a}_i^\dagger\hat{b}_i + \hat{b}_i^\dagger\hat{a}_i\right), \end{aligned} \tag{4.1.3}$$

where $i = 0\ldots N-1$, N being the number of spins in our spin chain, and periodic boundary conditions (PBCs) are naturally imposed.

Since we have a closed system, the master equation for $\hat{\rho}$ is given by:

$$\frac{\partial\hat{\rho}}{\partial t} = -\frac{i}{\hbar}\left[\hat{H},\hat{\rho}\right]. \tag{4.1.4}$$

To proceed, we use the PPR and express $\hat{\rho}$ in the usual way, i.e.

$$\hat{\rho} = \int P(\vec{\alpha},\vec{\alpha}^+,\vec{\beta},\vec{\beta}^+)\hat{\Lambda}(\vec{\alpha},\vec{\alpha}^+,\vec{\beta},\vec{\beta}^+)d^2\vec{\alpha}d^2\vec{\alpha}^+d^2\vec{\beta}d^2\vec{\beta}^+, \tag{4.1.5}$$

where the projection operator is now given by the direct product over projection operators for different sites:

$$\hat{\Lambda}(\vec{\alpha},\vec{\alpha}^+,\vec{\beta},\vec{\beta}^+) = \prod_{i=0}^{N-1}\otimes\frac{|\alpha_i\rangle\langle\alpha_i^{+*}|}{\langle\alpha_i^{+*}|\alpha_i\rangle}\otimes\frac{|\beta i\rangle\langle\beta_i^{+*}|}{\langle\beta_i^{+*}|\beta_i\rangle} \tag{4.1.6}$$

and $\vec{\alpha} = (\alpha_0,\ldots,\alpha_{N-1}), \vec{\alpha}^+ = (\alpha_0^+,\ldots,\alpha_{N-1}^+), \vec{\beta} = (\beta_0,\ldots,\beta_{N-1})$ and $\vec{\beta}^+ = (\beta_0^+,\ldots,\beta_{N-1}^+)$. Since there are two types of bosons per site, we have further introduced the complex variables $\{\beta,\beta^+\}\in\mathbb{C}$, which are the phase space variable associated $\hat{b}$. The correspondence relations in eq. 2.3.13 still applies and at each site, i, we now have:

$$\begin{aligned}\hat{\Lambda}\hat{a}_i^\dagger &= \alpha_i^+\hat{\Lambda}, & \hat{\Lambda}\hat{b}_i^\dagger &= \beta_i^+\hat{\Lambda}\\ \hat{a}_i\hat{\Lambda} &= \alpha_i\hat{\Lambda}, & \hat{b}_i\hat{\Lambda} &= \beta_i\hat{\Lambda}\\ \hat{a}_i^\dagger\hat{\Lambda} &= (\alpha_i^+ + \frac{\partial}{\partial\alpha_i})\hat{\Lambda}, & \hat{b}_i^\dagger\hat{\Lambda} &= (\beta_i^+ + \frac{\partial}{\partial\beta_i})\hat{\Lambda}\\ \hat{\Lambda}\hat{a}_i &= (\alpha_i + \frac{\partial}{\partial\alpha_i^+})\hat{\Lambda}, & \hat{\Lambda}\hat{b}_i &= (\beta_i + \frac{\partial}{\partial\beta_i^+})\hat{\Lambda}\end{aligned} \tag{4.1.7}$$

where $i = 0\ldots N-1$. Substituting the correspondence relations in eq. 4.1.7 into the Master equation in eq. 4.1.4, we obtain the following FPE after integrating by parts and ignoring

$$\mathbf{D} = \frac{iJ}{4\hbar}\begin{bmatrix} \frac{\partial^2}{\partial\alpha_i\partial\alpha_j} & 0 & \frac{\partial^2}{\partial\alpha_i\partial\beta_j}, \frac{\partial^2}{\partial\beta_i\partial\alpha_j} & 0 \\ 0 & \frac{\partial^2}{\partial\beta_i\partial\beta_j} & 0 & \frac{\partial^2}{\partial\alpha_i^+\partial\beta_j^+}, \frac{\partial^2}{\partial\beta_i^+\partial\alpha_j^+} \\ \frac{\partial^2}{\partial\alpha_i\partial\beta_j}, \frac{\partial^2}{\partial\beta_i\partial\alpha_j} & 0 & \frac{\partial^2}{\partial\alpha_i^+\partial\alpha_j^+} & 0 \\ 0 & \frac{\partial^2}{\partial\alpha_i^+\partial\beta_j^+}, \frac{\partial^2}{\partial\beta_i^+\partial\alpha_j^+} & 0 & \frac{\partial^2}{\partial\beta_i^+\partial\beta_j^+} \end{bmatrix}. \tag{4.1.10}$$

Each term in the diffusion matrix, represents an $N \times N$ matrix whose matrix elements are specified by the derivatives themselves. For example the matrix labeled by $\mathbf{D}^{(\alpha)} = \frac{\partial^2}{\partial\alpha_i\partial\alpha_j}$ (located at the top left corner of $\mathbf{D}$ in eq. 4.1.10) is given by $\alpha_i\alpha_j$ can be explicitly written out as:

$$\mathbf{D}^{(\alpha)} = \frac{iJ}{4\hbar}\begin{bmatrix} 0 & \alpha_0\alpha_1 & 0 & \dots & \alpha_0\alpha_{N-1} \\ \alpha_1\alpha_0 & 0 & \alpha_1\alpha_2 & \dots & 0 \\ 0 & \alpha_2\alpha_1 & 0 & \ddots & 0 \\ \vdots & 0 & \ddots & \dots & 0 \\ \alpha_{N-1}\alpha_0 & 0 & \dots & \dots & 0 \end{bmatrix}. \tag{4.1.11}$$

A particular factorization of the diffusion matrix in eq. 4.1.8 results in a noise matrix[1] which then gives us a set of Ito stochastic differential equations for $4N$ of our phase space variables, i.e.

$$\begin{aligned} d\alpha_i &= \left\{\frac{iJ}{4\hbar}\alpha_i\left[(n^{\alpha}_{i+1} - n^{\beta}_{i+1}) + (n^{\alpha}_{i-1} - n^{\beta}_{i-1})\right] + \frac{ih(t)}{2\hbar}\beta_i\right\}dt \\ &+\frac{1}{2}\sqrt{\frac{iJ}{2\hbar}}\left[-\sqrt{\alpha_i\alpha_{i+1}}(dW^{\alpha}_{2i} + idW^{\alpha}_{2i+1}) - \sqrt{\alpha_i\alpha_{i-1}}(dW^{\alpha}_{2i-2} - idW^{\alpha}_{2i-1})\right] \\ &+\frac{i}{2}\sqrt{\frac{iJ}{2\hbar}}\left[-\sqrt{\alpha_i\beta_{i-1}}(dW^{\alpha\beta}_{2i-2} + idW^{\alpha\beta}_{2i-1}) - \sqrt{\alpha_i\beta_{i+1}}(dW^{\beta\alpha}_{2i} - idW^{\beta\alpha}_{2i+1})\right] \end{aligned} \tag{4.1.12}$$

$$\begin{aligned} d\beta_i &= \left\{\frac{iJ}{4\hbar}\beta_i\left[(n^{\beta}_{i+1} - n^{\alpha}_{i+1}) + (n^{\beta}_{i-1} - n^{\alpha}_{i-1})\right] + \frac{ih(t)}{2\hbar}\alpha_i\right\}dt \\ &+\frac{1}{2}\sqrt{\frac{iJ}{2\hbar}}\left[-\sqrt{\beta_i\beta_{i+1}}(dW^{\beta}_{2i} + idW^{\beta}_{2i+1}) - \sqrt{\beta_i\beta_{i-1}}(dW^{\beta}_{2i-2} - idW^{\beta}_{2i-1})\right] \\ &+\frac{i}{2}\sqrt{\frac{iJ}{2\hbar}}\left[-\sqrt{\alpha_{i+1}\beta_i}(dW^{\alpha\beta}_{2i} - idW^{\alpha\beta}_{2i+1}) - \sqrt{\alpha_{i-1}\beta_i}(dW^{\beta\alpha}_{2i-2} + idW^{\beta\alpha}_{2i-1})\right] \end{aligned} \tag{4.1.13}$$

[1] For a detailed description on how the $\mathbf{D}$ was factorized can be found in Appendix B

$$
\begin{aligned}
d\alpha_i^+ &= \left\{ \frac{iJ}{4\hbar}\alpha_i^+ \left[(n_{i+1}^{\beta} - n_{i+1}^{\alpha}) + (n_{i-1}^{\beta} - n_{i-1}^{\alpha}) \right] - \frac{ih(t)}{2\hbar}\beta_i^+ \right\} dt \qquad (4.1.14)\\
&+\frac{i}{2}\sqrt{\frac{iJ}{2\hbar}} \left[-\sqrt{\alpha_i^+ \alpha_{i+1}^+}(dW_{2i}^{\alpha^+} + idW_{2i+1}^{\alpha^+}) - \sqrt{\alpha_i^+ \alpha_{i-1}^+}(dW_{2i-2}^{\alpha^+} - idW_{2i-1}^{\alpha^+}) \right]\\
&+\frac{1}{2}\sqrt{\frac{iJ}{2\hbar}} \left[-\sqrt{\alpha_i^+ \beta_{i-1}^+}(dW_{2i-2}^{\alpha^+\beta^+} + idW_{2i-1}^{\alpha^+\beta^+}) - \sqrt{\alpha_i^+ \beta_{i+1}^+}(dW_{2i}^{\beta^+\alpha^+} - idW_{2i+1}^{\beta^+\alpha^+}) \right]
\end{aligned}
$$

$$
\begin{aligned}
d\beta_i^+ &= \left\{ \frac{iJ}{4\hbar}\beta_i^+ \left[(n_{i+1}^{\alpha} - n_{i+1}^{\beta}) + (n_{i-1}^{\alpha} - n_{i-1}^{\beta}) \right] - \frac{ih(t)}{2\hbar}\alpha_i^+ \right\} dt \qquad (4.1.15)\\
&+\frac{i}{2}\sqrt{\frac{iJ}{2\hbar}} \left[-\sqrt{\beta_i^+ \beta_{i+1}^+}(dW_{2i}^{\beta^+} + idW_{2i+1}^{\beta^+}) - \sqrt{\beta_i^+ \beta_{i-1}^+}(dW_{2i-2}^{\beta^+} - idW_{2i-1}^{\beta^+}) \right]\\
&+\frac{1}{2}\sqrt{\frac{iJ}{2\hbar}} \left[-\sqrt{\alpha_{i+1}^+ \beta_i^+}(dW_{2i}^{\alpha^+\beta^+} - idW_{2i+1}^{\alpha^+\beta^+}) - \sqrt{\alpha_{i-1}^+ \beta_i^+}(dW_{2i-2}^{\beta^+\alpha^+} + idW_{2i-1}^{\beta^+\alpha^+}) \right]
\end{aligned}
$$

where we have introduced eight $2N \times 1$ Wiener increment vectors with the usual statistical properties that $\langle dW_i^x dW_j^y \rangle = dt\delta_{xy}\delta_{ij}$ and $\langle dW_i^x \rangle = 0$ where $i = 0 \ldots N-1$ and $x, y = \alpha, \alpha^+, \beta, \beta^+, \beta\alpha, \alpha\beta, \beta^+\alpha^+, \alpha^+\beta^+$ labels each Wiener increment vector. The subscript labels of the Wiener increment vector is not unique and the labeling scheme[2] was chosen simply for convenience.

4.2 Inclusion of anisotropy

Had we begun with the full anisotropic Hamiltonian:

$$\hat{H} = \sum_{\langle i,j \rangle} \left[-J\hat{S}_i^z.\hat{S}_j^z - \Delta\frac{1}{2}(\hat{S}_i^+\hat{S}_j^- + \hat{S}_i^-\hat{S}_j^+) \right] - \frac{1}{2}h(t)\sum_i \left[\hat{S}_i^+ + \hat{S}_i^- \right] \qquad (4.2.1)$$

instead and carried out the same steps as in section 4.1, it can be shown that anisotropy can be taken into account just by modifying the SDEs of eq. 4.1.12 to eq. 4.1.15 in a trivial way. The drift terms remain the same with the exception of the following additional terms:

$$
\begin{aligned}
d\alpha_i &\sim +\frac{i\Delta}{2\hbar}\beta_i(m_{i-1} + m_{i+1})dt \qquad (4.2.2)\\
d\beta_i &\sim +\frac{i\Delta}{2\hbar}\alpha_i(m_{i-1}^+ + m_{i+1}^+)dt \qquad (4.2.3)\\
d\alpha_i^+ &\sim -\frac{i\Delta}{2\hbar}\beta_i^+(m_{i-1}^+ + m_{i+1}^+)dt \qquad (4.2.4)\\
d\beta_i^+ &\sim -\frac{i\Delta}{2\hbar}\alpha_i^+(m_{i-1}^+ + m_{i+1}^+)dt \qquad (4.2.5)
\end{aligned}
$$

[2]Note that with the inclusion of periodic boundary conditions: $\alpha_{-1} \to \alpha_{N-1}$ and $\alpha_N \to \alpha_0$ spin. However since there are $2N \times 1$ Wiener increments, then for e.g. $dW_{-1}^x = dW_{2N-1}^x$ and $dW_{2N}^x = 0$.

where the following shorthand $m_i = \alpha_i\beta_i^+, m_i^+ = \alpha_i^+\beta_i$ was used. For the stochastic terms however, only the mixed derivative diffusion terms (i.e. those containing $\alpha\beta$ and $\alpha^+\beta^+$) are modified in the following way

$$d\alpha_i \sim +\frac{i}{2}\sqrt{\frac{i}{2\hbar}}\left[-\sqrt{J\alpha_i\beta_{i-1} - 2\Delta\beta_i\alpha_{i-1}}(\dots) - \sqrt{J\alpha_i\beta_{i+1} - 2\Delta\alpha_{i+1}\beta_i}(\dots)\right] \tag{4.2.6}$$

$$d\beta_i \sim +\frac{i}{2}\sqrt{\frac{i}{2\hbar}}\left[-\sqrt{J\beta_i\alpha_{i+1} - 2\Delta\beta_{i+1}\alpha_i}(\dots) - \sqrt{J\beta_i\alpha_{i-1} - 2\Delta\alpha_i\beta_{i-1}}(\dots)\right] \tag{4.2.7}$$

$$d\alpha_i^+ \sim +\frac{i}{2}\sqrt{\frac{i}{2\hbar}}\left[-\sqrt{J\beta_{i-1}^+\alpha_i^+ - 2\Delta\beta_i^+\alpha_{i-1}^+}(\dots) - \sqrt{J\beta_{i+1}^+\alpha_i^+ - 2\Delta\alpha_{i+1}^+\beta_i^+}(\dots)\right] \tag{4.2.8}$$

$$d\beta_i^+ \sim +\frac{i}{2}\sqrt{\frac{i}{2\hbar}}\left[-\sqrt{J\beta_i^+\alpha_{i-1}^+ - 2\Delta\beta_{i-1}^+\alpha_i^+}(\dots) - \sqrt{J\beta_i^+\alpha_{i+1}^+ - 2\Delta\alpha_i^+\beta_{i+1}^+}(\dots)\right] \tag{4.2.9}$$

where the terms in $(\dots)$ represent the same Wiener increment combinations as in eq. 4.1.12 to 4.1.15.

The Ito SDEs we have derived are also able to describe other types of spins models (see table 1.1) such as the XXX (isotropic case), XY model or even the XYZ model (to name a few), just by adjusting or including a few parameters. For the last two cases, we would have to take a trivial generalization in the derivations by introducing two different anisotropy terms in eq. 4.2.1. A current review article on the quantum quench dynamics of other variants of the Heisenberg Hamiltonian using other numerical methods can be found in [24].

4.3 Results and discussion

As an initial test for our formalism, we simulated the FM ($J > 0$) spin Hamiltonian for the TFIM ($\Delta = 0$) and the isotropic case ($\Delta = 1.0$) in eq. 4.2.1 for high ($H = 10/J$) and low ($H = 0.5/J$) field values. This was compared to results from exact diagonalization calculations using a small system with $N = 4$ spins. The Stratonovich version of the SDES [3] in eq. 4.1.12 to eq. 4.1.15 were simulated using a semi-implicit Stratonovich algorithm as they are known to exhibit superior convergent properties [46].

To track the dynamics of the system, we calculated the expectation values of all three spin components at each site i: $\langle\hat{S}_i^x\rangle, \langle\hat{S}_i^y\rangle, \langle\hat{S}_i^z\rangle$. Utilizing the translation symmetry of the system, we further averaged them over the entire lattice to obtain an average expectation value of the spin components per site: $[S^x], [S^y], [S^z]$. These expectation values were calculated using the stochastic averages of their respective phase space functions, i.e.

$$[S^x] = \sum_{i=0}^{N-1}\langle\frac{1}{2}(\hat{a}_i^\dagger\hat{b}_i + \hat{b}_i^\dagger\hat{a}_i)\rangle = \sum_{i=0}^{N-1}\langle\langle\frac{1}{2}(\alpha_i^+\beta_i + \beta_i^+\alpha_i)\rangle\rangle \tag{4.3.1}$$

[3] The Stratonovich correction terms worked out to be zero and hence the Stratonovich form of the SDEs from eq. 4.1.12 to eq. 4.1.15 have the exact same form as the derived Ito SDEs.

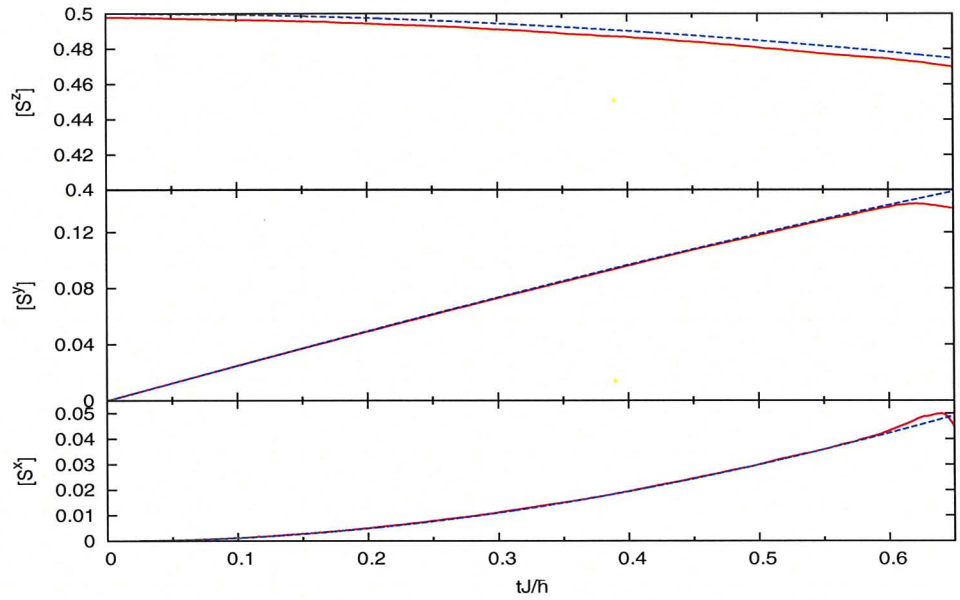

Figure 4.1: TFIM for $N = 4$ spins, following a transverse-field quench at $tJ/\hbar = 0$ from $h/J = 0$ to $h/J = 0.5$, beginning in the FM ground state: $|\uparrow\uparrow \ldots \uparrow\rangle$. FM interactions assumed: $sign(J) = +1$. From top to bottom: plots of $[S^x], [S^y], [S^z]$ vs $tJ/\hbar$ respectively. The stochastic averages, $\langle\langle . \rangle\rangle$ are given by red solid lines while exact diagonlization results are represented by the blue dashed lines. Simulation parameters: $n_{traj} = 10^6, dt = 0.001, \Delta/J = 0.0$. Agreement remains good till approximately $tJ/\hbar \sim 0.6$.

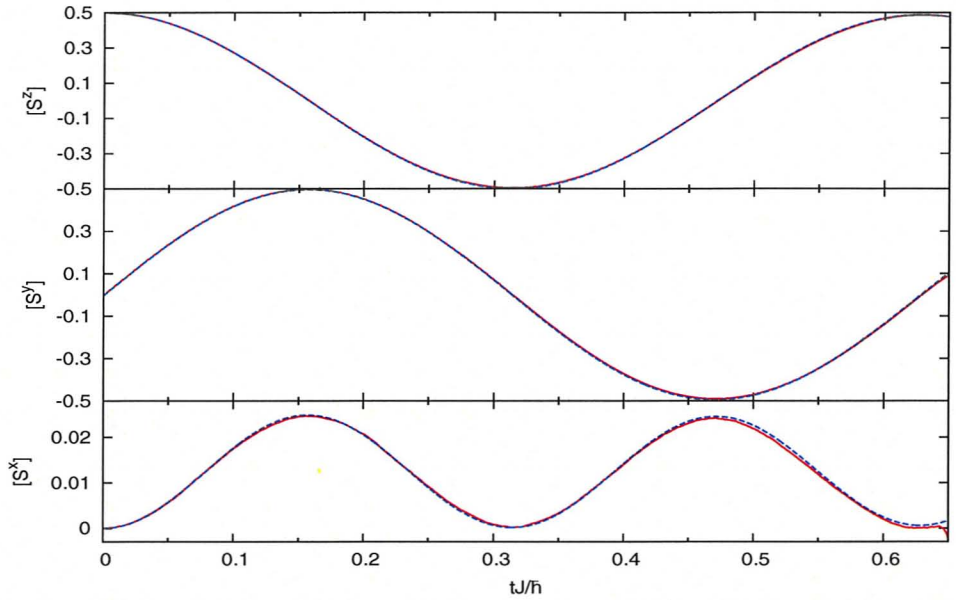

Figure 4.2: TFIM for $N = 4$ spins, following a transverse-field quench at $tJ/\hbar = 0$ from $h/J = 0$ to $h/J = 10.0$, beginning in the FM ground state: $|\uparrow\uparrow \ldots \uparrow\rangle$. From top to bottom: plots of $[S^x], [S^y], [S^z]$ vs $tJ/\hbar$ respectively. The stochastic averages, $\langle\langle . \rangle\rangle$ are given by red solid lines while exact diagonalization results are represented by the blue dashed lines. Simulation parameters: $n_{traj} = 2 \times 10^5, dt = 0.001, \Delta/J = 0.0$. Agreement remains good and results are nearly indistinguishable. The simulations diverge at approximately $tJ/\hbar = 0.65$.

$$[S^y] = \sum_{i=0}^{N-1} \langle \frac{1}{2i}(\hat{a}_i^\dagger \hat{b}_i - \hat{b}_i^\dagger \hat{a}_i)\rangle = \sum_{i=0}^{N-1} \langle\langle \frac{1}{2i}(\alpha_i^+ \beta_i - \beta_i^+ \alpha_i)\rangle\rangle \tag{4.3.2}$$

$$[S^z] = \sum_{i=0}^{N-1} \langle \frac{1}{2}(\hat{a}_i^\dagger \hat{a}_i - \hat{b}_i^\dagger \hat{b}_i)\rangle = \sum_{i=0}^{N-1} \langle\langle \frac{1}{2}(\alpha_i^+ \alpha_i - \beta_i^+ \beta_i)\rangle\rangle \tag{4.3.3}$$

The initial state of the system was taken to be the classical ferromagnetic state: $|\uparrow\uparrow \ldots \uparrow\rangle$ and the dynamics were observed for $tJ/\hbar \geq 0$ during which a transverse field is applied. The results for the TFIM are shown in Fig. 4.1 and Fig. 4.2 for different field strengths while the results for the isotropic $(\Delta/J = 1.0)$ model are shown in Fig. 4.3 and Fig. 4.4. Both models show good agreement with exact diagonalization calculations.

The only drawback of the PPR is that the simulations are usually valid only for relatively short lifetimes (roughly $tJ/\hbar \sim 0.45 - 0.65$ for the models examined) before sampling errors caused by diverging trajectories take over. In Fig. 4.1 for example, the onset of the effects of diverging trajectories can be seen at around $tJ/\hbar \sim 0.58$ where a deviation of the SDE results and exact calculations begin to appear. However, for the time scales where the simulations remain finite, it does yield good results.

One should not be alarmed as this is a common problem associated in using the PPR (as mentioned in section 2.8) and can be attributed to the nature of the SDEs derived and not due to a non-converging numerical algorithm [31, 36, 49]. In fact, Deuar[38] examined

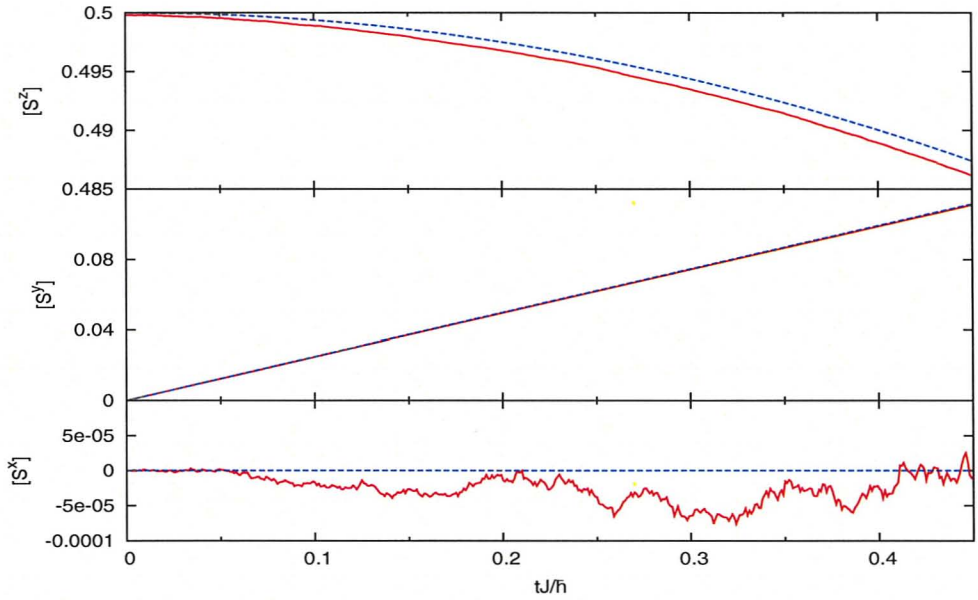

Figure 4.3: Isotropic Heisenberg model for $N = 4$ spins, following a transverse-field quench at $tJ/\hbar = 0$ from $h/J = 0.0$ to $h/J = 0.5$, beginning in the FM ground state: $|\uparrow\uparrow \ldots \uparrow\rangle$. FM interactions assumed: $sign(J) = +1$. From top to bottom: plots of $[S^x], [S^y], [S^z]$ vs $tJ/\hbar$ respectively. The stochastic averages, $\langle\langle . \rangle\rangle$ are given by red solid lines while exact diagonlization results are represented by the blue dashed lines. Simulation parameters: $n_{traj} = 10^6, dt = 0.001, \Delta/J = 1.0$. Agreement remains good and results are nearly indistinguishable. The simulations diverge at approximately $tJ/\hbar \sim 0.45$.

this issue thoroughly when applying the PPR to the exact dynamics of many-body systems. If we abide by Deuar's findings strictly (c.f. eq. 2.8.1 and 2.8.2), we see that there are no drift and noise divergences present in the SDEs in eq. 4.1.12 - 4.1.15. However, we suspect drift terms of the form $\sim iX_i \left[(\mp n^{\alpha}_{i+1} \pm n^{\beta}_{i+1}) + (n^{\alpha}_{i-1} \pm n^{\beta}_{i-1}) \right]$, where $X_i = \alpha_i, \alpha_i^+, \beta, \beta^+$ can be problematic. This is because if we take into consideration the translational symmetry of the system, then we can approximately say that

$$iX_i \left[\left(\mp n^{\alpha}_{i+1} \pm n^{\beta}_{i+1} \right) + \left(\mp n^{\alpha}_{i-1} \pm n^{\beta}_{i-1} \right) \right] \approx 2iX_i \left(\mp n^{\alpha}_{i} \pm n^{\beta}_{i} \right), \tag{4.3.4}$$

which now clearly exhibits offending terms [38] that cause trajectories to escape to infinity, since now $dX_i \sim X_i^2 [\ldots] dt + \ldots$ (see eq. 2.8.1 and eq. 2.8.2).

One should not discount the PPR however. In 2005, the gauge-P representation [37, 38, 49–51] was developed to specifically deal with such drift instabilities. In the gauge-P representation, arbitrary gauge functions, $\{g_k\}$ can be introduced into the SDEs whose effect is a modification of the deterministic evolution. This can be done at the expense of introducing another stochastic variable, Ω (in $\hat{\Lambda}$), which manifests itself as a weight term when calculating stochastic averages. To be more specific, using the gauge-P representation[37],

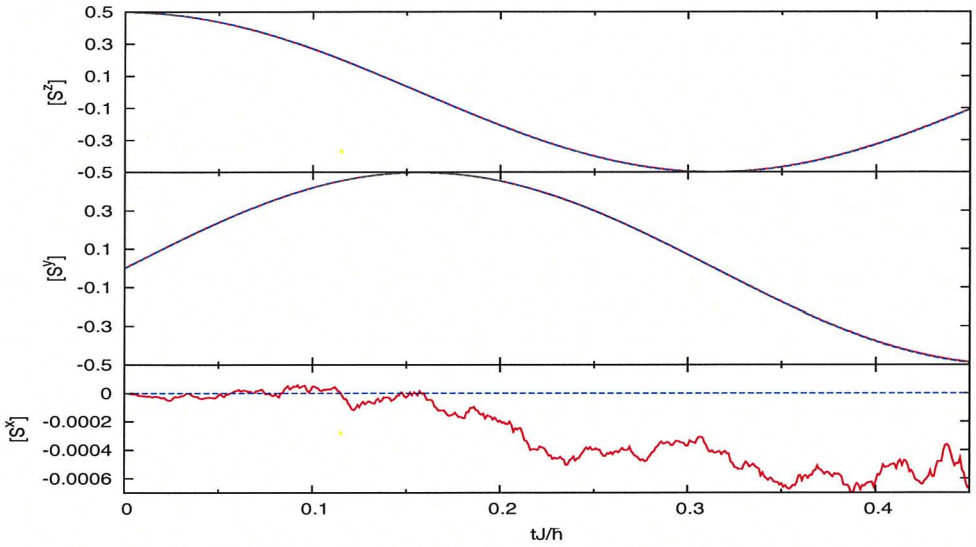

Figure 4.4: Isotropic Heisenberg model for $N = 4$ spins, following a transverse-field quench at $tJ/\hbar = 0$ from $h/J = 0.0$ to $h/J = 10.0$, beginning in the FM ground state: $|\uparrow\uparrow \ldots \uparrow\rangle$. FM interactions assumed: $sign(J) = +1$. From top to bottom: plots of $[S^x], [S^y], [S^z]$ vs $tJ/\hbar$ respectively. The stochastic averages, $\langle\langle . \rangle\rangle$ are given by red solid lines while exact diagonlization results are represented by the blue dashed lines. Simulation parameters: $n_{traj} = 10^5, dt = 0.001, \Delta/J = 1.0$. Agreement remains good and results are nearly indistinguishable. The simulations diverge at approximately $tJ/\hbar \sim 0.45$.

the Ito SDEs are altered such that:

$$d\alpha_i = \left(A_i^+ - g_k B_{jk}\right) dW_k \tag{4.3.5}$$

$$d\Omega = \Omega \left(V dt + g_k dW_k\right), \tag{4.3.6}$$

where summation over k is implied and V is the constant term that may appear, after one substitutes the correspondence relations into an equation of motion for $\hat{\rho}$.

The gauge-P representation has been very successful in simulating the dynamics of many-mode bose gases [21, 22, 52] partly because such systems result in neat diagonal noise matrices that are easier to handle as seen in eq. 4.3.5. However, it is obviously not as straightforward to apply it in our case as we have a much more complicated non-diagonal noise matrix. This makes calculating Stratonovich correction terms messy even with the help of Mathematical software, thus being impractical for numerical simulations. We believe that the application of the gauge-P is possible in principle but requires a bit more thought for Heisenberg systems if using the Schwinger boson approach.

4.3.1 Finite size effects

The main advantage of the PPR is its abilities to overcome the Hilbert space problem and this thesis would be missing a crucial element if we did not discuss this. We first demonstrate the capabilities of the PPR at simulating large system sizes by showing results

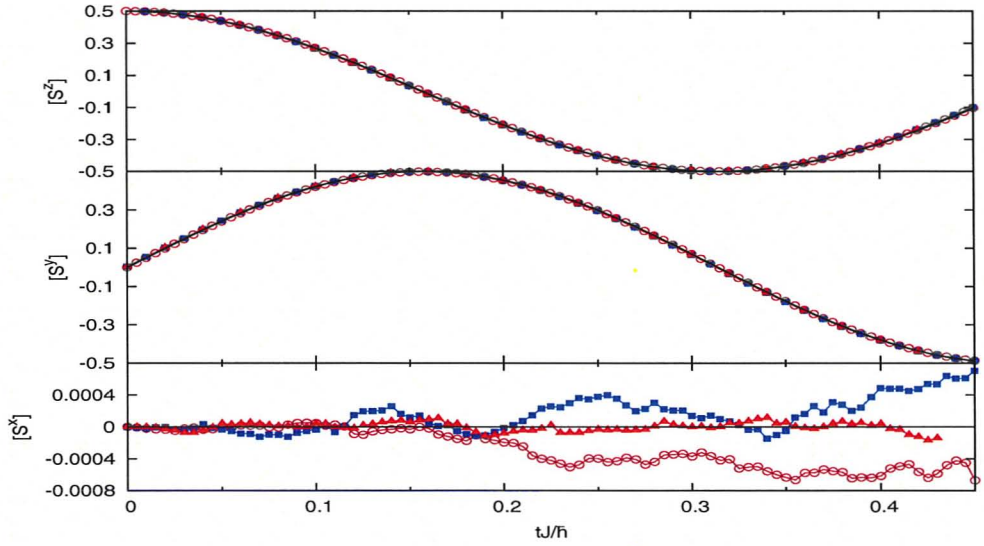

Figure 4.5: Isotropic Heisenberg model following a transverse-field quench at $tJ/\hbar = 0$ from $h/J = 0.0$ to $h/J = 10.0$, beginning in the FM ground state: $|\uparrow\uparrow \ldots \uparrow\rangle$. FM interactions assumed: $sign(J) = +1$. From top to bottom: plots of $[S^x], [S^y], [S^z]$ vs $tJ/\hbar$ respectively. The stochastic averages, $\langle\langle . \rangle\rangle$ are for $N = 4$: (—■—), $N = 10$: (—○—), $N = 100$: (—▲—), while exact diagonlization results for $N = 4$ are represented by the black solid line. Simulation parameters: $n_{traj}^{(N=4)} = 10^5, n_{traj}^{(N=10)} = 2 \times 10^5, n_{traj}^{(N=100)} = 5 \times 10^4, dt = 0.001, \Delta/J = 1.0$. Agreement remains good and finite size effects are negligible. The simulations diverge at approximately $tJ/\hbar \sim 0.45$.

for the FM isotropic Heisenberg case at a field value of $h/J = 10$, prepared in the initial FM state as in Fig. 4.4. As expected, we do not observe any finite size effects within the life time of the stochastic simulations even with a chain consisting of 100 spins. The simulations are compared against the exact diagonalization results for an $N = 4$ system and exhibit identical real time evolution of the spin components as expected for a $1D$ chain with FM interactions, i.e. finite size effects are negligible.

This is not the case for a $1D$ AFM ($sign(J) = -1$) however. In order to verify that finite size effects do exist, we performed $N = 4$ and $N = 10$ exact calculations for the anisotropic AFM with different values of anisotropy: Δ/J. Two sample exact calculations are shown in Fig. 4.6 and Fig. 4.7 respectively for $\Delta/J = -0.8$ and $\Delta/J = -1.5$. For the AFM Heisenberg Hamiltonian, the system is initialized in the classical AFM Neel state: $|\uparrow\downarrow \ldots \uparrow\downarrow\rangle$. An immediate observation is that increasing the value of Δ, reduces the time: t_{finite}, which we define as the time that significant finite size effects are noticeable. A natural thing to do in order to take advantage of the SDES we have derived, is to increase the value Δ/J such that $t_{life} < t_{finite}$, thus allowing us to explore the finite size effects of macroscopically large systems at smaller t_{finite}.

We observe finite size effects through the same observables as in eq. 4.3.1 to eq. 4.3.3. However for the initial Neel state, it is necessary to take into consideration the alternating

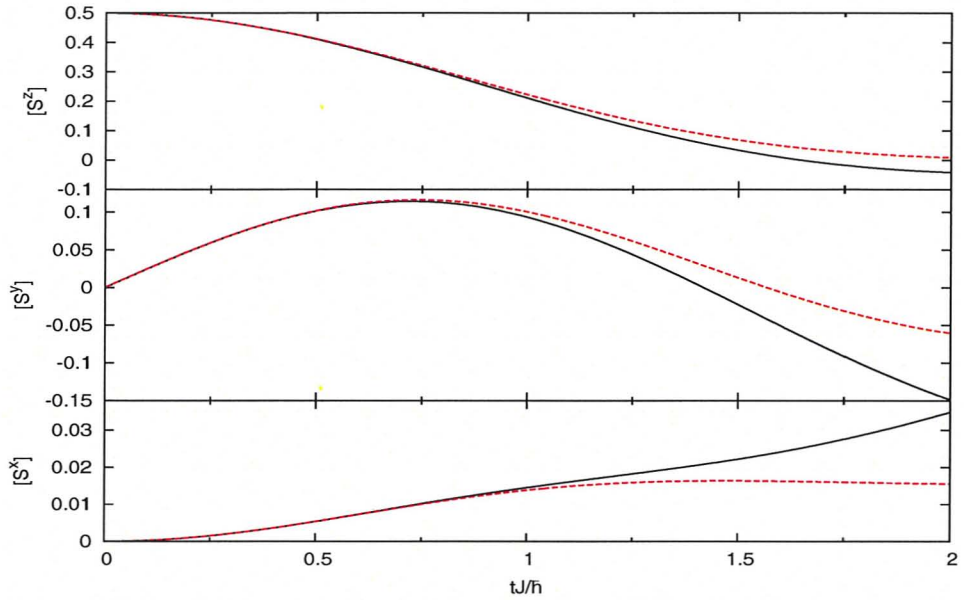

Figure 4.6: Anisotropic Heisenberg model following a transverse-field quench at $tJ/\hbar = 0$ from $h/J = 0.0$ to $h/J = 10.0$, beginning in the AFM Neel state: $|\uparrow\downarrow \ldots \uparrow\downarrow\rangle$. AFM interactions assumed: $sign(J) = -1$. From top to bottom: plots of $[S^x], [S^y], [S^z]$ vs $tJ/\hbar$ respectively. The exact calculations for the $N = 4$ (solid black lines) and $N = 10$ (dashed red lines) are compared. We observe $t_{finite}J/\hbar \sim 0.8$ for $\Delta/J \sim -0.8$

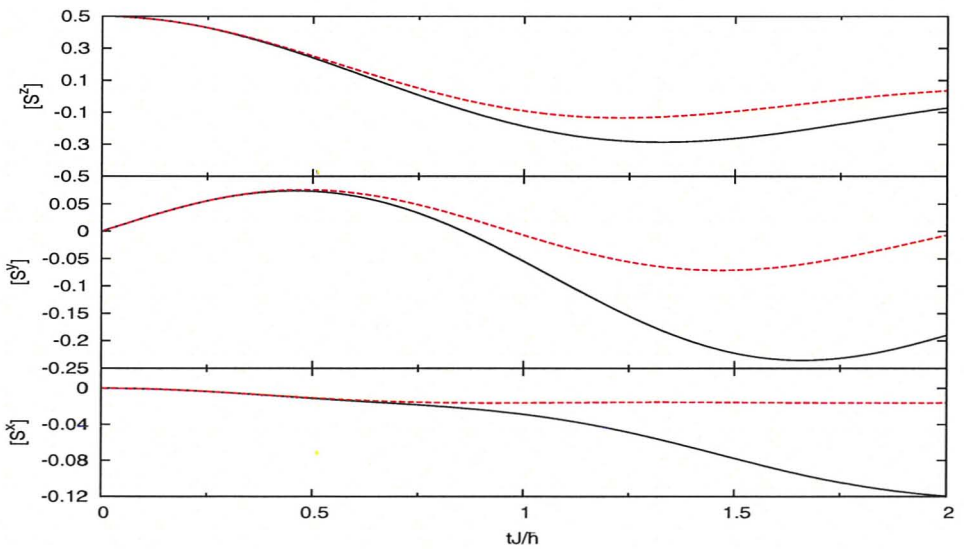

Figure 4.7: Anisotropic Heisenberg model following a transverse-field quench at $tJ/\hbar = 0$ from $h/J = 0.0$ to $h/J = 10.0$, beginning in the AFM Neel state: $|\uparrow\downarrow \ldots \uparrow\downarrow\rangle$. AFM interactions assumed: $sign(J) = -1$. From top to bottom: plots of $[S^x], [S^y], [S^z]$ vs $tJ/\hbar$ respectively. The exact calculations for the $N = 4$ (solid black lines) and $N = 10$ (dashed red lines) are compared. We observe $t_{finite}J/\hbar \sim 0.5$ for a given anisotropy of $\Delta/J \sim -1.5$

sign of spins when calculating the averaged spin components[4], i.e.:

$$[S^x] = \sum_{i=0}^{N-1} \langle \frac{1}{2}(\hat{a}_i^\dagger \hat{b}_i + \hat{b}_i^\dagger \hat{a}_i) \rangle = \sum_{i=0}^{N-1} \langle\langle \frac{1}{2}(\alpha_i^+ \beta_i + \beta_i^+ \alpha_i) \rangle\rangle, \tag{4.3.7}$$

$$[S^y] = \sum_{i=0}^{N-1} \langle \frac{1}{2i}(-1)^i(\hat{a}_i^\dagger \hat{b}_i - \hat{b}_i^\dagger \hat{a}_i) \rangle = \sum_{i=0}^{N-1} (-1)^i \langle\langle \frac{1}{2i}(\alpha_i^+ \beta_i - \beta_i^+ \alpha_i) \rangle\rangle, \tag{4.3.8}$$

and

$$[S^z] = \sum_{i=0}^{N-1} \langle \frac{1}{2}(-1)^i(\hat{a}_i^\dagger \hat{a}_i - \hat{b}_i^\dagger \hat{b}_i) \rangle = \sum_{i=0}^{N-1} (-1)^i \langle\langle \frac{1}{2}(\alpha_i^+ \alpha_i - \beta_i^+ \beta_i) \rangle\rangle. \tag{4.3.9}$$

Increasing Δ/J however has the adverse effect of decreasing t_{life} significantly. Thus while it is possible to simulate macroscopically large system sizes, we find that the SDE simulations diverge much sooner than t_{finite}. Fig. 4.8 reinforces our claim that t_{finite} decreases with Δ/J as no finite size effects are observed up to $tJ/\hbar = 1$, in sharp comparison to Fig. 4.5 and Fig. 4.6. Our last effort to observe finite size effects was to increase Δ/J to -1.2 with hopes that $t_{life} > t_{finite}$. As seen in Fig. 4.9, our simulations do not survive beyond t_{finite}. Since t_{finite} depends on the anisotropy Δ/J, increasing the system size while possible will result in t_{life} of the same order. In general, we find that $\uparrow \Delta/J \longrightarrow \downarrow t_{life}, \downarrow t_{finite}$ such that $t_{life} < t_{finite}$. This thwarts our efforts on examining finite size effects for the AFM case. We suspect the following points as possible culprits:

1. The Δ terms in the SDEs (see section 4.2) may contain drift instabilities as well, however we are unsure of what gauge functions to employ to cull them
2. The initial distribution for the initial AFM state may be much broader than that of the FM state and as the distribution broadens due to the diffusion term in the FPE, the boundaries of phase space are more likely to be explored, resulting in numerical spikes.

Furthermore, we find that using an initial Neel state results in poor convergence for the observable: $[S^x]$ as seen in Fig. 4.8, compared to an initial FM ground state and it is likely that we have used an insufficient number of trajectories in our simulations. Simulations employing a larger number of trajectories than 10^6 are currently being run but will unfortunately not complete within the time of this thesis' writing. Nevertheless, we have demonstrated the applicability of the PPR to AFM systems.

[4]Note that there is no need to account for a sign change for the observable: $[S_x]$

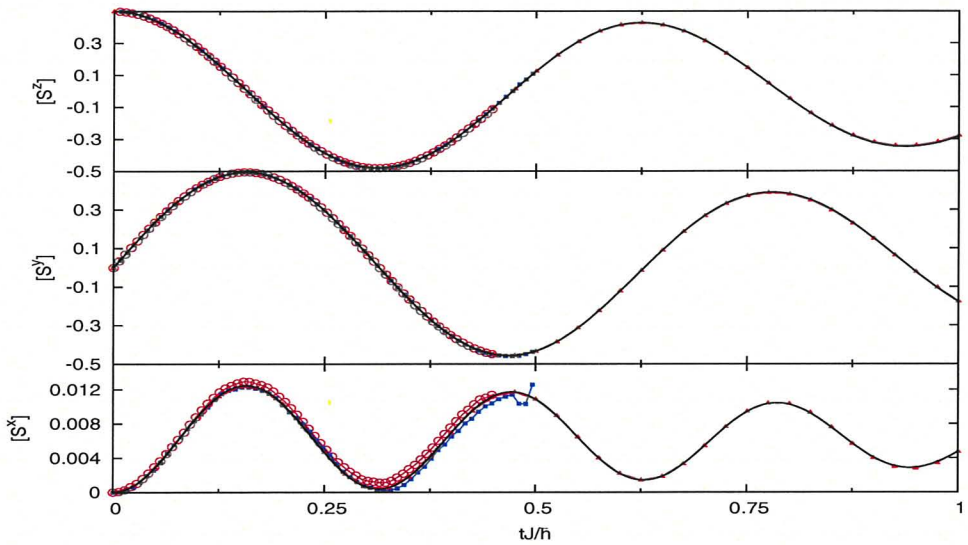

Figure 4.8: Anisotropic Heisenberg model following a transverse-field quench at $tJ/\hbar = 0$ from $h/J = 0.0$ to $h/J = 10.0$, beginning in the AFM ground state: $|\uparrow\downarrow \ldots \uparrow\downarrow\rangle$. AFM interactions assumed: $sign(J) = -1$. From top to bottom: plots of $[S^x], [S^y], [S^z]$ vs $tJ/\hbar$ respectively. The stochastic averages, $\langle\langle . \rangle\rangle$ are for $N = 4$:(—■—)and $N = 10$:(—○—), while exact diagonalization results are for $N = 4$: (black solid lines) and $N = 10$: (—▲—). Simulation parameters: $n_{traj}^{(N=4)} = 10^6, n_{traj}^{(N=10)} = 10^5, dt = 0.001, \Delta/J = -0.5$. Agreement remains good and finite size effects are unnoticeable up to $tJ\hbar = 1$. The SDEs diverge at $t_{life}J/\hbar \sim 0.48$.

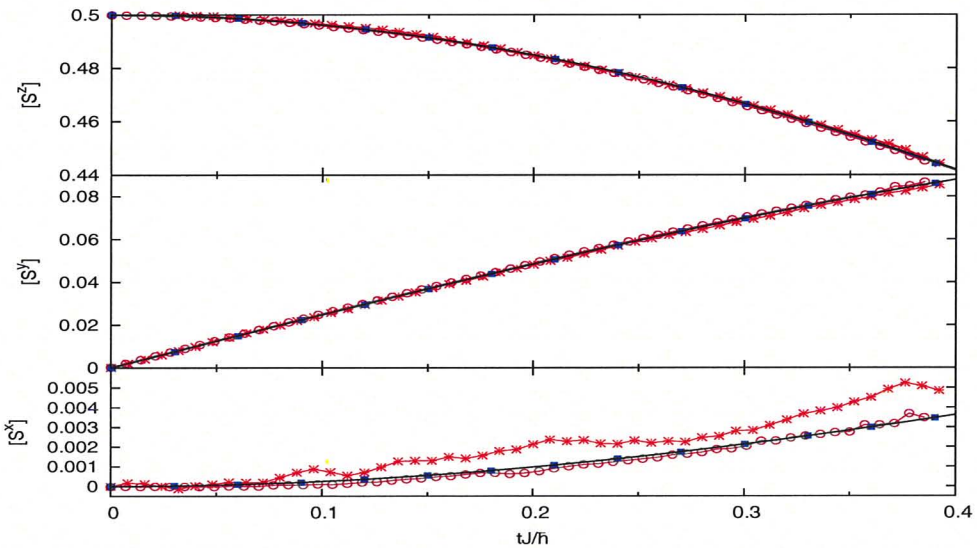

Figure 4.9: Anisotropic Heisenberg model following a transverse-field quench at $tJ/\hbar = 0$ from $h/J = 0.0$ to $h/J = 0.5$, beginning in the AFM ground state: $|\uparrow\downarrow \ldots \uparrow\downarrow\rangle$. AFM interactions assumed: $sign(J) = -1$. From top to bottom: plots of $[S^x], [S^y], [S^z]$ vs $tJ/\hbar$ respectively. The stochastic averages, $\langle\langle . \rangle\rangle$ are for $N = 4$:(—○—)and $N = 10$:(—✳—), while exact diagonalization results are for $N = 4$: (black solid lines) and $N = 10$: (—■—). Simulation parameters: $n_{traj}^{(N=4)} = 10^6, n_{traj}^{(N=10)} = 10^5, dt = 0.001, \Delta/J = -0.8$. Finite size effects are unnoticeable at $t_{life}J/\hbar \sim 0.4$.

Chapter 5

Conclusion

The main thrust of this research was to illustrate how the real-time quantum quench dynamics of spin systems can be simulated via the use of SDEs. The number of spins in a real system are macroscopically large and therefore generally impossible to solve numerically, let alone analytically. We embarked on a novel approach to solving the dynamics of such spin systems by using the quantum phase space method known as the PPR. The PPR is only applicable to Hamiltonians comprising of bosonic annihilation and creation operators and so to proceed, it is necessary to have a bosonic representation of the spin operators. We found that the most convenient way of doing this was to use Schwinger representation of spin.

In doing so, we showed that substituting the PPR for the density operator and the correspondence relations into the Master equation yields an FPE, after integrating by parts and ignoring boundary terms. This FPE can then be equivalently represented in terms of a set of coupled complex Ito SDEs. The number of SDES scales linearly with N, thereby making the simulation of such many-body systems tractable. In this formalism, the quantum mechanical expectation values of normal-ordered operators can be replaced by stochastic averages (in the limit that an infinite number of trajectories are used) of their corresponding complex phase space functions, which are much simpler to calculate.

In this thesis, we first simulated the quench dynamics of the average spin components, $[S^x], [S^y], [S^z]$, for two variants of the Heisenberg model, i.e. the TFIM and the isotropic Heisenberg model. Our stochastic simulation results were verified against exact diagonalization calculations to show good agreements. In both instances, we assumed ferromagnetic interactions, $J > 0$ in eq. 4.1.1 and at $t < 0$, initialized both models in the classical ferromagnetic ising chain ground state: $|\uparrow\uparrow \ldots \uparrow\rangle$. At $t \geq 0$, the transverse-field and anisotropy was turned on and the system allowed to evolve.

In order to observe finite size effects of the lattice, we simulated the quantum quench dynamics of the AFM anisotropic Heisenberg model beginning in the classical Neel state. Using exact diagonalization calculations, we demonstrated that finite size effects can be

expected at a certain time scale: t_{finite}, which has been empirically shown to depend on the anisotropy: Δ/J. In general making Δ/J more negative, decreases t_{finite} as well as the $t_{lifetime}$. Unfortunately, the relation is such that $t_{finite}J/\hbar > t_{life}J/\hbar$ for all values of Δ/J. Our bare simulations are therefore unable to detect finite size effects of the lattice. Within the time scales of t_{life} however, they do indeed produce good agreement with the exact calculations. We would finally like to point out that initializing the system in a Neel state requires much more trajectories than the classical FM state to attain convergence, however we are still unclear as to why this is the case.

The main drawback of the positive-P representation however, is its notoriously short life time, t_{life}, which prevents us from obtaining useful results beyond a certain time. For the TFIM and the isotropic Heisenberg model, we found a bare application of the PPR to have $t_{life}J/\hbar \sim 0.45 - 0.65$, whereas for anisotropic AFM chains beginning in the Neel state, $t_{life}J/\hbar$ was reduced to < 0.4 depending on the value of Δ/J. We suspect that this is due to drift instability terms present in the SDEs that cause trajectories to make large excursions into the boundaries of phase space within this time scale. If this was the case, then the neglect of boundary terms which we made after the step of partial integration is no longer valid and the entire formalism breaks down.

5.1 Future work

5.1.1 Extension of t_{life}: gauge-P representation and diffusion gauges

An obvious future direction of our research involves applying the gauge-P representation in a bid to extend simulation life times. The gauge-P representation was formulated for the exact purpose of dealing with drift instabilities (see section 4.3). In fact, we have looked into this and carefully chosen appropriate gauge functions, that we believe will suppress the drift divergences for the TFIM case. As all our simulations have to be carried out with the Stratonovich version of SDEs, it is necessary to be able to calculate Stratonovich correction terms. For our non-diagonal complicated looking noise matrix, this is no longer a trivial task and is still currently under research. For the anisotropic case however, we have yet to come up with reasonable gauge functions and is another point of interest.

Another possible way to overcome the aforementioned problem is by using diffusion gauges [31]. This method takes advantage of the ambiguity of the noise matrix in order to reduce sampling errors. It is not clear to us at the moment how to use this explicitly but Plimak et al [31] has shown remarkable results using diffusion gauges to extend t_{life} of the real time dynamics of an anharmonic oscillator. If the gauge-P representation is successful, we intend to tackle more complicated problems such as 2D lattices with different geometries, and presumably preparing the system in different initial states with antiferromagnetic exchanges.

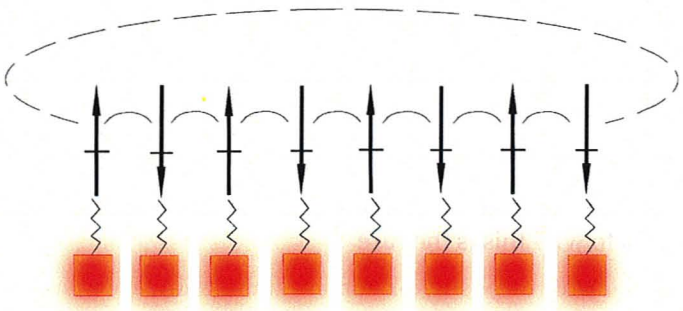

Figure 5.1: Schematic diagram of the Heisenberg spin system coupled to isolated single mode bosonic baths .

5.1.2 Heisenberg spin-boson Model

Another interesting problem which we intend to look into, is the generalization of the spin-boson model to extended systems. The traditional spin-boson model [53] explores the dynamics of a single spin coupled to its environment which could be modeled as either a bath of harmonic oscillators or spins. However, there has not been any research exploring the dissipative dynamics of an extended system, such as the Heisenberg model, coupled to its environment (see fig. 5.1). The work we have presented in this thesis provides a starting point for this problem and allows a simple generalization of the Hamiltonian to include a bosonic bath to describe a Heisenberg spin-boson model. As a first attempt, we will assume that the spins are coupled to their own single-mode baths as shown in fig. 5.1 and is described by a Hamiltonian which takes the form:

$$\hat{H} = -J \sum_{\langle i,j \rangle} \hat{\mathbf{S}}_i . \hat{\mathbf{S}}_j - h \sum_i \hat{S}_i^x + \sum_i \omega_i \hat{a}^{(i)\dagger} \hat{a}^{(i)} + \frac{g_i}{2} \sum_i \hat{S}_i^z \left(\hat{a}^{(i)\dagger} + \hat{a}^{(i)} \right), \tag{5.1.1}$$

where g_i is measures the coupling of the i-th spin to its bosonic bath. SDEs including the single mode bath have already been derived but have yet to be numerically simulated.

5.1.3 Dynamics in imaginary time.

The last possible extension of this project would be the simulation of the system in imaginary time. Formally, one assumes the system to be described by a statistical mechanical ensemble, such as the canonical ensemble and derive an equation of motion for $\hat{\rho}$ in imaginary time (or inverse temperature) $\tau = 1/\beta$. By evolving the system in τ, it allows us to obtain the equilibrium statistics of the system at lower temperatures. This technique has been successfully applied by Ghabari et al [21] on the Bose-Hubbard model. They assume an unnormalized grand canonical ensemble, i.e.:

$$\hat{\rho} = e^{\tau \hat{K}}, \tag{5.1.2}$$

where $\hat{K} = \hat{H} - \mu\hat{N}$, and evolve it in τ according to the equation of motion:

$$\frac{\partial\hat{\rho}}{\partial\tau} = -\frac{1}{2}\left[\frac{\partial\hat{K}\tau}{\partial\tau}, \hat{\rho}\right]_+, \tag{5.1.3}$$

where $[\ldots,\ldots]_+$ stands for an anticommutator. Also, note that eq. 5.1.3 holds, provided that $\left[\frac{\partial\hat{K}}{\partial\tau}, \hat{K}\right]$ is true.

5.2 Final remarks

We present extremely preliminary results in this thesis as it was only recently that we successfully implemented the Schwinger bosons with the PPR. Nonetheless, we are very optimistic in the potential capabilities of this approach. Should the gauge-P representation manage to extend simulation life times, the PPR presents itself as a potential state-of-the-art method that may surpass traditional methods and easily overcome the Hilbert space problem. At the very least, it will allows us to explore the dissipative dynamics of extended spin systems, which has never been done before.

Appendix A

An abridged introduction to stochastic differential equations

This Appendix provides a brief review of Fokker-Planck equations (FPEs) and stochastic differential equations (SDEs) and explains how a correspondence between them exist. As this is a central theme of the PPR, it is worthwhile to spend some time familiarizing oneself with the mathematics. To make things less technical, most of the examples in this chapter will be carried out in $1D$ with their multi-dimensional generalization simply stated. The theory of SDEs and FPEs is by no means trivial and we will only provide the bare essentials necessary to understand this thesis. The interested reader can refer to standard mathematical textbooks such as [35] (which is dedicated solely to the Fokker-Planck Equation) and [18] (which is an introductory text on SDES) for a more detailed and rigorous treatment.

A.1 The Fokker-Planck equation

The Fokker-Planck Equation is simply defined as an equation of motion for a conditional probability density $P(\vec{x}, t|\vec{x}_o, 0)$ and has the generic form:

$$\frac{\partial}{\partial t}P(\vec{x}, t|\vec{x}_o, 0) = \left(-\sum_{i=1}^{N} \frac{\partial}{\partial x_i} A_i(\vec{x}) + \frac{1}{2} \sum_{i,j=1}^{N} \frac{\partial^2}{\partial x_i \partial x_j} D_{ij}(\vec{x}) \right) P(\vec{x}, t|\vec{x}_o, 0), \tag{A.1.1}$$

where $\vec{x}_i = (x_1, x_2, \ldots, x_N)$ is a vector of n random variables. $\vec{A}(\vec{x})$ is called the drift vector and $\mathbf{D}(\vec{x})$ is called the diffusion matrix which is semi positive-definite and symmetric by definition. In principle, if one is able to solve for the probability distribution: $P(\vec{x}, t|\vec{x}_o, 0)$ subject to the initial condition $\vec{x}(t = 0) = \vec{x}_o$ then it would be possible to calculate the expectation values of any arbitrary function of $\vec{x}$, $f(\vec{x})$ for all times, using the formula:

$$\langle f(\vec{x}(t),t)\rangle = \int d\vec{x}P(\vec{x},t|\vec{x}_o,0)f(\vec{x}). \tag{A.1.2}$$

What we are interested in calculating in particular, are moments of arbitrary order: $(\prod_{i=1}^{N} x_i)^{n_i}$ for all times where n_i indicates the order of the moment of the variable x_i. Using eq. A.1.2, this is given by the formula

$$\langle \prod_{i=1}^{N}(x_i)^{n_i}\rangle = \int d\vec{x}P(\vec{x},t|\vec{x}_o,0)\prod_{i=1}^{N}(x_i)^{n_i} \tag{A.1.3}$$

A.1.1 The one-dimensional FPE

One can imagine that solving an FPE can prove to be a highly non-trivial task and it is not always possible to find an analytic solution. As we will see there are ways around this, but to gain some physical insight regarding the FPE, we will just examine the $1D$ case and omit unnecessary mathematical details which can be found in [29]. Let us begin by stating the $1D$ version of eq. A.1.1:

$$\frac{\partial P(x)}{\partial t} = \left[-\frac{\partial}{\partial x}A(x) + \frac{1}{2}\frac{\partial^2}{\partial x^2}D(x)\right]P(x). \tag{A.1.4}$$

What we would like to do is to illustrate the physical relevance of $A(x)$ and $\mathbf{D}(x)$. First we will calculate the mean of the random variable, x which is given by

$$\langle x(t)\rangle = \int_{-\infty}^{\infty} dxP(x,t)x \tag{A.1.5}$$

and obeys the equation of motion

$$\begin{aligned}
\frac{d}{dt}\langle x(t)\rangle &= \int_{-\infty}^{\infty} dx\frac{d}{dt}P(x,t)x & \text{(A.1.6)}\\
&= -\int_{-\infty}^{\infty} dx\frac{\partial}{\partial x}\left[A(x)P(x,t)\right]x + \frac{1}{2}\int_{-\infty}^{\infty} dx\frac{\partial^2}{\partial x^2}\left[D(x)P(x,t)\right]x\\
&= \int_{-\infty}^{\infty} A(x)P(x,t)dx\\
&= \langle A(x)\rangle, & \text{(A.1.7)}
\end{aligned}$$

where we substituted eq. A.1.4 into eq. A.1.4 and performed an integration by parts. We also made the assumption that $P(x,t)$ and its derivatives vanish sufficiently rapidly at $x \to \infty$ so that boundary terms can be safely ignored. If we wish to proceed explicitly, we need to specify the drift term of the FPE. However, we can already see that the evolution of the mean of the distribution $P(x,t)$ depends solely on $A(x)$ (i.e. $\mathbf{D}$ does not appear). This explains why $A(x)$ is called the drift term, i.e. it is the term that causes a "drift" in the peak[1] of the probability distribution. As an explicit example, let us consider the case of a

[1] Location of the mean

linear FPE which is defined to have: $A(x) = Ax$ and D =constant. The solution for the mean value of x can be obtained by solving eq. A.1.6, which is obviously given by

$$\langle x(t)\rangle = \langle x(0)\rangle e^{At}. \tag{A.1.8}$$

For a linear FPE then, a constant A causes an exponential decay ($A < 0$) or growth ($A > 0$) of the value of $\langle x\rangle$ thereby causing a shift in the distribution with time.

On the other hand, the physical interpretation of the diffusion term can be made clear by calculating the width of the distribution which is quantified by the variance, $\langle\sigma^2(t)\rangle$:

$$\langle\sigma(t)^2\rangle = \langle x(t)^2\rangle - \langle x(t)\rangle^2. \tag{A.1.9}$$

We can carry out a similar calculation as in eq. A.1.6 for the second moment of x to get:

$$\begin{aligned}\frac{d}{dt}\langle x^2\rangle &= \int_{-\infty}^{\infty} dx \frac{dP(x,t)}{dt} x^2 \\ &= 2\langle xA(x)\rangle + \langle D(x)\rangle.\end{aligned} \tag{A.1.10}$$

Using eq. A.1.10 then, we can derive an equation of motion for $\langle\sigma^2(t)\rangle$:

$$\begin{aligned}\frac{d}{dt}\sigma(t)^2 &= \frac{d}{dt}\left[\langle x^2\rangle - \langle x\rangle^2\right] \\ &= 2\langle xA(x)\rangle - 2\langle x\rangle\langle D(x)\rangle + \langle D(x)\rangle.\end{aligned} \tag{A.1.11}$$

For simplicity, if we imagine a probability distribution centered initially at $x(0) = 0$ and no drift term ($A = 0$), we see that:

$$\frac{d}{dt}\sigma(t)^2 = \langle D(x)\rangle, \tag{A.1.12}$$

which implies that the evolution of the width of the distribution depends on the $D(x)$, hence the name "diffusion matrix". For a linear FPE (i.e. constant D and $A(x) = Ax$), eq. A.1.11 has the solution (see [29]):

$$\langle\sigma(t)^2\rangle = \sigma(0)^2 e^{2At} - \left(\frac{D}{2A}\right)\left(1 - e^{2At}\right) \tag{A.1.13}$$

and for the case of an initially sharp distribution where $\langle\sigma(0)\rangle = 0$, we see that the time evolution of the width of the distribution depends on a competition between D and A. For $D > 0, A < 0$, D acts as a source for fluctuations and causes broadening as is intuitively expected for a "diffusion term".

A.2 Stochastic differential equations

So far we have seen that an FPE describes the dynamics of the conditional probability distribution, $P(x,t)$ of a random variable, x. Once solved, it allows us to calculate the time

dependent average value $\langle x(t) \rangle$, which can be interpreted as the average of repeated samplings from independent experiments. An interesting question to be raised is: Is it possible to find a set of differential equations whose solutions generate independent trajectories of $x(t)$, representative of a single, unique experimental observation. In which case, it would allow us to get around the arduous task of solving an FPE, thus providing the motivation of using stochastic differential equations. The SDEs provide an equivalent way of describing the FPE in the sense that averages calculated from either method are identical. We will examine SDEs in more detail in A.2.1 where we carry out a brief review of stochastic differential equations before examining their correspondence with the FPE.

A.2.1 What is an SDE?

We are all surely familiar with the concept of an ordinary differential equation (ODE), for example in $1D$

$$dx(t) = \bar{A}(x(t), t)dt \tag{A.2.1}$$

which has a well-defined trajectory[2] in time, regardless of how many times we choose to numerically simulate $x(t)$. We will therefore call $\bar{A}(x(t))$ in eq. A.2.1 a deterministic term. An SDE on the other hand, comprises of two components, namely a deterministic term, $A(x(t))$ and a noise term, $B(x(t))$, and takes the general form:

$$dx(t) = A(x(t))dt + B(x(t))dW(t). \tag{A.2.2}$$

$dW(t)$ introduces irregularity in the system by acting as a source of fluctuations, whose properties are only defined probabilistically. This means that we need to specify its mean, variance and correlations with noise terms at different times. This issue will be addressed in section A.2.2.

For an SDE then, the same initial condition: $x(0)$ will result in an infinite number of realizations of $x(t)$ due to the random (or stochastic) nature of $dW(t)$. Individually, each trajectory has little significance, and what we are interested in is an average over many equally-weighted trajectories called a stochastic average. Using SDEs, the stochastic averages are computed using the simple formula:

$$\langle\langle x(t) \rangle\rangle = \frac{\left(\sum_{i=1}^{N_{exps}} x_i(t)\right)}{N_{exps}}, \tag{A.2.3}$$

where $x_i(t)$ represents different realizations of $x(t)$ trajectories and N_{exps} is the total number of trajectories we are averaging over[3]. What we are looking for then is to define stochastic noise fluctuations $dW(t)$ such that the following correspondence can be made:

$$\langle O(x(t)) \rangle_{FPE} = \langle\langle O(x(t)) \rangle\rangle \tag{A.2.4}$$

[2] Assuming the same initial condition is used, of course.

[3] Note that we denote stochastic averages with: $\langle\langle \cdot \rangle\rangle$ instead of single brackets. $\langle \cdot \rangle$ may be used for stochastic averages as well but it will be apparent from the context in which it is used

where $O(x(t))$ is any function of $x(t)$. If this were possible, then one could simply work with SDEs like eq. A.2.2 which is usually much simpler than solving an FPE. Especially since the latter usually involves complicated multi-dimensional partial differential equations which are not usually analytically accessible and difficult to solve even on computer.

A.2.2 The Wiener increments

It turns out that the increments $dW(t)$ that we are interested in (see eq. A.2.2), are known as Wiener increments or white noise terms which have the following statistical properties:

$$\langle dW(t) \rangle = 0 \tag{A.2.5}$$
$$\langle dW(t_i) dW(t_j) \rangle = \delta(t_i - t_j) dt. \tag{A.2.6}$$

In the multi-dimensional case, where we have a vector of Wiener increments, $\vec{dW}(t) = \langle dW_1(t), dW_2(t), \ldots \rangle$ instead, we have the relation:

$$\langle dW_i(t) \rangle = 0 \tag{A.2.7}$$
$$\langle dW_k(t_i) dW_l(t_j) \rangle = \delta(t_i - t_j)\delta_{kl} dt. \tag{A.2.8}$$

We can calculate the variance of dW_i at a given time, t using eq. A.2.7 and eq. A.2.8 to get:

$$\begin{aligned} \langle dW_i(t)^2 \rangle - \langle dW_i(t) \rangle^2 &= \langle dW_i(t)^2 \rangle \\ &= dt, \end{aligned} \tag{A.2.9}$$

which tells us that Wiener increments can be easily simulated if we are able to generate a random variable with mean 0 and variance dt, or in terms of a standard normal distribution: $N(0,1)$[4]:

$$dW_i(t) = N(0, dt) \sim \sqrt{dt} N(0,1) \tag{A.2.10}$$

where we have used the property of normal random variables that:

$$aX + b \sim N(a\mu + b, a^2\sigma^2) \tag{A.2.11}$$

given that $X \sim N(\mu, \sigma^2)$. Fortunately, generating standard normal random variables in computers can be done quickly and trivially, as numerous algorithms are available.

A.2.3 Ito vs Stratonovich SDEs

Stochastic differential equations are quite different from ODEs, not only because of the inclusion of stochastic noise terms as in eq. A.2.2. Unlike ODES, depending on the instant in time, τ_i

[4]We denote a normal variable using the convention $N(\mu, \sigma^2)$ where μ is the mean and σ^2 is the variance.

$$\tau_i = t_i + \alpha \Delta t, \tag{A.2.12}$$

where $\alpha \in [0,1]$, at which we evaluate the noise terms of SDEs, will generate quantitatively and possibly qualitatively different results. $\alpha = 1$ corresponds to the explicit case and $\alpha = 0$ corresponds to the fully implicit case i.e., an Euler-type approach. Suppose we are dealing with ordinary differential calculus, and now consider the differential equation of some variable $x(t), t \in [t_0, t_N]$:

$$dx(t_i) = x(t_i + \Delta t) - x(t_i) = A(x(\tau_i))\Delta t, \tag{A.2.13}$$

where we break up the time domain into N equal time slices of length $\Delta t = (t_N - t_0)/N$. Also, let us evaluate the RHS of eq. A.2.13 at the instant in time: $\tau_i = t_i + \alpha t_i$, which lies in the interval $[t_i, t_{i+1}]$. Regardless of the value of $\alpha \in [0,1]$, the trajectory of $x(t)$ does not change. Different values of α results in different numerical schemes with higher order error corrections in dt but does not affect the quantitative or qualitative behavior of the trajectory. Therein lies the difference. In stochastic calculus, different choices of α will result in completely different behaviors both quantitatively and possibly qualitatively. Let us illustrate this point with a simple example.

Consider the following stochastic differential equation [5] for X_i

$$dX_i = X_{i+1} - X_i = A(X_i)dt + B(X_i)dW_i \tag{A.2.14}$$

or

$$X_{i+1} = X_i + A(X_i)dt + B(X_i)dW_i \tag{A.2.15}$$

where the subscript i denotes the i-th time step. This SDE corresponds to the choice $\alpha = 0$ and is known as an ***Ito SDE***. The noise term, $B(X_i)$ is a function of X_i and therefore depends only on the variables, X_j and dW_j for $j = 0 \ldots i-1$ which are all independent of present noise term, dW_i. Thus for an Ito SDE, the stochastic average of X_i is easy to calculate:

$$\begin{aligned} d\langle X_i \rangle &= \langle A(X_i) \rangle dt + \langle B(X_i) dW_i \rangle \\ &= \langle A(X_i) \rangle dt + \langle B(X_i) \rangle \langle dW_i \rangle \\ &= \langle A(X_i) \rangle dt \end{aligned} \tag{A.2.16}$$

where we have used the statistical independence of $B(X_i)$ and dW_i as well as eq. A.2.7 in the second line of eq. A.2.16.

Now if we were to evaluate the noise term of the SDE in eq. A.2.14 at the mid-point interval (corresponding to $\alpha = 1/2$) however, then we **cannot** make a similar assumption that $\langle B(X_{i+\frac{1}{2}}) dW_i \rangle = \langle B(X_{i+\frac{1}{2}}) \rangle \langle dW_i \rangle$ since B is now being evaluated at a slightly later

[5] Note that we will denote the i-th time step with a subscript for brevity, so $X(t_i) \equiv X_i$ and similarly $dW(t_i) = dW_i$

time and are no longer statistically independent of dW_i. The choice $\alpha = 0.5$ corresponds to another type of stochastic different equation, called the ***Stratonovich SDE***, and is given by:

$$dX_i = X_{i+1} - X_i = A(X_i)dt + B(X_{i+1/2})dW_i. \tag{A.2.17}$$

Our goal now, is to express the Stratonovich SDE in terms of X_i and X_{i+1} so that stochastic averaging as in eq. A.2.16 is possible. To proceed, let us approximate $B(X_{i+1/2})$ by first using linear interpolation to write:

$$X_{i+1/2} = X_i + \frac{1}{2}(X_i + X_{i+1}) \tag{A.2.18}$$

and use it to expand $B(X_{i+1/2})$ to first order in X_i, i.e.

$$\begin{aligned} B(X_{i+1/2}) &= B\left(X_i + \frac{1}{2}(X_{i+1} - X_i)\right) \\ &= B(X_i) + \frac{1}{2}(X_{i+1} - X_i)\frac{dB}{dX}(X_i). \end{aligned} \tag{A.2.19}$$

Substituting eq. A.2.19 into eq. A.2.17 then gives:

$$X_{i+1} = X_i + [A(X_i)]\,dt + \left[B(X_i) + \frac{1}{2}\,(X_{i+1} - X_i)\right] dW_i. \tag{A.2.20}$$

We may, in addition use an Euler-type approximation that

$$X_{i+1} = X_i + dtA(X_i) + B(X_i)dW_i \tag{A.2.21}$$

and substitute eq. A.2.21 into eq. A.2.20 to solve for X_{i+1} explicitly to get:

$$X_{i+1} = X_i + A(X_i)\left[1 + \frac{1}{2}B'(dW_i)\right]dt + B(X_i)dW_i\left[1 + \frac{1}{2}B'(X_i)dW_i\right], \tag{A.2.22}$$

where we have used the following abbreviation for the derivative, i.e. $\frac{dB}{dX}(X_i) \equiv B'(X_i)$.

Now, what we need is to keep terms that are of order dt only. Since on average $\langle dW(t)^2\rangle = dt$ (c.f. e.q. A.2.8) then in this sense, we can say that $dW \sim \sqrt{dt}$. Thus the term $A(X_i)B'dtdW_i$ in eq. A.2.22 is actually of order $dt^{3/2}$ and can be neglected. On the other hand, the term $B(X_i)\frac{1}{2}B'(X_i)dW_i^2$ is of order dt and cannot be neglected. Finally we arrive at the result:

$$X_{i+1} = X_i + dtA(X_i) + B(X_i)dW_i + B(X_i)\frac{1}{2}B'(X_i)dW_i^2, \tag{A.2.23}$$

which upon averaging becomes

$$d\langle X_i\rangle = \langle X_{i+1}\rangle - \langle X_i\rangle = \langle A(X_i) + \frac{1}{2}B(X_i)B'(X_i)\rangle dt, \tag{A.2.24}$$

and is clearly different from the result obtain from the Ito SDE in eq. A.2.16 in the sense that there is a modification of the drift term such that

$$A(X_t) \to A(X_t) + \frac{1}{2}B(X_i)B'(X_i). \tag{A.2.25}$$

A.2.4 Ito vs Stratonovich calculus

Another key difference between Stratonovich and Ito SDEs is that they obey different rules of calculus. Stratonovich SDEs obey the rules of conventional calculus

$$d(XY) = X \circ dY + Y \circ dX \tag{A.2.26}$$

where X and Y are stochastic variables and $\circ$ defines Stratonovich differential equations whereas Ito calculus obeys slightly different rules:

$$d(XY) = YdX + XdY + dXdY. \tag{A.2.27}$$

For Ito calculus, it is important to keep the extra product of differentials: $dXdY$ which is normally neglected in conventional calculus. This is because, we have to be careful not to neglect terms of order dW_i^2 which may result from $dXdY$ as they scale like $\sim dt$ in the mean (c.f. section A.2.3). In general, however, Stratonovich SDEs are preferred over Ito SDEs because Stratonovich numerical algorithms are known to exhibit stronger convergent properties [46]. Although the SDES that correspond to the FPE are of Ito form[6], we should not despair as it is possible convert an Ito SDE to a Stratnovich SDE and vice versa by modifying only the drift term using the relation (for the multi-dimensional case):

$$A_i^{Strat} = A_i^{Ito} - \frac{1}{2}\sum_{j,k} B_{kj}(\vec{x})\frac{\partial}{\partial x_k}B_{ij}(\vec{x}). \tag{A.2.28}$$

We see that eq. A.2.28 does indeed yield the same correction term as in eq. A.2.25 for the $1D$ case. On the other hand, there is no change to the noise terms. To put it explicitly, the following multidimensional Ito SDE

$$d\vec{X} = \vec{A}^{Ito}(\vec{X})dt + \mathbf{B}(\vec{X})d\vec{W} \tag{A.2.29}$$

and Stratonovich SDE:

$$d\vec{X} = \vec{A}^{Strat}(\vec{X})dt + \mathbf{B}(\vec{X}) \circ d\vec{W} \tag{A.2.30}$$

will produce the same results where A^{Strat} and A^{Ito} are related through eq. A.2.28 and the $\circ$ indicates that $\mathbf{B}$ has to be evaluated at the midpoint interval of each time interval $\tau_i \in [t_i, t_{i+1}]$.

[6] This will be shown in section A.2.5

A.2.5 Calculation of averages

For an Ito SDE, we found that the mean obeys the equation of motion in eq. A.1.6, i.e.

$$\frac{d}{dt}\langle X_t\rangle = \langle A(X_t)\rangle. \tag{A.2.31}$$

Using the rules of Ito calculous (see eq. A.2.27) we can then calculate the time evolution of X_t using the standard definition of an Ito differential (eq. A.2.14):

$$\begin{aligned} d(X_t^2) &= d(X_t \times X_t) \\ &= X_t dX_t + X_t dX_t + dX_t dX_t \\ &= 2X_t(A(X_t)dt + 2B(X_t)dW_t + B(X_t)^2 dW_t^2 \\ &\quad + A(X_t)^2 dt^2 + 2B(X_t)A(X_t)dtdW_t \end{aligned} \tag{A.2.32}$$

which upon stochastic averaging and keeping terms that are only of order dt becomes:

$$\begin{aligned} d\langle X_t^2\rangle &= 2\langle X_t A(X_t)\rangle dt + \langle B^2\rangle\langle dW(t)^2\rangle \\ &= 2\langle X_t A(X_t))\rangle dt + \langle B(X_t)^2\rangle dt \end{aligned} \tag{A.2.33}$$

or

$$\frac{d}{dt}\langle X_t^2\rangle = 2\langle X_t A(X_t)\rangle + \langle B(X_t)^2\rangle. \tag{A.2.34}$$

These are exactly the results that were obtained from using the $1D$ FPE in eq. A.1.5 and eq. A.1.10 provided we make the distinction:

$$D(X_t) = B(X_t)^2. \tag{A.2.35}$$

For a system of equations that are higher dimensions however, we get the generalized condition:

$$\mathbf{D}(\vec{\mathbf{X}}) = \mathbf{B}(\vec{\mathbf{X}})\mathbf{B}(\vec{\mathbf{X}})^T. \tag{A.2.36}$$

Simply put, the probabilistic dynamics generated by an FPE with drift vector $\vec{A}(\vec{X}(t))$ and diffusion matrix $\mathbf{D}(\vec{X}(t))$ will be the same as the that generated from a stochastic averaging of trajectories governed by the Ito SDE:

$$dX_t = \vec{A}(X_t)dt + \mathbf{B}(X_t)d\vec{W}(t) \tag{A.2.37}$$

as long as the factorization in eq. A.2.36 exists. This establishes the correspondence between the FPE and its corresponding Ito SDE. The conversion between an Ito SDE and its Stratonovich counterpart can be obtained using eq. A.2.28.

Appendix B

Noise matrix derivation for TFIM

In chapter 4, we did not explain in detail how the diffusion matrix was factorized as we conveniently mentioned that *"... a particular factorization of the diffusion matrix in eq. 4.1.8 ..."*. The details were relegated to this section so as to not distract the reader from the technical details but does not imply that it is a trivial process. Let us now go through this step in the derivation in more detail. Recall the FPE for TFIM:

$$
\begin{aligned}
\frac{\partial P(\vec{\alpha},\vec{\alpha}^{+},\vec{\beta},\vec{\beta}^{+})}{dt} = \sum_i \Bigg(& -\frac{\partial}{\partial\alpha_i}\left\{\frac{iJ}{4\hbar}\alpha_i\left[(n^{\alpha}_{i+1}-n^{\beta}_{i+1})+(n^{\alpha}_{i-1}-n^{\beta}_{i-1})\right]+\frac{ih(t)}{2\hbar}\beta_i\right\} \\
& -\frac{\partial}{\partial\beta_i}\left\{\frac{iJ}{4\hbar}\alpha^{+}_i\left[(n^{\beta}_{i+1}-n^{\alpha}_{i+1})+(n^{\beta}_{i-1}-n^{\alpha}_{i-1})\right]+\frac{ih(t)}{2\hbar}\alpha_i\right\} \\
& -\frac{\partial}{\partial\beta_i}\left\{\frac{iJ}{4\hbar}\beta_i\left[(n^{\beta}_{i+1}-n^{\alpha}_{i+1})+(n^{\beta}_{i-1}-n^{\alpha}_{i-1})\right]-\frac{ih(t)}{2\hbar}\alpha^{+}_i\right\} \\
& -\frac{\partial}{\partial\beta^{+}_i}\left\{\frac{iJ}{4\hbar}\beta^{+}_i\left[(n^{\alpha}_{i+1}-n^{\beta}_{i+1})+(n^{\alpha}_{i-1}-n^{\beta}_{i-1})\right]-\frac{ih(t)}{2\hbar}\alpha^{+}_i\right\} \\
& +\frac{1}{2}\left(\frac{iJ}{4\hbar}\right)\left[\frac{\partial^2}{\partial\alpha_i\partial\alpha_{i+1}}\alpha_i\alpha_{i+1}+\frac{\partial^2}{\partial\alpha_{i+1}\partial\alpha_i}\alpha_i\alpha_{i+1}-\frac{\partial^2}{\partial\alpha^{+}_i\partial\alpha^{+}_{i+1}}\alpha^{+}_i\alpha^{+}_{i+1}\right. \\
& -\frac{\partial^2}{\partial\alpha^{+}_{i+1}\partial\alpha^{+}_i}\alpha^{+}_i\alpha^{+}_{i+1}+\frac{\partial^2}{\partial\beta_i\partial\beta_{i+1}}\beta_i\beta_{i+1}+\frac{\partial^2}{\partial\beta_{i+1}\partial\beta_i}\beta_i\beta_{i+1} \\
& -\frac{\partial^2}{\partial\beta^{+}_i\partial\beta^{+}_{i+1}}\beta^{+}_i\beta^{+}_{i+1}-\frac{\partial^2}{\partial\beta^{+}_{i+1}\partial\beta^{+}_i}\beta^{+}_i\beta^{+}_{i+1}+\frac{\partial^2}{\partial\alpha^{+}_i\partial\beta^{+}_{i+1}}\alpha^{+}_i\beta^{+}_{i+1} \\
& +\frac{\partial^2}{\partial\beta^{+}_{i+1}\partial\alpha^{+}_i}\alpha^{+}_i\beta^{+}_{i+1}+\frac{\partial^2}{\partial\alpha^{+}_{i+1}\partial\beta^{+}_i}\alpha^{+}_{i+1}\beta^{+}_i+\frac{\partial^2}{\partial\beta^{+}_i\partial\alpha^{+}_{i+1}}\alpha^{+}_{i+1}\beta^{+}_i \\
& -\frac{\partial^2}{\partial\alpha_i\partial\beta_{i+1}}\alpha_i\beta_{i+1}-\frac{\partial^2}{\partial\beta_{i+1}\partial\alpha_i}\alpha_i\beta_{i+1}-\frac{\partial^2}{\partial\alpha_{i+1}\partial\beta_i}\alpha_{i+1}\beta_i \\
& \left.-\frac{\partial^2}{\partial\beta_i\partial\alpha_{i+1}}\alpha_{i+1}\beta_i\right]\Bigg) P(\vec{\alpha},\vec{\alpha}^{+},\vec{\beta},\vec{\beta}^{+}),
\end{aligned}
\tag{B.0.1}
$$

By inspecting eq. B.0.1, the diffusion matrix (which is a $4N \times 4N$ matrix), has matrix elements that are specified by the functions associated with their derivatives. Obviously, calculating the noise matrix is not a trivial task and comprises the bulk of the analytical work. Instead of simply taking the straightforward $\mathbf{B} = \sqrt{\mathbf{D}}$ choice, we used the trick mentioned in 2.3.2 and decomposed our diffusion matrix into eight different constituents, i.e.:

$$\mathbf{D} = \mathbf{D}^{\alpha} + \mathbf{D}^{\beta} + \mathbf{D}^{\alpha^+} + \mathbf{D}^{\beta^+} + \mathbf{D}^{\beta\alpha} + \mathbf{D}^{\alpha\beta} + \mathbf{D}^{\beta^+\alpha^+} + \mathbf{D}^{\alpha^+\beta^+}, \tag{B.0.2}$$

where the obvious choice for these constituents would be

$$\begin{aligned}
\left(\mathbf{D}^{\alpha}\right)_{i,i+1} &= \left(\mathbf{D}^{\alpha}\right)_{i+1,i} = & \frac{iJ}{4\hbar}\alpha_i\alpha_{i+1} \\
\left(\mathbf{D}^{\beta}\right)_{i,i+1} &= \left(\mathbf{D}^{\beta}\right)_{i+1,i} = & \frac{iJ}{4\hbar}\beta_i\beta_{i+1} \\
\left(\mathbf{D}^{\alpha^+}\right)_{i,i+1} &= \left(\mathbf{D}^{\alpha^+}\right)_{i+1,i} = & \frac{iJ}{4\hbar}\alpha_i^+\alpha_{i+1}^+ \\
\left(\mathbf{D}^{\beta^+}\right)_{i,i+1} &= \left(\mathbf{D}^{\beta^+}\right)_{i+1,i} = & \frac{iJ}{4\hbar}\beta_i^+\beta_{i+1}^+ \\
\left(\mathbf{D}^{\beta\alpha}\right)_{i,i+1} &= \left(\mathbf{D}^{\beta\alpha}\right)_{i+1,i} = & \frac{iJ}{4\hbar}\alpha_i\beta_{i+1} \\
\left(\mathbf{D}^{\alpha\beta}\right)_{i,i+1} &= \left(\mathbf{D}^{\alpha\beta}\right)_{i+1,i} = & \frac{iJ}{4\hbar}\beta_i\alpha_{i+1} \\
\left(\mathbf{D}^{\beta^+\alpha^+}\right)_{i,i+1} &= \left(\mathbf{D}^{\beta^+\alpha^+}\right)_{i+1,i} = & \frac{iJ}{4\hbar}\alpha_i^+\beta_{i+1}^+ \\
\left(\mathbf{D}^{\alpha^+\beta^+}\right)_{i,i+1} &= \left(\mathbf{D}^{\alpha^+\beta^+}\right)_{i+1,i} = & \frac{iJ}{4\hbar}\beta_i^+\alpha_{i+1}^+.
\end{aligned}$$

The idea is that instead of factorizing one complicated diffusion matrix, $\mathbf{D}$ we can instead factorize eight relatively simpler looking noise matrices, i.e. solving $\mathbf{B}^{\mathbf{x}}\left(\mathbf{B}^{\mathbf{x}}\right)^T = \mathbf{D}^x$. To make things slightly more transparent we will write out the general form for the first constituent, i.e. $x = \alpha$:

$$\mathbf{D}^{\alpha} = \frac{iJ}{4\hbar}\begin{bmatrix}
\begin{bmatrix}
0 & \alpha_0\alpha_1 & 0 & \dots & \alpha_0\alpha_{N-1} \\
\alpha_1\alpha_0 & 0 & \alpha_1\alpha_2 & \dots & 0 \\
0 & \alpha_2\alpha_1 & 0 & \ddots & 0 \\
\vdots & 0 & \ddots & \dots & 0 \\
\alpha_{N-1}\alpha_0 & 0 & \dots & \dots & 0
\end{bmatrix} & & & \mathbf{0} & \mathbf{0} & \mathbf{0} \\
 & & & & & \\
 & & \mathbf{0} & & \mathbf{0} & \mathbf{0} & \mathbf{0} \\
 & & \mathbf{0} & & \mathbf{0} & \mathbf{0} & \mathbf{0} \\
 & & \mathbf{0} & & \mathbf{0} & \mathbf{0} & \mathbf{0}
\end{bmatrix} \tag{B.0.3}$$

where $\mathbf{0}$ represents an $N \times N$ null matrix. If it were possible to find $\mathbf{B}^x$ for all x, then the total noise matrix takes the form of eq. 2.3.26.

Unfortunately, using the obvious choice $\sqrt{B^x}$ would still be messy and it would appear that we have not made things any easier. However, we can apply the same trick once more

and decompose each $\mathbf{D}^{\mathbf{x}}$ into N subconstituents: $\left\{\mathbf{D}_j^x,\ j = 0 \ldots N-1\right\}$. Once again taking the $x = \alpha$ matrix as an example, the intuitive way of choosing the subconstituents is:

$$\mathbf{D}^{\alpha} = \mathbf{D}_0^{\alpha} + \mathbf{D}_1^{\alpha} + \cdots + \mathbf{D}_{N-1}^{\alpha} \tag{B.0.4}$$

$$= \frac{iJ}{4\hbar}\begin{bmatrix} 0 & \alpha_0\alpha_1 & \ldots & \ldots & 0 \\ \alpha_1\alpha_0 & 0 & \ldots & \ldots & \\ \vdots & \vdots & \ddots & \ldots & \vdots \\ \vdots & \vdots & \ddots & \ldots & \vdots \\ 0 & 0 & \ldots & \ldots & 0 \end{bmatrix} + \frac{iJ}{4\hbar}\begin{bmatrix} 0 & 0 & \ldots & \ldots & 0 \\ 0 & 0 & \alpha_1\alpha_2 & \ldots & \\ 0 & \alpha_2\alpha_1 & \ddots & \ldots & \\ \vdots & \vdots & \ldots & \ddots & \vdots \\ 0 & \ldots & \ldots & \ldots & 0 \end{bmatrix} + \cdots +$$

$$\frac{iJ}{4\hbar}\begin{bmatrix} 0 & \ldots & \ldots & \ldots & \alpha_0\alpha_{N-1} \\ 0 & \ldots & \vdots & \ldots & \\ \vdots & \ldots & \ddots & \ldots & \\ \vdots & \vdots & \ldots & \ddots & \vdots \\ \alpha_{N-1}\alpha & \ldots & \ldots & \ldots & 0 \end{bmatrix}, \tag{B.0.5}$$

where the only non-trivial matrix elements of $\mathbf{D}_j^{\alpha}$ are given by

$$(\mathbf{D}_j^{\alpha})_{i,i+1} = (\mathbf{D}_j^{\alpha})_{i+1,i} = \alpha_j\alpha_{j+1}. \tag{B.0.6}$$

Each subconstituent diffusion matrix $\mathbf{D}_i^{\alpha}$ can then be individually factorized. This reduces the original problem to the much more trivial problem of factorizing matrices of the following form:

$$\mathbf{D}' = \begin{bmatrix} 0 & X \\ X & 0 \end{bmatrix} \tag{B.0.7}$$

for which we can easily show that either

$$\mathbf{B}' = \begin{bmatrix} -\sqrt{X/2} & -i\sqrt{X/2} \\ -\sqrt{X/2} & i\sqrt{X/2} \end{bmatrix} \tag{B.0.8}$$

or

$$\mathbf{B}'' = \begin{bmatrix} -\sqrt{X/2} & i\sqrt{X/2} \\ -\sqrt{X/2} & -i\sqrt{X/2} \end{bmatrix} \tag{B.0.9}$$

satisfies the necessary relation in eq. A.2.35. Now, granted that the decomposition for each $\mathbf{D}_i^{\alpha}$ exists, we can write eq. B.0.4 as:

$$\mathbf{D}^{\alpha} = \mathbf{B}_0^{\alpha}\left(\mathbf{B}_0^{\alpha}\right)^T + \mathbf{B}_1^{\alpha}\left(\mathbf{B}_1^{\alpha}\right)^T + \cdots + \mathbf{B}_{N-1}^{\alpha}\left(\mathbf{B}_{N-1}^{\alpha}\right)^T \tag{B.0.10}$$

so that using eq. 2.3.26 again, the total noise matrix for $\mathbf{D}^\alpha$ takes the obvious form:

$$\mathbf{B}^\alpha = \begin{bmatrix} | & | & | & | & | & | \\ \mathbf{B}_0^\alpha & \mathbf{B}_1^\alpha & \dots & \mathbf{B}_j^\alpha & \dots & \mathbf{B}_{N-1}^\alpha \\ | & | & | & | & | & | \end{bmatrix} \tag{B.0.11}$$

obviously satisfying eq. A.2.35, with the only non-zero elements being:

$$\begin{aligned} \left(\mathbf{B}_j^\alpha\right)_{j,2j} &= -\sqrt{\frac{iJ}{2\hbar}}\frac{1}{2}\sqrt{\alpha_j\alpha_{j+1}} \\ \left(\mathbf{B}_j^\alpha\right)_{j,2j+1} &= -i\sqrt{\frac{iJ}{2\hbar}}\frac{1}{2}\sqrt{\alpha_j\alpha_{j+1}} \\ \left(\mathbf{B}_j^\alpha\right)_{j+1,2j} &= -\sqrt{\frac{iJ}{2\hbar}}\frac{1}{2}\sqrt{\alpha_j\alpha_{j+1}} \\ \left(\mathbf{B}_j^\alpha\right)_{j+1,2j+1} &= i\sqrt{\frac{iJ}{2\hbar}}\frac{1}{2}\sqrt{\alpha_j\alpha_{j+1}}, \end{aligned}$$

where $j = 0 \dots N-1$. As an explicit example, the $N = 4$ case of eq. B.0.11 is shown below:

$$\mathbf{B}^\alpha = \sqrt{\frac{iJ}{2\hbar}}\frac{1}{2}\begin{bmatrix}\begin{bmatrix} -\sqrt{\alpha_0\alpha_1} & -i\sqrt{\alpha_0\alpha_1} \\ -\sqrt{\alpha_0\alpha_1} & +i\sqrt{\alpha_0\alpha_1} \\ 0 & 0 \\ 0 & 0 \\ \vdots & \vdots \\ 0 & 0 \end{bmatrix} & \begin{bmatrix} 0 & 0 \\ -\sqrt{\alpha_1\alpha_2} & -i\sqrt{\alpha_1\alpha_2} \\ -\sqrt{\alpha_1\alpha_2} & i\sqrt{\alpha_1\alpha_2} \\ 0 & 0 \\ \vdots & \vdots \\ 0 & 0 \end{bmatrix} & \begin{bmatrix} 0 & 0 \\ 0 & 0 \\ -\sqrt{\alpha_2\alpha_3} & -i\sqrt{\alpha_2\alpha_3} \\ -\sqrt{\alpha_2\alpha_3} & i\sqrt{\alpha_2\alpha_3} \\ \vdots & \vdots \\ 0 & 0 \end{bmatrix} & \begin{bmatrix} -\sqrt{\alpha_0\alpha_3} & -i\sqrt{\alpha_0\alpha_3} \\ 0 & 0 \\ 0 & 0 \\ -\sqrt{\alpha_0\alpha_3} & +i\sqrt{\alpha_0\alpha_3} \\ \vdots & \vdots \\ 0 & 0 \end{bmatrix}\end{bmatrix} \tag{B.0.12}$$

which is an $4N \times 2N$ matrix with most elements being trivial. This noise matrix would therefore introduce $2N$ independent Wiener increments (see section. A.2.2) can be stored as the components of the Wiener increment vector: $d\vec{W}^\alpha$. In this fashion, the noise terms for the SDEs in eq. 4.1.12 to eq. 4.1.15 can be derived. If we label $d\vec{W}^\alpha$ in the conventional way[1] then:

[1]The labelings for $dW^{\alpha\beta}, dW^{\beta\alpha}, dW^{\beta^+\alpha^+}$ and $dW^{\alpha^+\beta^+}$ does not follow the usual convention and can be deduced from the corresponding noise terms in eq. 4.1.12 to eq. 4.1.15

$$d\vec{W}^{\alpha} = \begin{bmatrix} dW_0^{\alpha} \\ dW_1^{\alpha} \\ \vdots \\ \vdots \\ dW_{N-1}^{\alpha} \end{bmatrix}, \tag{B.0.13}$$

and the resulting stochastic terms only contribute to $d\vec{\alpha}$, i.e.:

$$d\alpha_i \propto -\sqrt{\alpha_i \alpha_{i+1}}\left(dW_{2i} + i dW_{2i+1}\right) - \sqrt{\alpha_i \alpha_{i-1}}\left(dW_{2i-2} + i dW_{2i-1}\right). \tag{B.0.14}$$

where we assumed "periodic boundary conditions" for the Wiener increment vectors in the sense that $dW_{-i} = dW_{2N-i}$ where $i \in [0, N-1]$.

Appendix C

Numerical algorithm

The Stratonovich semi-implicit algorithm is known to have strong convergent properties [46] compared to the numerical methods for Ito SDEs. Thus the Stratonovich version of the SDEs derived were numerically solved instead. We now provide an outline of an algorithm which is surprisingly trivial. The simulations produced required a self-consistent type algorithm as the SDEs given are all expressed in Stratonovich form. The latter form implies that we need to evaluate the noise matrix, $\underline{B}$ at the midpoint of each time interval. Although Stratonovich SDEs does not require us evaluate the drift terms at the midpoint, we will do so anyway as it provides a more accurate calculation. More explicitly, the semi-implicit Stratonovich differential equation is given by:

$$y(t+h) - y(t) = h\left[a[y(t+\frac{h}{2})] + b[y(t+\frac{h}{2})]\xi(t)\right], \tag{C.0.1}$$

where $\xi(t) \sim N(0, 1/dt) = \sqrt{dt}N(0,1)$ and we are evaluating the RHS at midpoint values. The problem is that we have no idea what the value of $y(t+\frac{h}{2})$ is, i.e. its future value at half a time step. The best we can do then is approximate this value and iterate till convergence is reached. We therefore write an SDE for the midpoint value as

$$y(t+\frac{h}{2}) - y(t) = \frac{h}{2}\left[a[y(t+\frac{h}{2})] + b[y(t+\frac{h}{2})]\xi(t)\right] \tag{C.0.2}$$

or

$$y(t+\frac{h}{2}) = y(t) + \frac{h}{2}\left[a[y(t+\frac{h}{2})] + b[y(t+\frac{h}{2})]\xi(t)\right]. \tag{C.0.3}$$

In eq. C.0.3, we take the Taylor expansion as out first approximation so that

$$\begin{aligned} y(t+\frac{h}{2}) &\approx y(t) + \frac{h}{2}y'(t) \\ &= y(t) + \frac{h}{2}\left(a[y(t)] + b[y(t)]\xi(t)\right). \\ &= y_1 \end{aligned} \tag{C.0.4}$$

where y_1 denotes that our first approximation for $y(t+\frac{h}{2})$. Now substitute this back into eq. C.0.3 to get

$$\underline{y(t+\frac{h}{2})} = y(t) + \frac{h}{2}\left[a[y_1(t)] + b[y_1(t)\xi(t)]\right] \tag{C.0.5}$$

and $\underline{y(t+\frac{h}{2})}$ becomes our new estimate: y_2. This generates a self-consistency condition that gives us better and better estimates the more iterations we have. For the purposes of the simulations in this paper, three iterations are more than enough for good agreement. One difference to note is that, we have written the noise terms in terms of the gaussian variables with mean 0 and variance $\frac{1}{\sqrt{dt}}$. Recall:

$$dW(t) = W(t+dt) - W(t) = \xi(t)dt \tag{C.0.6}$$

and since

$$dW(t) \sim N(0,dt) = \sqrt{dt}N(0,1) \tag{C.0.7}$$

then

$$\xi(t) = \frac{1}{\sqrt{dt}}N(0,1). \tag{C.0.8}$$

Our SDEs which were defined to be of generic form

$$d\vec{\alpha} = A(\vec{\alpha},\vec{\beta})dt + B(\vec{\alpha},\vec{\beta})d\vec{W}(t) \tag{C.0.9}$$

can be written as

$$d\vec{\alpha} = \left(A(\vec{\alpha},\vec{\beta}) + B(\vec{\alpha},\vec{\beta})\vec{\xi}(t)\right)dt \tag{C.0.10}$$

instead.

Bibliography

[1] I. Bose. Quantum magnets: a brief overview. *ArXiv Condensed Matter e-prints*, July 2001.

[2] P. Mendels and F Bert. Quantum kagome antiferromagnet zncu$_3$(oh)$_6$cl$_2$. *Journal of the Physical Society of Japan*, 79(1):011001, 2010.

[3] M. Ramazanoglu, C. P. Adams, J. P. Clancy, A. J. Berlinsky, Z. Yamani, R. Szymczak, H. Szymczak, J. Fink-Finowicki, and B. D. Gaulin. Spin waves in the ferromagnetic ground state of the kagome staircase system $co_3v_2o_8$. *Phys. Rev. B*, 79(2):024417, Jan 2009.

[4] N. Oba et al. Collinear order in frustrated quantum antiferromagnet on square lattice (cubr)lanb$_2$o$_7$. *Journal of the Physical Society of Japan*, 75(11):113601, 2006.

[5] J. Matsuno, Y. Okimoto, Z. Fang, X. Z. Yu, Y. Matsui, N. Nagaosa, M. Kawasaki, and Y. Tokura. Metallic ferromagnet with square-lattice *coo*2 sheets. *Phys. Rev. Lett.*, 93(16):167202, Oct 2004.

[6] H. Q. Lin. Exact diagonalization of quantum-spin models. *Phys. Rev. B*, 42(10):6561–6567, Oct 1990.

[7] R. M. Noack and S. R. Manmana. Diagonalization- and Numerical Renormalization-Group-Based Methods for Interacting Quantum Systems. In A. Avella & F. Mancini, editor, *Lectures on the Physics of Highly Correlated Electron Systems IX*, volume 789 of *American Institute of Physics Conference Series*, pages 93–163, September 2005.

[8] H. Q. Lin and J. E. Gubernatis. Exact diagonalization methods for quantum systems. *Computers in Physics*, 7(4):400–407, 1993.

[9] A.J. Daley, C. Kollath, U. Schollwöck, and G. Vidal. Time-dependent density-matrix renormalization-group using adaptive effective hilbert spaces. *Journal of Statistical Mechanics: Theory and Experiment*, 2004:P04005, 2004.

[10] S.R. White and A.E. Feiguin. Real-time evolution using the density matrix renormalization group. *Physical review letters*, 93(7):76401, 2004.

[11] M.C. Bañuls, M.B. Hastings, F. Verstraete, and J.I. Cirac. Matrix product states for dynamical simulation of infinite chains. *Physical review letters*, 102(24):240603, 2009.

[12] K. E. Cahill and R. J. Glauber. Density operators and quasiprobability distributions. *Phys. Rev.*, 177(5):1882–1902, Jan 1969.

[13] E. Wigner. On the quantum correction for thermodynamic equilibrium. *Phys. Rev.*, 40(5):749–759, Jun 1932.

[14] J. E. Moyal. Quantum mechanics as a statistical theory. *Proc. Cambridge Phil. Sock*, 45(99):99–124, Nov 1949.

[15] D. J. Tannor, editor. *Introduction to Quantum Mechanics: A Time-Dependent Perspective*. University Science Books, 2006.

[16] P. D. Drummond and C. W. Gardiner. Generalised p-representations in quantum optics. *Journal of Physics A: Mathematical and General*, 13(7):2353, 1980.

[17] R. J. Glauber. Coherent and incoherent states of the radiation field. *Phys. Rev.*

[18] L. Arnold. *Stochastic Differential Equations*. New York: Wiley, 1974.

[19] A. M. Smith and C. W. Gardiner. Simulations of nonlinear quantum damping using the positive p representation. *Phys. Rev. A*, 39(7):3511–3524, Apr 1989.

[20] K. J. McNeil and I. J. D. Craig. Positive-p representation for second-harmonic generation: Analytic and computational results. *Phys. Rev. A*, 41(7):4009–4018, Apr 1990.

[21] S. Ghanbari, J. F. Corney, and T. D. Kieu. Finite temperature correlations in the Bose-Hubbard model: application of the Gauge-P representation. *ArXiv e-prints*, February 2010.

[22] P. Deuar, A. G. Sykes, D. M. Gangardt, M. J. Davis, P. D. Drummond, and K. V. Kheruntsyan. Nonlocal pair correlations in the one-dimensional bose gas at finite temperature. *Phys. Rev. A*, 79(4):043619, Apr 2009.

[23] L. I. Plimak, M J. Steel, M. K. Olsen, P. D. Drummond, S. M. Tan, M. J. Collett, D. F. Walls, and R. Graham. Dynamical quantum noise in trapped bose-einstein condensates. *Phys. Rev. A*, 58(6):4824–4835, Dec 1998.

[24] P. Barmettler, M. Punk, V. Gritsev, E. Demler, and E. Altman. Quantum quenches in the anisotropic spin-1/2 heisenberg chain: different approaches to many-body dynamics far from equilibrium. *New Journal of Physics*, 12(5):055017, 2010.

[25] A. Iucci and M. A. Cazalilla. Quantum quench dynamics of the sine-gordon model in some solvable limits. *New Journal of Physics*, 12(5):055019, 2010.

[26] I. Bloch, J. Dalibard, and W. Zwerger. Many-body physics with ultracold gases. *Rev. Mod. Phys.*, 80(3):885–964, Jul 2008.

[27] I. Bloch and A. Rosch. Exploring strongly correlated quantum many-body systems with ultracold atoms in optical lattices. *physica status solidi (b)*, 247(3):530–536, Mar 2010.

[28] S. Fillling M. Feld U. Schnorrberger A. M. Rey A. Polkovnikov E. A. Demler M. D. Lukin I. Bloch S. Trotzky, P. Cheinet. Time-resolved observation and control of superexchange interactions with ultracold atoms in optical lattices. *Science*, 18(1150841):295–299, Jan 2008.

[29] H. J. Carmichael. *Statistical Methods in Quantum Optics 1: Master Equations and Fokker-Planck Equations*. Springer, 2002.

[30] M. K. Olsen, L. I. Plimak, S. Rebic, and A.S. Bradley. Phase-space analysis of bosonic spontaneous emission. *Optics Communications*, 254(4-6):271 – 281, 2005.

[31] L. I. Plimak, M. K. Olsen, and M. J. Collett. Optimization of the positive-p representation for the anharmonic oscillator. *Phys. Rev. A*, 64(2):025801, Jul 2001.

[32] P. Deuar and P. D. Drummond. Correlations in a bec collision: First-principles quantum dynamics with 150 000 atoms. *Phys. Rev. Lett.*, 98(12):120402, Mar 2007.

[33] R. J. Glauber. The quantum theory of optical coherence. *Phys. Rev.*, 130(6):2529–2539, Jun 1963.

[34] E. C. G. Sudarshan. Equivalence of semiclassical and quantum mechanical descriptions of statistical light beams. *Phys. Rev. Lett.*, 10(7):277–279, Apr 1963.

[35] H. Risken. *The Fokker-Planck Equation*. Berlin: Springer, 1989.

[36] A. Gilchrist, C. W. Gardiner, and P. D. Drummond. Positive p representation: Application and validity. *Phys. Rev. A*, 55(4):3014–3032, Apr 1997.

[37] P. Deuar and P. D. Drummond. Gauge p representations for quantum-dynamical problems: Removal of boundary terms. *Phys. Rev. A*, 66(3):033812, Sep 2002.

[38] P. Deuar. First-principles quantum simulations of many-mode open interacting Bose gases using stochastic gauge methods. *ArXiv Condensed Matter e-prints*, July 2005.

[39] H. Van Dam and L. C. Biedenharn, editor. *Quantum Theory of Angular Momentun*. Academic Press, 1965.

[40] J. J. Sakurai. *Modern Quantum Mechanics*. Addison-Wesley, 1994.

[41] T. Holstein and H. Primakoff. Field dependence of the intrinsic domain magnetization of a ferromagnet. *Phys. Rev.*, 58(12):1098–1113, Dec 1940.

[42] S V Maleev. *Sov. Phys. JETP*, 6:776, 1958.

[43] D. W. Barry and P. D. Drummond. Qubit phase space: $su(n)$ coherent-state p representations. *Phys. Rev. A*, 78(5):052108, Nov 2008.

[44] J M Radcliffe. Some properties of coherent spin states. *Journal of Physics A: General Physics*, 4(3):313, 1971.

[45] J. F. Corney S. E. Hoffmann and P. D. Drummond. Hybrid phase-space simulation method for interacting bose fields. *Phys. Rev. A*, 78(1):013622, Jul 2008.

[46] P. D. Drummond and I. K. Mortimer. Computer simulations of multiplicative stochastic differential equations. *Journal of Computational Physics*, 93(1):144 – 170, 1991.

[47] M.K. Olsen and A.S. Bradley. Numerical representation of quantum states in the positive-p and wigner representations. *Optics Communications*, 282(19):3924 – 3929, 2009.

[48] G. Marsaglia and W. W. Tsang. A simple method for generating gamma variables. *ACM Trans. Math. Softw.*, 26(3), 2000.

[49] P. Deuar and P. D. Drummond. First-principles quantum dynamics in interacting bose gases ii: stochastic gauges. *Journal of Physics A: Mathematical and General*, 39(11):2723, 2006.

[50] P. Deuar and P. D. Drummond. Stochastic gauges in quantum dynamics for many-body simulations. *Computer Physics Communications*, 142(1-3):442 – 445, 2001.

[51] P. D. Drummond and P. Deuar. Quantum dynamics with stochastic gauge simulations. *Journal of Optics B: Quantum and Semiclassical Optics*, 5(3):S281, 2003.

[52] P. D. Drummond, P. Deuar, and K. V. Kheruntsyan. Canonical bose gas simulations with stochastic gauges. *Phys. Rev. Lett.*, 92(4):040405, Jan 2004.

[53] A. J. Leggett, S. Chakravarty, A. T. Dorsey, M. P. A. Fisher, A. Garg, and W. Zwerger. Dynamics of the dissipative two-state system. *Rev. Mod. Phys.*, 59(1):1–85, Jan 1987.